Negative microfilm received from university

Mic 61-1762

McKENZIE, William Moore. FUNDAMENTAL ASPECTS OF THE WOOD CUTTING PROCESS.

University of Michigan, Ph.D., 1961
Agriculture, forestry and wildlife

University Microfilms, Inc., Ann Arbor, Michigan

FUNDAMENTAL ASPECTS

OF THE WOOD CUTTING PROCESS

by
William Moore McKenzie

A dissertation submitted in partial fulfilment
of the requirements for the degree of
Doctor of Philosophy in the
University of Michigan
1960

Doctoral Committee:

Associate Professor Norman C. Franz, Chairman
Professor Samuel K. Clark
Professor Lester V. Colwell
Professor Alan A. Marra
Professor Stephen B. Preston

ACKNOWLEDGMENTS

Professor Norman C. Franz under whose guidance this study was carried out, is a pioneer in the analytical approach to the wood cutting process. For his invaluable advice and constant encouragement the author is deeply grateful. Professor Stephen B. Preston has always been ready with a fresh and pungent approach, and Professor Alan A. Marra has also contributed freely from his experience. The soundness of this work owes much to the generous attention of Professor Lester V. Colwell of the University's Department of Mechanical Engineering, and of Professor Samuel K. Clark of the Department of Engineering Mechanics, who suggested the model comprising a string on an elastic foundation. The patience, ever-willing advice, and assistance of Glenn P. Bruneau in the experimental work is also gratefully acknowledged.

This work was carried out while the author was on leave from the Division of Forest Products, Commonwealth Scientific and Industrial Research Organization, South Melbourne, Australia, and the author is grateful for this support.

Finally, the project would not have been possible without considerable sacrifice by my wife, in addition to a

direct contribution in the form of typing and checking the manuscript.

TABLE OF CONTENTS

		Page
LIST OF TABLES		vi
LIST OF FIGURES		vii
INTRODUCTION		1
	PART I. THE EFFECT OF CUTTING SPEED ON CUTTING FORCES	
Chapter		
1.	INTRODUCTION	5
2.	EXPERIMENTAL	10
3.	DISCUSSION	16
	PART II. THE GENERAL ORTHOGONAL CUTTING SITUATION IN WOOD	
4.	THE ANISOTROPY OF WOOD	18
	PART III. PRELIMINARY INVESTIGATION OF THE 90°-90° CUTTING SITUATION	
5.	INITIAL OBSERVATIONS	24
6.	SHEAR ABOVE THE CUTTING PLANE - VOSKRESENSKI'S ANALYSIS	42
7.	THE INDENTATION PHASE OF CUTTING	50
8.	THE EFFECT OF LATERAL VIBRATION ON THE INDENTATION PHASE.	57
9.	THE EFFECTS OF LUBRICATION ON THE INDENTATION PHASE	68
10.	CONCLUSIONS PROVIDING THE BASIS FOR AN ANALYSIS	73

PART IV. ANALYTICAL MODELS FOR THE 90°-90° CUTTING SITUATION

Chapter		Page
11.	STRING ON ELASTIC FOUNDATION	81
12.	BEAM ON ELASTIC FOUNDATION	87
13.	CRITERION FOR TYPE II FAILURE BASED ON THE ELASTICALLY SUPPORTED BEAM .	122
14.	APPLICATION OF THE BEAM MODELS TO CUTTING AT 90°-0° AND 0°-90°	133
	PART V.	
15.	GENERAL DISCUSSION	141
SUMMARY		146
BIBLIOGRAPHY		149

LIST OF TABLES

Table		Page
1.	Comparison of Observed Cutting Forces with Values Computed from Equations (3) and (4)	45
2.	The Effect of Induced Lateral Vibrations at 60 c.p.s. on Cutting Forces and Apparent Friction Coefficients in Cutting at 90°-90°	62
3.	The Effect of Induced Lateral Vibration at 60 c.p.s. on Cutting Forces and Apparent Friction Coefficients in Orthogonal Cutting at 90°-0° and 0°-90° . .	64
4.	The Effect of Lubrication with S.A.E.30 Oil on Maximum Parallel Cutting Force and the Cutting Friction Coefficient . .	70
5.	Mean Wavelengths of Recorded Cutting Forces	101
6.	Mechanical and Physical Properties Used in Computations Based on Equations (3) and (39)	106
7.	Effect of Species, Moisture Content and Cutting Angle on Cutting Friction Coefficients	119
8.	Comparison of Theoretical Maximum Stresses with Tensile Strength	(a) 128 (b) 129

LIST OF FIGURES

Figure		Page
1.	Orthogonal cutting	3
2.	Suggested effects of cutting speed on cutting force	8
3.	Arrangement of laminated work-piece, dynamometer and grooving tool on lathe . . .	11
4.	Oscilloscope records of cutting force components, in cutting on the edge of a disk of yellow-poplar at 5 per cent moisture content	12
5.	The effect of cutting speed on tool forces in cutting on the edge of a disk of yellow-poplar at 5 per cent moisture content, grain direction diametral	14
6.	Specification of the general three-dimensional cutting situation	19
7.	The three main cutting directions, specified with respect to the grain direction	21
8.	The 90°-90° cutting situation	25
9.(a)	Irregular failure types; x 30	28
(b)	" " " ; x 10	29
10.	Type I(a) failure in saturated eastern white pine	30
11.	Type I(b) failure in eastern white pine at 5 per cent moisture content	31
12.	Type II(a) failure in yellow-poplar at 5 per cent moisture content	33

Figure		Page
13.	Type II(b) failure in common persimmon at 5 per cent moisture content	34
14.	Transition from type I(a), through types I(b) and II(a), to type II(b) failure in sugar maple at 5 per cent moisture content as cutter emerges from a zone lubricated with oil	35
15.	Sequence of four cuts in sugar maple at 8 per cent moisture content, associated with type II(a) failure	37
16.	Zones of failure in 90°-90° cutting . . .	39
17.	Diagram for deriving friction angle at the shear plane	43
18.	Recordings of cutting force components associated with the four failure types . . .	53
19.	Indentation by cutter edge, with deflection of cell walls	55
20.	Effect of taking section in resultant cutting direction on apparent cutting angle and apparent wall thickness	59
21.	Lateral vibration at 60 c.p.s. prevented type II failure and improved surface quality in cutting yellow-poplar and common persimmon at 0.5 in. per min.	61
22.	Lateral vibration at 60 c.p.s. (centre section) prevented fuzzy grain in cutting at 90°-0° in eastern white pine at 5 per cent moisture content . . .	65
23.	The effect of lateral vibration in cutting at 0°-90° (veneer cutting) in saturated yellow birch	67
24.	The effect of applying S.A.E. 30 lubricating oil (dark-stained areas) on failure type in sugar maple at 5 per cent moisture content	71
25.	Basic postulate concerning incision. Failure in tension	76

Figure		Page
26.	Hypothetical distribution of tension stress along the fibre below cutter edge	80
27.	Model for indentation phase. String on elastic foundation	82
28.	Relation between cutting force and assumed stress distribution along cutting plane	88
29.	Double-beam model - Beam 1	95
30.	Double-beam model - Beam 2	99
31.	Comparison of theoretical relationship between cutting force and cutting angle with experimental points : matched material, nominal chip thickness 0.030 in.	108
32.	Comparison of theoretical relationship between cutting force and cutting angle with experimental points : matched material, 0.010 in. nominal chip thickness	109
33.	Comparison of theoretical relationship between cutting force and cutting angle, based on species-mean properties, with experimental points	110
34.	Comparison of theoretical relationship between cutting force and nominal chip thickness with experimental points : sugar pine	111
35.	Comparison of theoretical relationship between cutting force and nominal chip thickness with experimental points : yellow birch	112
36.	Comparison of theoretical relationship between cutting force and nominal chip thickness with experimental points : white ash	113
37.	Criterion for type II failure - Beam 3 . .	123
38.	The effect of moisture content on failure type	132
39.	Model for 90°-0° cutting situation	135

Figure Page

40. Relationship between axial force and shear at cutting plane in model for $90^{\circ}-0^{\circ}$ cutting situation 137

INTRODUCTION

Historically, research in wood machining has progressed from investigation of a particular problem of a certain machining process to study of the problems basic to a particular process, as exemplified by the work of Franz (1) in planing, Reineke (2) in sawing, and Leney (3) in veneer cutting. It is apparent that the more fundamental such work becomes, the less it is concerned with the details of the machine or the tool, and the more it is concerned with the action of a highly simplified cutter on a work-piece of wood. Attention is focussed on the behaviour of the material of the work-piece rather than that of the tool.

To carry this trend further, it is logical to ask "Are there problems basic to all wood machining processes?" and further,"Are such problems vital?" If the answers to these questions are affirmative, there remains the question, "How far can attempts to find a general solution to such problems be carried?"

Concerning the first question, it is evident from the work on particular operations, referred to above, and from metal cutting research (4), that the problem basic to the more important cutting processes concerns the situation known as orthogonal cutting. This is the term applied where a simple wedge-shaped cutter, with a straight edge

wider than the work-piece, moves with uniform velocity in a plane parallel to the surface of a semi-infinite work-piece, as in Fig. 1. Quasi-equilibrium is assumed, and there is presented a static problem in mechanics. Variables to be considered are those associated with the geometry of the cutter, the properties of the material of the work-piece, the thickness of the uncut chip (nominal chip thickness), and in the first instance, the cutting speed. The information to be expected from an analysis of the stresses in the vicinity of the cutter edge is of two kinds. Firstly, it should be possible to derive the forces acting on the tool or work-piece for given cutting conditions, and secondly, the analysis should enable prediction of the mode of chip formation and the nature of the associated cut surface. In considering the question as to whether these types of information are important, it is asserted that, in any wood-cutting operation, efforts to improve efficiency and product quality are concerned with some or all of the following aspects:- surface accuracy and smoothness, chip form, amount and form of waste, power consumption, tool and machine wear, and machine design. It is contended that each of these aspects is primarily related to either the forces involved or the mode of chip formation, or both, and hence that this information, obtainable in principle from a study of orthogonal cutting, is of vital importance.

The provision of an answer to the third question posed above, that is, exploration of the possibilities of a general approach, was the primary purpose of the work

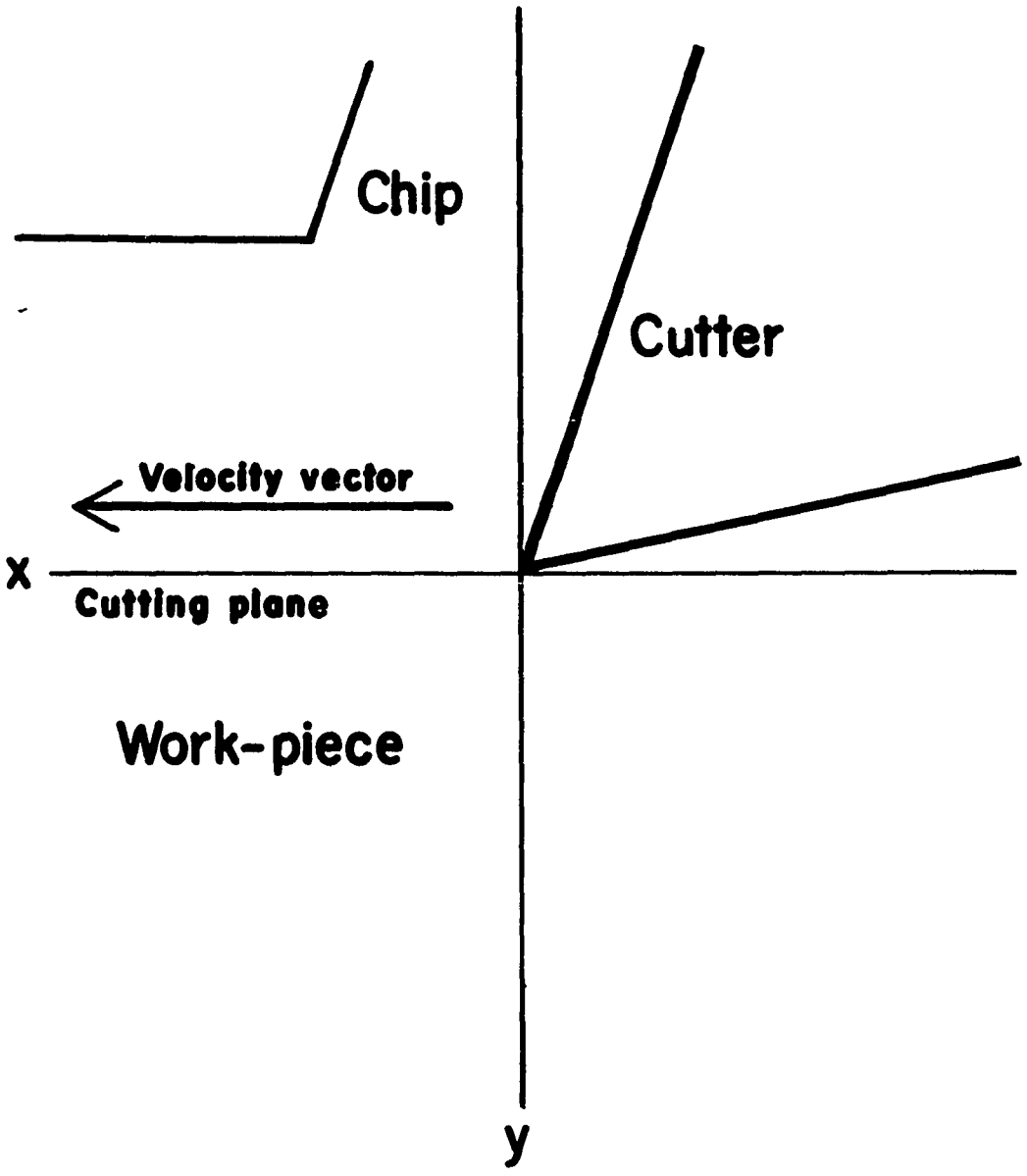


Fig. 1. Orthogonal cutting.

reported here. For two reasons, it was considered necessary, before proceeding to exploratory studies, to assess the significance of cutting speed in the orthogonal cutting situation - that is, apart from effects on tool behaviour, chip geometry etc. Observations of events during cutting are made most conveniently at very low cutting speeds, and further, mechanical properties of wood are normally measured under "static" conditions. Hence study and analysis of the cutting process would be greatly facilitated if it could be established that the effects of cutting speed were essentially linear. Since the available evidence was somewhat contradictory, and reported cutting experiments showed certain weaknesses, an investigation of this aspect has been undertaken, as reported in Part I.

On proceeding to examine the general orthogonal cutting situation, it was evident that the greatest obstacle to general analysis was the extreme anisotropy of wood. Since it seemed impossible to visualize relationships between events in cutting situations differing widely with respect to grain angle, it was expedient to choose a particular grain angle for exploratory study of the other important cutting factors. For reasons given later, attention was directed to the situation in which both the cutter edge and its velocity vector are perpendicular to the grain. This was done in the hope that principles elicited and analytical results obtained might be extended to other grain angles. This possibility has been briefly investigated.

PART I

THE EFFECT OF CUTTING SPEED ON CUTTING FORCES

CHAPTER 1

INTRODUCTION

Work on the effect of cutting speed is well reviewed by Lubkin (5), and it is evident that some results show practically no effect on cutting power, while others show a curve with a minimum at some speed, or a linear change with increasing velocity.

The commonness of the belief that surface quality improves at higher speeds may be partly attributed to the fact that in practice a higher cutting speed is almost always accompanied by the cutting of a thinner chip, so that the cutting forces and surface damage are both reduced.

Voskresenski (6) states that cutting speed has a negligible effect on forces, but claims positive evidence as to an effect of cutting speed on surface quality. He asserts that this may be expected, due to dynamic effects in the wood, and this is plausible, but he makes no attempt to assess the likelihood of a significant effect in the normal range of cutting speeds. His treatment of the dynamics of a lamina such as occurs in cutting end grain may have significance in

the case of a multi-knife cutter head, since speed would be related to frequency of knife contact, but this is a different question to that being posed here.

The essential question is whether cutting speed affects the relevant physical and mechanical properties of the wood. Therefore the evidence of Liska (7) on the effect of strain rate on wood properties is of interest. He found that strength in compression parallel to the grain and in flexure increased eight per cent for every ten-fold increase in testing speed up to 24 in. per min. If these results could legitimately be extrapolated so far, it could be concluded that wood should be many times stronger at normal cutting speeds, and that cutting forces should increase correspondingly. It is to be noted that most experiments have covered less than a six-fold increase in cutting velocity, so that, at most, an increase of 6.5 per cent in cutting forces should have been observed, and this could have been masked by experimental error in some cases. As pointed out by Koch (8), another factor tending to increase tool forces as cutting velocity increases is the energy required to change the momentum of the chips, but his computation shows that this would contribute no more than about 5 per cent of the tool forces at 10,000 ft. per min. Other factors suggested as contributing to an increase in cutting force are "chip compression" (9), and "dynamic support" (10) which may be references to a viscoelastic effect. Such an effect would also explain the results of Liska discussed above.

An initial decrease in cutting forces with increase of velocity is ascribed by Thunell (9) to reduced friction on the grounds that, in many materials, friction coefficient decreases with increasing sliding speed. Another factor which might cause cutting forces to decrease with velocity is increase in temperature, resulting from a tendency toward adiabatic conditions (11). It is known (12) that strength of wood decreases one-half to one-third per cent per degree F. increase in temperature. If a temperature of 150 degrees F. existed, and this is quite possible according to the work of Reichel (13) on tool temperatures, the resulting loss of strength would be about 40 per cent, which would roughly balance the increase in strength due to high straining rate mentioned above.

Hence, on lines suggested by Freudenthal (11) for metals, a possible explanation for the variation in results from the several studies of cutting speed is that there are counter influences, an increase in cutting forces due to increased straining rate (viscoelastic effect) being opposed by decreases due to the higher temperature, and possibly by reduced friction. This is illustrated in Fig. 2. The shape of the cutting force curve would depend on the variation of the three interacting effects with velocity, and according to the conditions of the experiment could approximate a horizontal line or a curve of varying shape. In addition to conflicting evidence concerning the normal range of cutting speeds, there is a region of uncertainty at

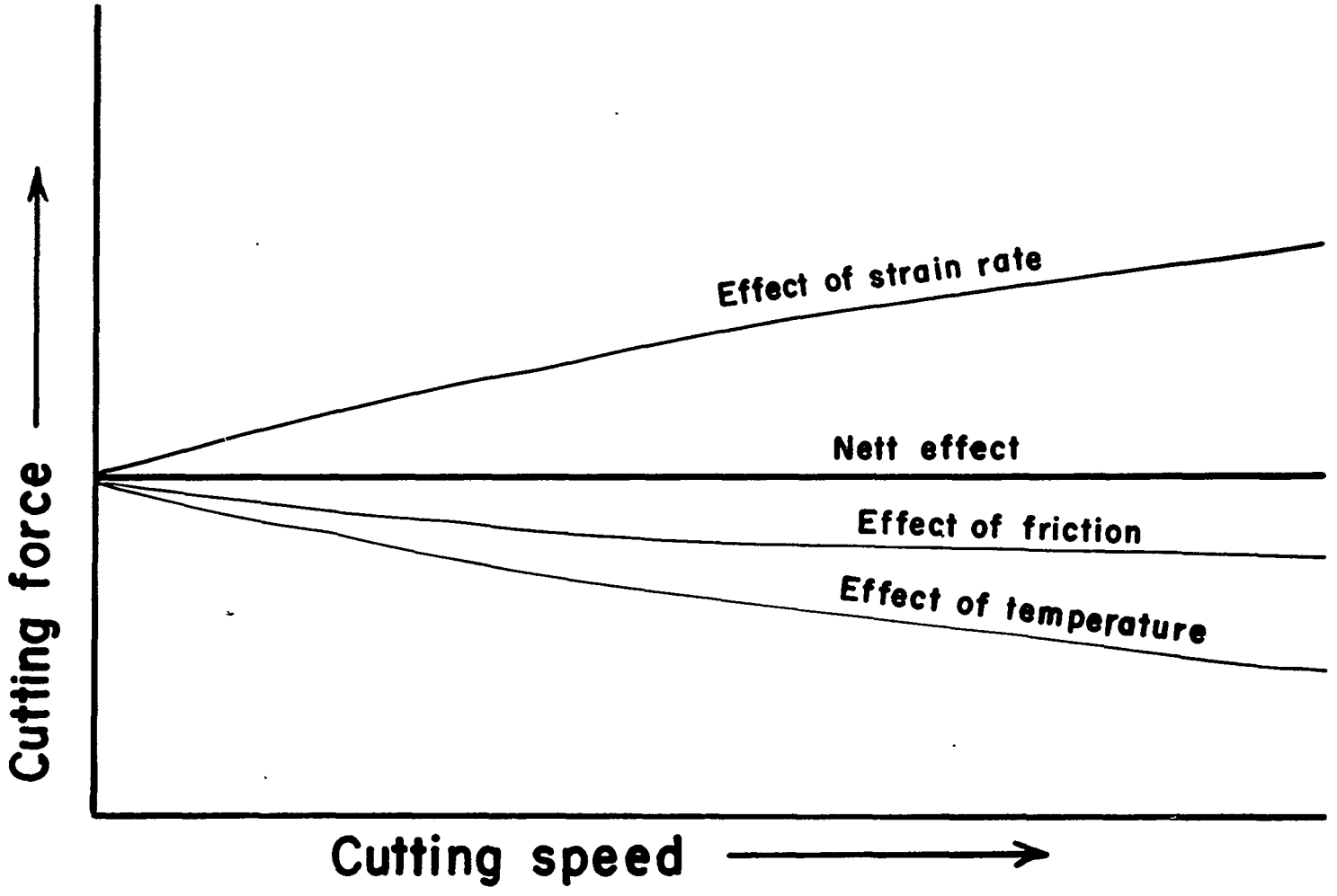


Fig. 2. Suggested effects of cutting speed on cutting force.

the very low end of the scale of cutting velocity, since Franz (1) has observed that as static conditions were approached, alteration of the cutting process took place, often resulting in changes of chip type. Only Kivimaa (14) reports a direct comparison of forces in this region, and the type of apparatus used by him is dynamically suspect (15). This indicates a hazard involved in developing a theory of chip formation based on static considerations, and a need for further investigation in this region of cutting velocity.

Criticisms that apply to most of the machining experiments reported are, firstly, that they deal with percussive action, so that results could be affected by dynamic properties of the system of wood, tool, machine and measuring device. Secondly, no evidence of statistical analysis is given in any of the articles. A third possibility, in some cases, is that wattmeter recordings of motor input may not have been adjusted for motor efficiency at various speeds. It would be necessary to meet all these criticisms before one would be justified in drawing anything but a horizontal straight line through a plot of cutting forces against speed.

It appeared that many of the difficulties concerning machine and dynamometer might be avoided by using a continuous type of cutting such as that of a lathe, thus reducing the effects of impact.

CHAPTER 2

EXPERIMENTAL

Continuous cutting conditions were obtained at speeds varying from 2,700 to 27,500 ft. per min. by cutting on the edge of a wood disk mounted on a high-speed lathe, controlling cutting and feed speeds by reference to electronic counters. The cutter and dynamometer were as described by Franz (1). The dynamometer, which had a natural frequency of 1,500 c.p.s. was connected through a multi-channel direct-current amplifier to a dual-beam oscilloscope, the X-sweep of which was triggered by a contact on the lathe nose-plate. The superimposed traces from up to 130 successive revolutions were photographed using a Polaroid camera. The work-piece illustrated in Fig. 3 was a laminated disk of 13 in. diameter from which a rim of yellow-poplar 0.25 in. wide was formed ahead of the cutter by an auxiliary cutter. Cuts at low speeds of 0.5 and 24 in. per min. were made on a milling machine (1) on pieces from the same disk as cut on the lathe. The moisture content was 5 per cent, cutting angle was 10 deg. and nominal chip thickness was 0.010 in. Photographs for 1,000 r.p.m. (2,700 to 3,000 ft. per min.) and 8,000 r.p.m. (23,300 to 27,200 ft. per min.) are shown in Fig. 4. Because the grain direction was diametral to the

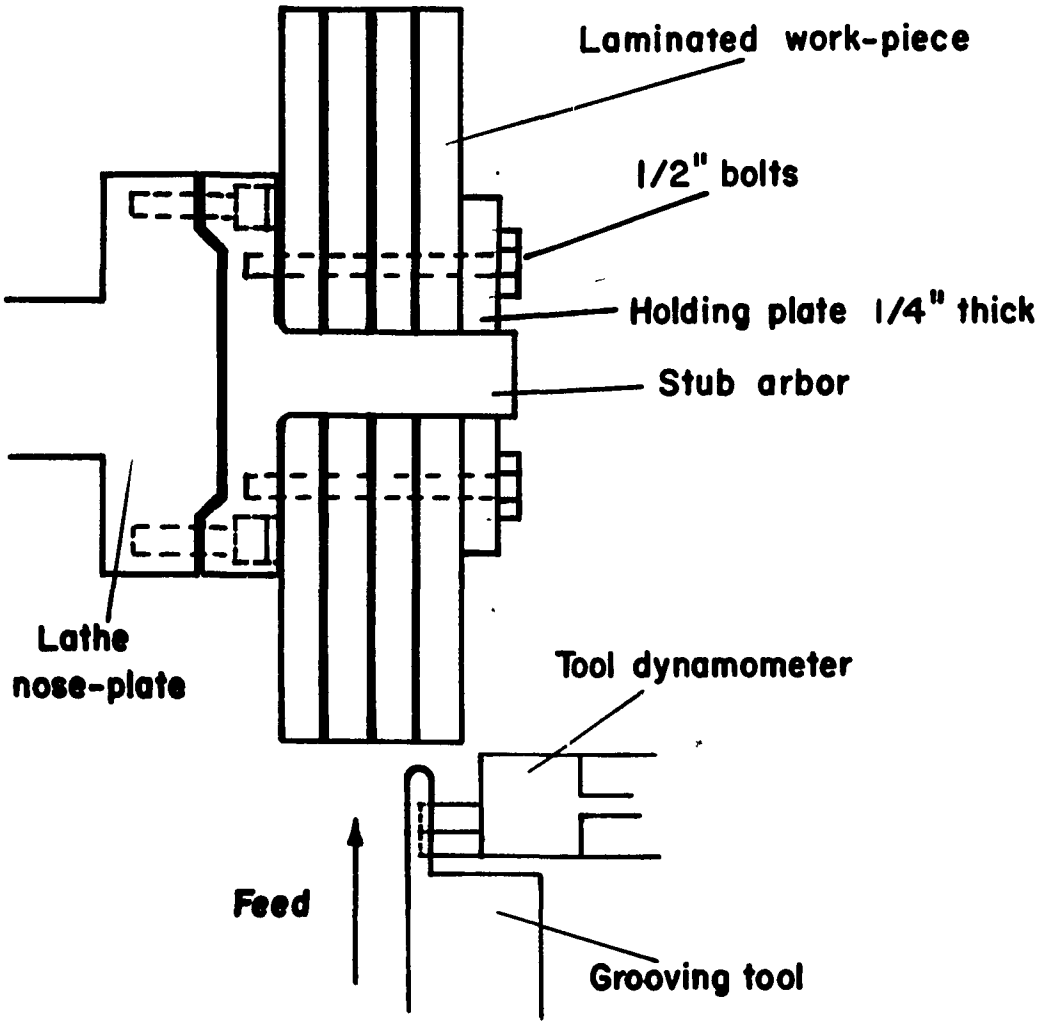
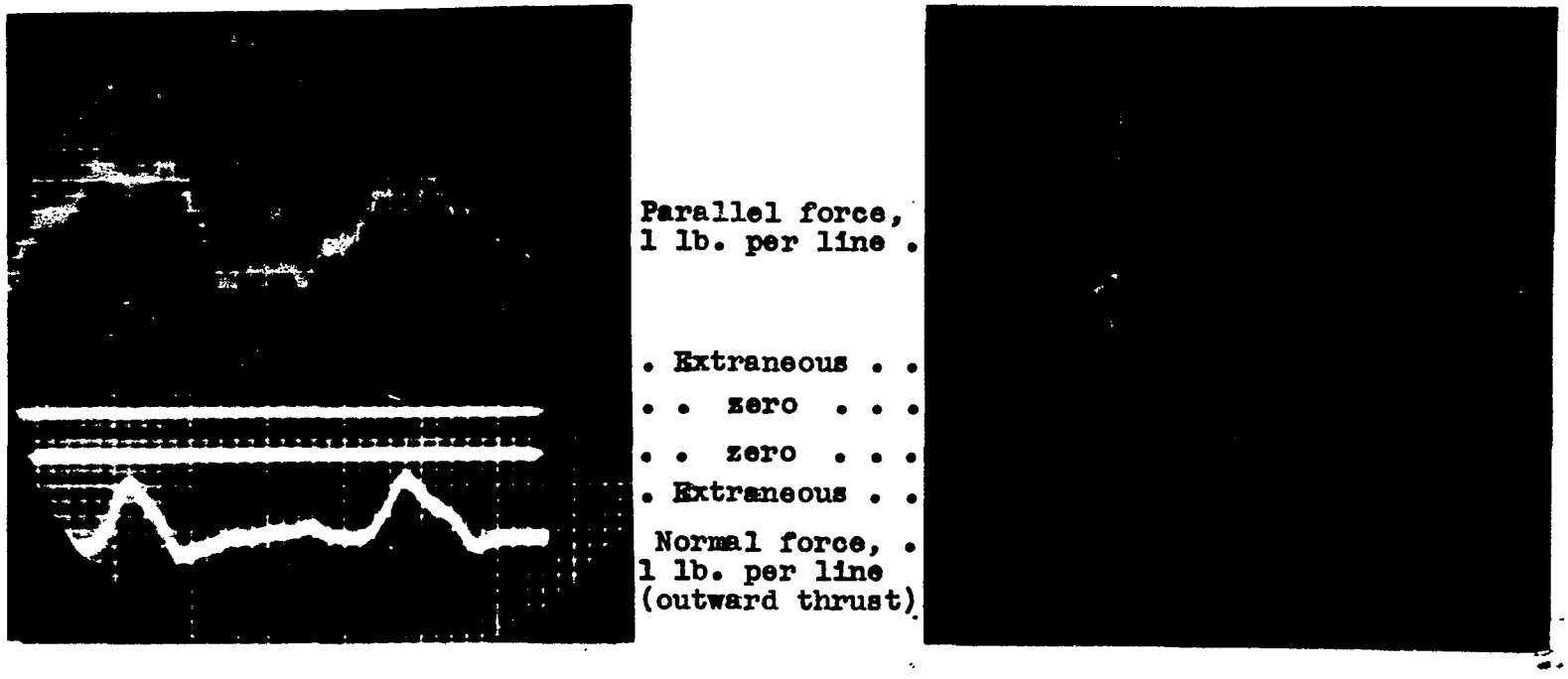


Fig. 3. Arrangement of laminated work-piece, dynamometer and grooving tool on lathe.



1,000 r.p.m. (2,700 to 3,000 ft.per min.)

8,000 r.p.m. (23,300 to 27,200 ft.per.min.)

Fig. 4. Oscilloscope records of cutting force components, in cutting on the edge of a disk of yellow-poplar at 5 per cent moisture content. Width of cut 0.25 in., cutting angle 10 deg., nominal chip thickness 0.010 in.

disk, the traces show two oscillations corresponding to a single revolution of the lathe. The amplitude of these was somewhat attenuated at the highest speeds, so that median values were taken and plotted as shown in Fig. 5, against their regression line represented by the equation

$$P_x = 13.52 + V \times 9.23 \times 10^{-5} \qquad (1)$$

in which P_x is the parallel cutting force (lb) and V is the cutting speed (ft. per min.).

Despite the smallness of the regression coefficient it was significantly different (probability level 0.05) from zero. It appears possible to explain this in terms of the energy required to reduce the speed of the chips to zero. The mean force associated with this energy is given by the equation

$$\delta P_x = \frac{btdV^2}{2g} \qquad (2)$$

where δP_x = increase in parallel force, lb.

b = width of work-piece, ft.

t = nominal chip thickness, ft.

d = density of wood, lb. per cu. ft.

V = cutting speed, ft. per sec.

g = gravity constant, ft. per sec.^{2}

For the measured density of the wood used, this equation gave an increase of 1.5 lb. for a cutting speed increase of 28,000 ft. per min., as against 2.6 lb. from the regression line. This difference was not statistically significant, and hence

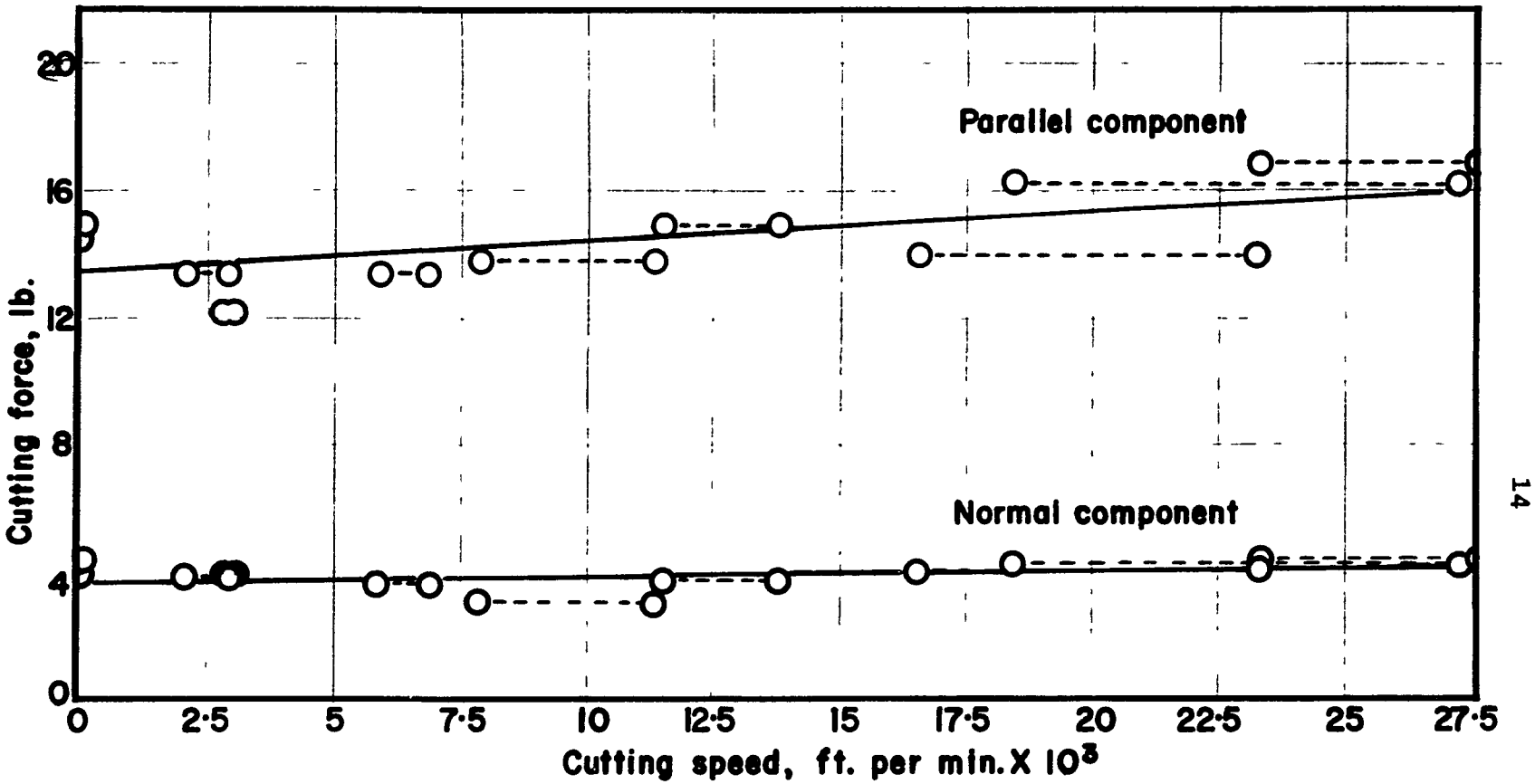


Fig. 5. The effect of cutting speed on tool forces in cutting on the edge of a disk of yellow-poplar at 5 per cent moisture content, grain direction diametral. Width of cut 0.25 in., cutting angle 10 deg., nominal chip thickness 0.010 in.

the slope of the regression line may be attributed to chip deceleration.

It was not possible to compare surfaces remaining after cutting for the full range of speeds since the hydraulic feed could not be reversed instantaneously and the final surface was formed by very light cuts. However, another lathe, with mechanical feed capable of sudden reversing, was used to form surfaces at 1,120 ft. per min., and these were indistinguishable from surfaces formed at 0.5 in. per min. In addition, study of movie film taken at 0.5 and 21 in. per min. and the flash photographs taken by Chardin (16) of saw teeth cutting at speeds of 3,600 to 10,000 ft. per min. showed very similar modes of chip formation.

CHAPTER 3

DISCUSSION

Despite the restricted cutting conditions, these results are regarded as conclusive, for there do not appear to be reasons other than chip acceleration why the effect of cutting speed should be different at other cutting angles, species and moisture contents. The theoretical implication is that the essential cutting process remains unchanged over this tremendous (300,000 - fold) range of cutting speed. In order to reconcile this result with those of Liska (7), it is necessary to postulate that his relation would not fit results at testing rates much higher than he used, and that the true relation is not logarithmic but asymptotic to a certain maximum value, occurring at some strain rate below that reached in cutting at 0.5 in. per min. with 10 deg. cutting angle. Further, if the suggestion represented by Fig. 2 is valid, these results suggest that in this range the effect of cutting speed on friction is negligible, and that the strain rate and temperature effects are exactly opposed, as might be expected if adiabatic conditions were reached at some cutting speed below 0.5 in. per min.

This leaves some doubt as to what strength values to assume in analysis of the cutting process, but it seems

probable that the values at the strain rates involved in cutting would not be much higher than the maximum obtained by Liska.

In any case it is evident that experimental or analytical results appropriate to cutting speeds as low as 0.5 in. per min. may be applied to cutting at and above normal working speeds. In light of this, it was concluded that cutting speed could be validly ignored in studying the orthogonal cutting situation.

PART II

THE GENERAL ORTHOGONAL CUTTING SITUATION IN WOOD

CHAPTER 4

THE ANISOTROPY OF WOOD

As applied to metals, orthogonal cutting is regarded as a plane problem in mechanics. Because of the anisotropy of wood, this is not the general case, but holds only when one of the axes of symmetry is parallel to the cutting edge. In the general situation in wood, in which the grain direction is arbitrary, it can be characterized completely and briefly as follows. If wood is considered to be orthotropic, with the longitudinal (L), tangential (T) and radial (R) directions mutually orthogonal, then the cutting situation is represented by the direction angles of the cutter edge and the velocity vector relative to these three axes (See Fig. 6). For instance, the rotary veneer cutting situation is given by

	L	T	R
Cutter edge	0°	90°	90°
Velocity vector	90°	0°	90°

If, as is often possible, the difference in properties in the tangential and radial directions is ignored,

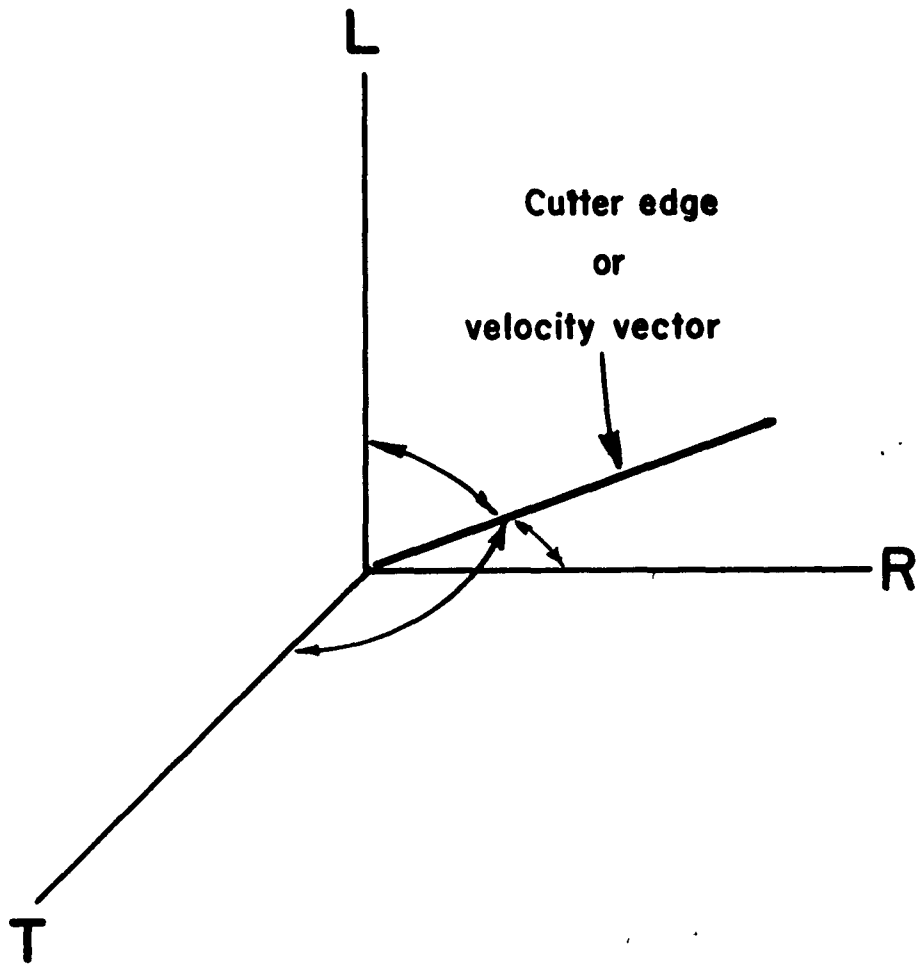


Fig. 6. Specification of the general three-dimensional cutting situation.

the notation is much simplified. The cutting situation may then be represented by giving the angles made respectively by the cutter edge and the velocity vector with the longitudinal or grain direction. Thus rotary veneer cutting, the example cited above, would have the simple notation 0°-90°, which gives the angles made respectively by the cutter edge and velocity vector with the grain direction. Other important cutting situations are 90°-0°, typifying the planing cut, and 90°-90°, typifying the action of the front edge of a ripsaw tooth. These are illustrated in Fig. 7.

Prior to considering the cutting process analytically, it is necessary to define some terms that will be used.

"Failure" of the wood at a certain point will be considered to have occurred when the combined stresses at the point have reached the maximum that the wood can sustain.

More than one failure may occur before a chip becomes separated from the work-piece, and a particular pattern of failures will be called for convenience, a "failure type".

A complete analysis would provide a continuous relationship between the stresses in the region of the cutter, the cutting force and the distance advanced by the cutter, enabling the instant and location of failure to be readily predicted. In considering the possibility of attaining such a solution, it is to be noted that Norris (17) has provided a strength criterion for orthotropic materials under combined stresses, based on and similar to the von Mises criterion for

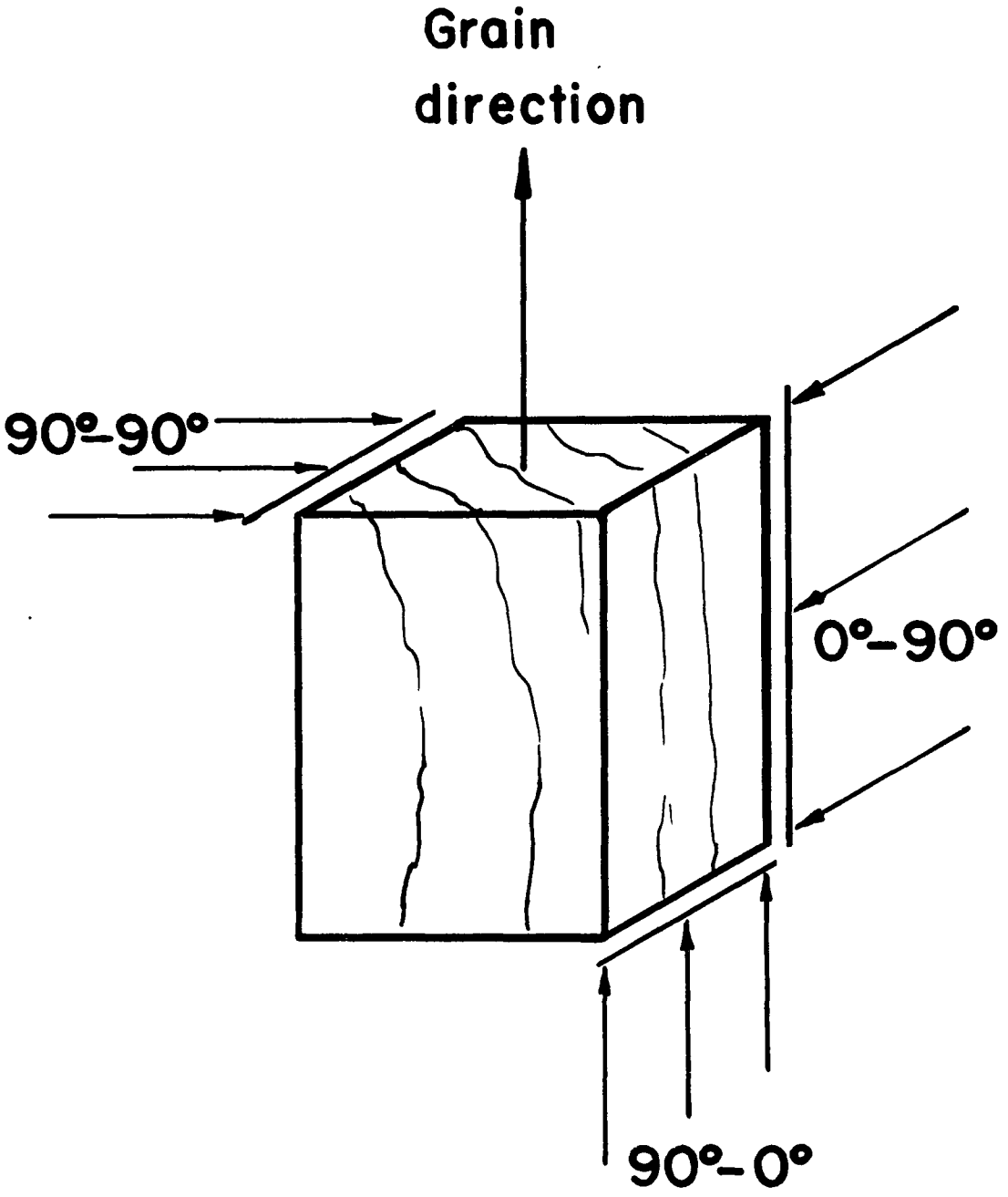


Fig. 7. The three main cutting directions, specified with respect to the grain direction.

isotropic materials, and has applied it to wood under very simple loading, with moderate success. However, the common difficulty of finding an analytical solution for the stresses satisfying boundary conditions is magnified in the case of cutting wood for the following reasons.

(1) If the cutter edge is considered as being ideally sharp, elasticity theory cannot be used directly since it calls for infinite stresses and immediate failure at first contact of the edge. Theory of plasticity is not appropriate to wood, since its behaviour does not approach ideal plasticity and in any case no solution is at present available for highly anisotropic materials.

(2) If the edge is considered to have a finite radius, so that elasticity theory can in principle be applied, the problem is highly intricate, since the boundaries are complicated, and the boundary conditions at the cutter difficult to establish. Numerical methods such as relaxation are inapplicable because the work-piece is considered to be semi-infinite.

(3) The general cutting situation is a three-dimensional problem.

(4) In any case, the more exact methods can be applied only to the situation before the first failure occurs to introduce further complication, and the first failure is not necessarily associated with maximum forces or with final chip and surface form.

It was therefore apparent that existing methods in

analytical mechanics did not provide a basis for obtaining a complete solution for the problem of orthogonal cutting in wood even if the situation were simplified by choosing one of the main cutting situations illustrated in Fig. 7. Nevertheless, it was evident that there were important factors affecting cutting in all directions with respect to the grain. Therefore it was decided to seek a more restricted analysis for a particular cutting direction, and to investigate the effects of other important factors in the hope of eliciting principles that might be applied to other cutting directions. Since the problem was too complex to be attacked from first principles, it appeared necessary to define it in terms of what was observed to occur under a range of conditions.

In choosing a cutting situation for investigation, it was noted that those associated with planing and veneer cutting had received some attention (1) (3) (18), whereas there had been little fundamental study of the action of a ripsaw tooth, which is of great practical importance. Further, the need for a critical examination of the 90°-90° cutting situation follows from the point made by Antoine (19) that cutting in this situation requires the wood to fail in its strongest direction. Therefore an intensive study of cutting at 90°-90° was undertaken.

PART III

PRELIMINARY INVESTIGATION OF THE 90°-90° CUTTING SITUATION

CHAPTER 5

INITIAL OBSERVATIONS

(a) Methods

The 90°-90° cutting situation is sketched in Fig. 8. In order to define the problem to be analysed more clearly, some preliminary observations were made of orthogonal cutting at 0.5 in. per min. using the equipment described earlier in connection with slow-speed cutting studies. A stereo microscope was used to view the cutting at up to 60 magnifications through plate glass bolted to the wood specimen, with the cutter carefully ground on the end to form a good corner against the glass. This prevented the fibres from being pushed outward and resulted in a more realistic view of the deformations in the vicinity of the cutting edge. Still and movie photographs were taken to record the various failure modes, and rough cutting force values were obtained. The most important variables involved were considered to be species properties, moisture content, cutting angle (α, Fig. 8) and chip thickness (t). The species used in this preliminary study covered a wide density range and included

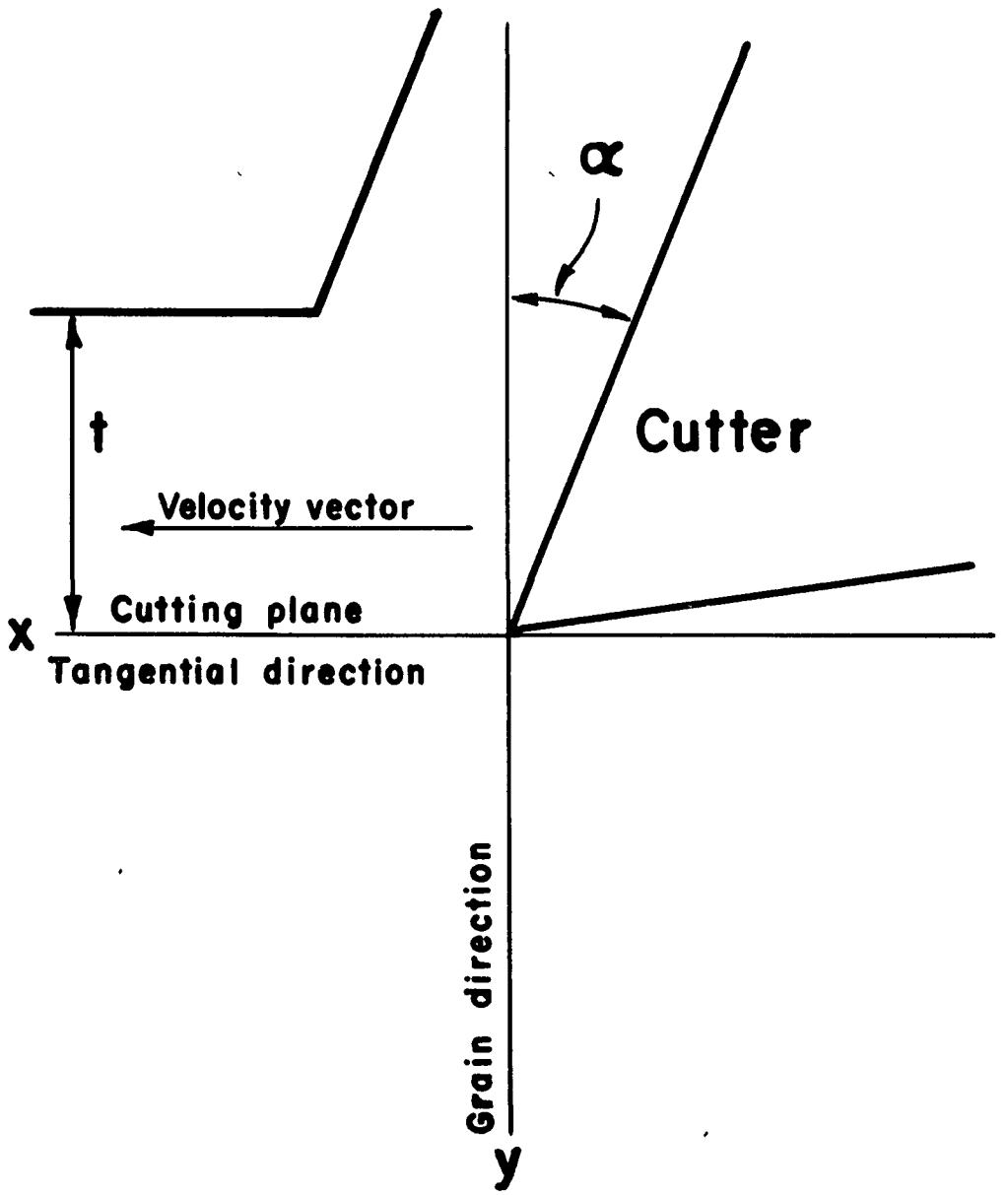


Fig. 8. The 90°-90° cutting situation.

eastern white pine (Pinus strobus), yellow-poplar (Liriodendron tulipifera), sugar maple (Acer saccharum) and common persimmon (Diospyros virginiana). They were cut saturated and at 5 per cent moisture content, using cutting angles of 5, 30 and 40 deg. and nominal chip thicknesses of 0.005, 0.010, 0.030 and 0.070 in. The pristine sharpness of the cutters was removed by a few preliminary cuts. The original end surfaces were prepared by deep sanding to remove sawing effects, followed by trimming cuts of 0.002 in. and the chip thicknesses given above were taken in ascending order, so that the surface for the first cut at each chip thickness was prepared by cutting at a lower one. Two or more successive cuts were taken at each chip thickness. Later, for checking analytical results more closely, cuts at cutting angles of 20, 30 and 40 deg. and nominal chip thicknesses of 0.010, 0.030 and 0.070 in. were made in specimens for which the mechanical properties were known from tests on matched material. The species were sugar pine (Pinus lambertiana), yellow birch (Betula allheganiensis) and white ash (Fraxinus americana). Specimens were cut at two moisture contents, 4 per cent and saturated.

(b) Failure Types

At a cutting angle of 5 deg. and at a chip thickness of 0.005 in. failure tended to occur either by shear parallel to the grain so that the fibres were not always cut at the edge, but were bent before the cutter, and eventually removed by attrition, or by irregular crumbling. Examples of these

irregular types of failure are illustrated in Fig. 9. For cutting angles larger than 20 deg. and chip thicknesses over 0.010 in., where incision by the edge was an essential phase of the cutting process, regular failure types could be recognized, the transition values being dependent on such factors as species and moisture content. Four types of failure were recognized for this regular region, but it was found convenient for analytical and practical purposes to consider only two major types with two sub-types in each, as described below.

Type I Failure (Repetitive) Figs. 10 and 11

The distinguishing feature of this type is that, after the first cut, the average cutting forces are essentially the same for successive cuts. Splits occur along the grain below the cutting plane. In type I(a) these may be short and regular (Fig. 10), associated with small wave-length and amplitude of the recorded cutting forces and comparatively high surface quality. In type I(b), (Fig. 11), two, three or sometimes more short splits may occur between fairly regularly spaced longer splits which detract from the surface quality. In both cases, after the first cut, the spacing and length of the split remains essentially the same, accounting for the regularity of the average cutting forces in successive cuts.

Above the cutting plane, each sub-chip is formed by shear along the grain simultaneously as a split forms below. In cuts after the first, the sub-chips are loosely

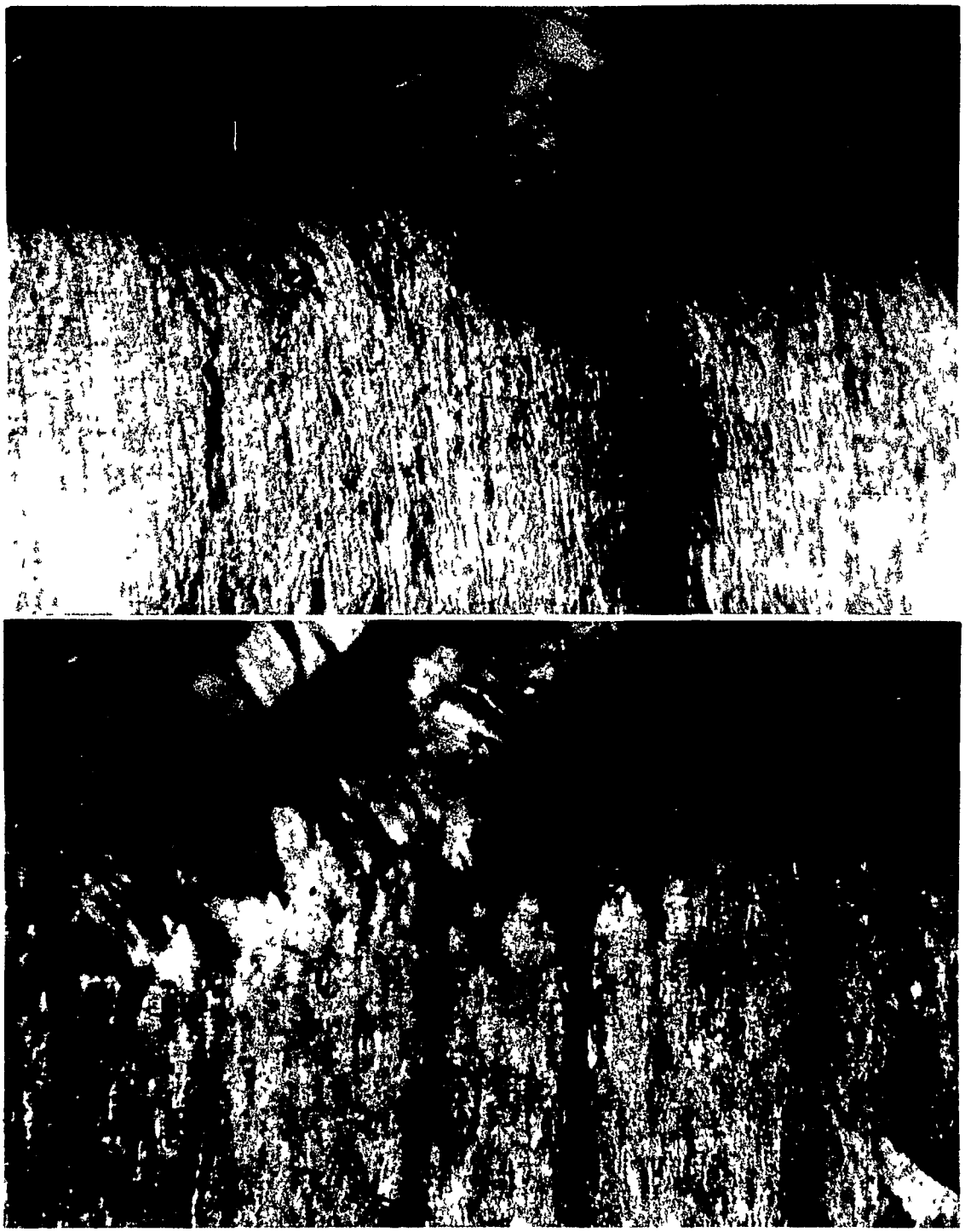


Fig. 9(a). Irregular failure types; x 30.
Top: Eastern white pine at 5 per cent moisture content, with 30 deg. cutting angle, 0.005 in. nominal chip thickness.
Bottom: Common persimmon at 5 per cent moisture content, with 40 deg. cutting angle and 0.005 in. nominal chip thickness.

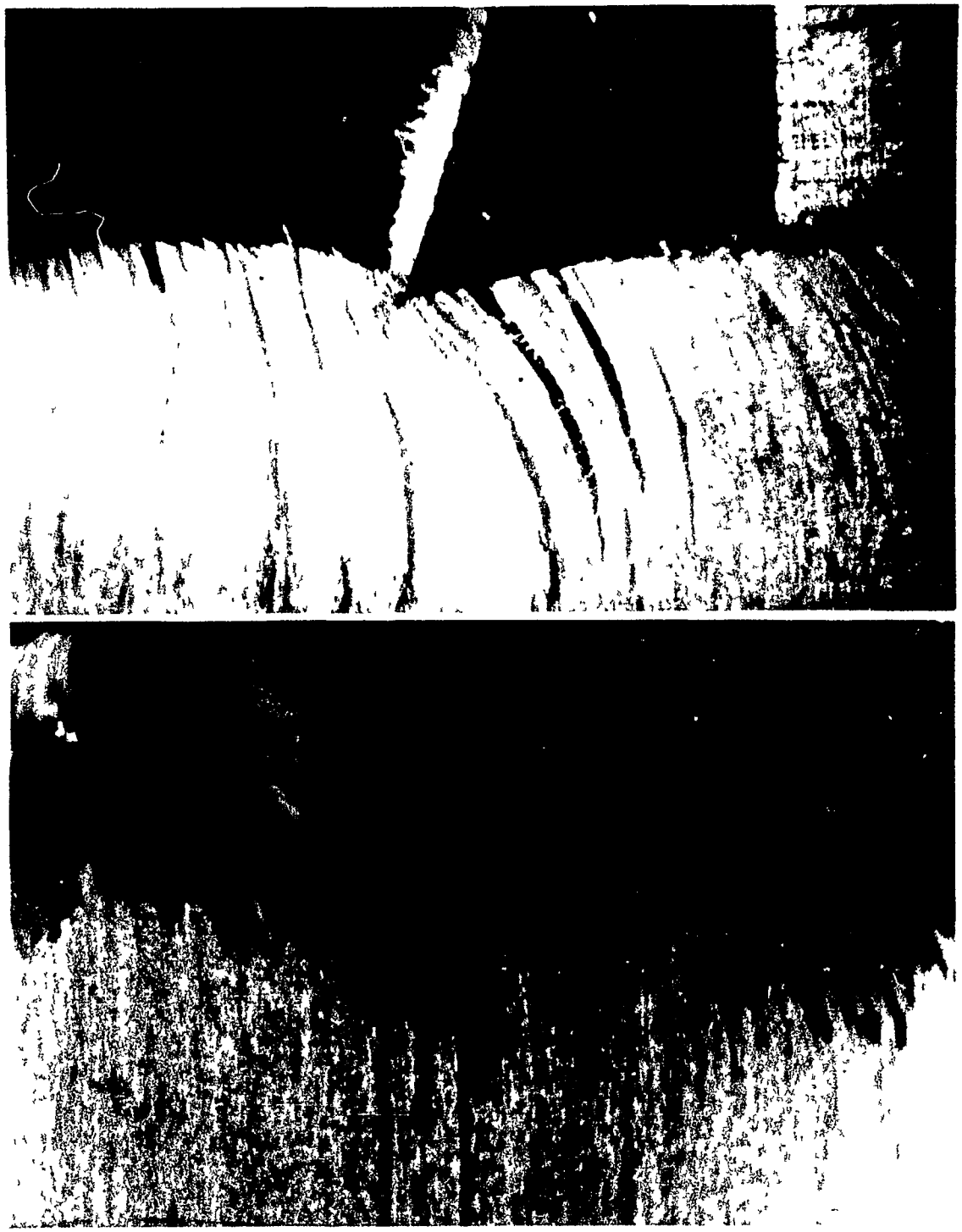


Fig. 9(b). Irregular failure types; x 10.
Top: Eastern white pine, saturated. Cutting angle 20 deg., nominal chip thickness 0.030 in.
Bottom: Eastern white pine at 5 per cent moisture content, cutting angle 5 deg., nominal chip thickness 0.030 in.

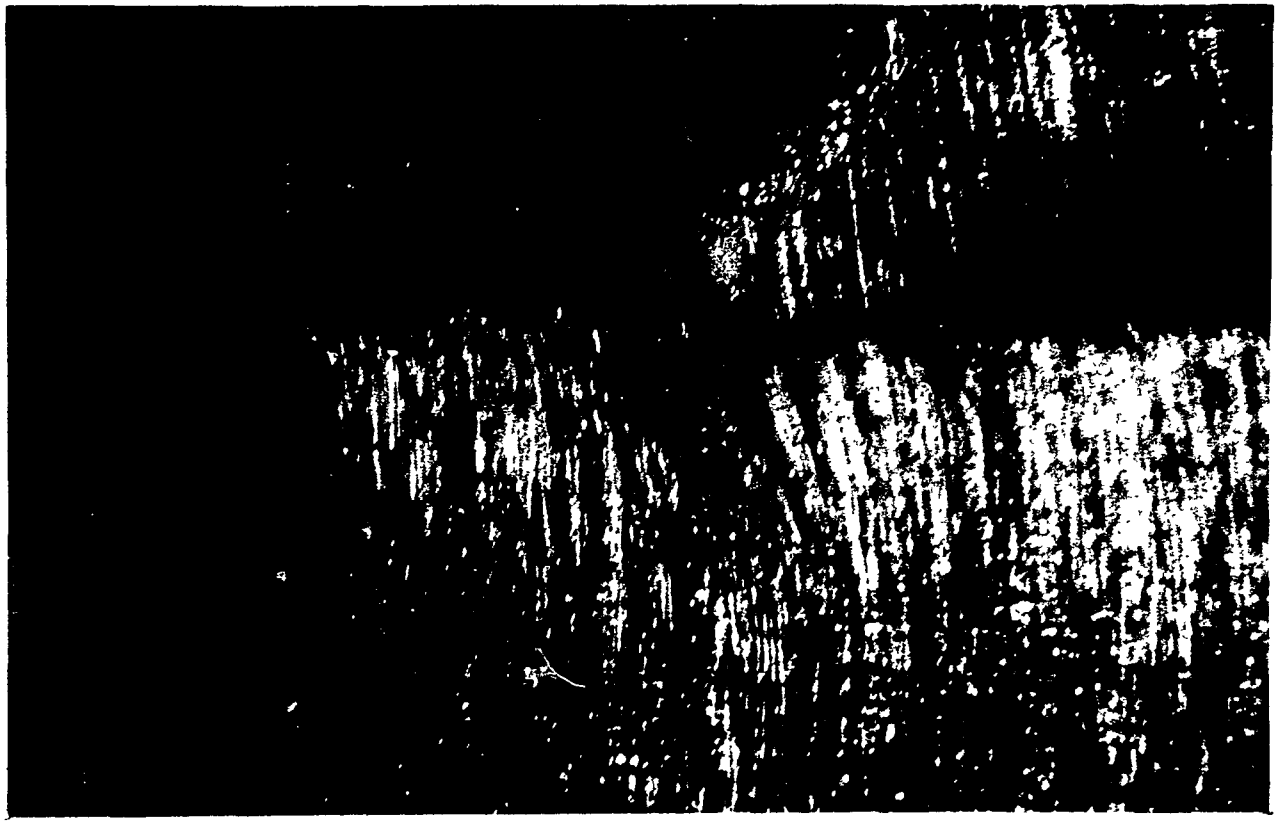


Fig. 10. Type I(a) failure in saturated eastern white pine. Cutting angle 40 deg., nominal chip thickness 0.010 in.

x 30

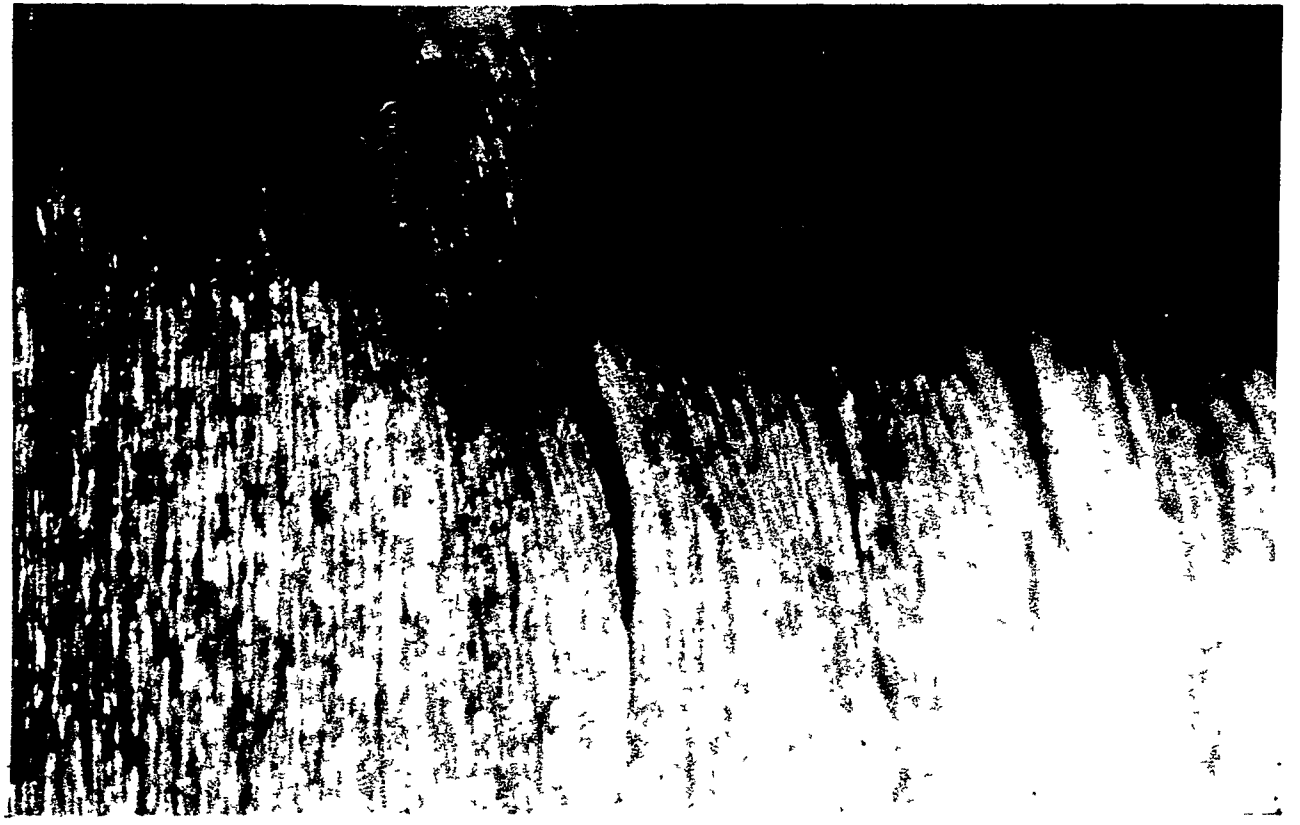


Fig. 11. Type I(b) failure in eastern white pine at 5 per cent moisture content. Cutting angle 30 deg., nominal chip thickness 0.030 in.

x 30

linked continuously in type I(a), but in type I(b) they are in groups corresponding to the spacing of the major splits.

Type II Failure (Cyclic) Figs. 12 and 13

This failure type is associated with a cyclic variation of average cutting forces with successive cuts. Failures occur in a plane perpendicular to the grain (parallel to the cutting plane), at a variable distance below it. They may be intermittent (type II(a), Fig. 12) or continuous (type II(b), Fig. 13). In type II(a) this failure is accompanied by severance at the cutting plane and shear above, forming sub-chips, so that the broken end of the lamina remains in place to be removed by the next one or two cuts. In type II(b) (Fig. 13) severance occurs continuously at the cutting plane. The chip above the cutting plane may be sheared into sub-chips or remain intact so that two practically continuous chips are formed, one above and one below the cutting plane, as in Fig. 13. Under certain conditions there occur transitions between failure types II(a) and II(b), and an example of such a transition in sugar maple is illustrated in Fig. 14. This is taken as evidence that there is no discontinuity in the conditions governing the two types of failure. In both types depending on the continuity and distance below the cutting plane of the failure, various types of cyclic variation occur in the average cutting forces in successive cuts. For instance there may be no contact with wood in one or two successive passes of the cutter after the first, then a gradual return to a condition similar to

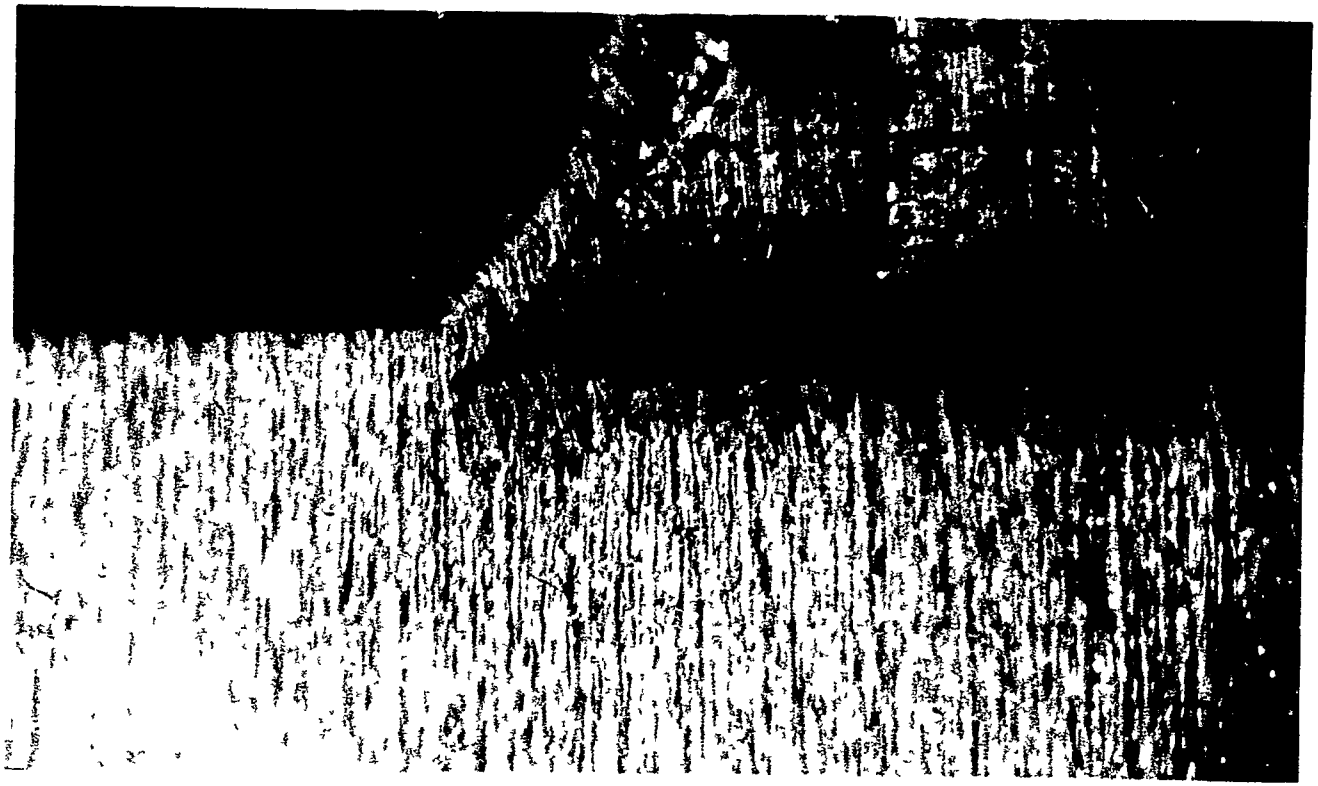


Fig. 12. Type II(a) failure in yellow-poplar at 5 percent moisture content. Cutting angle 40 deg., nominal chip thickness 0.030 in.

x 10

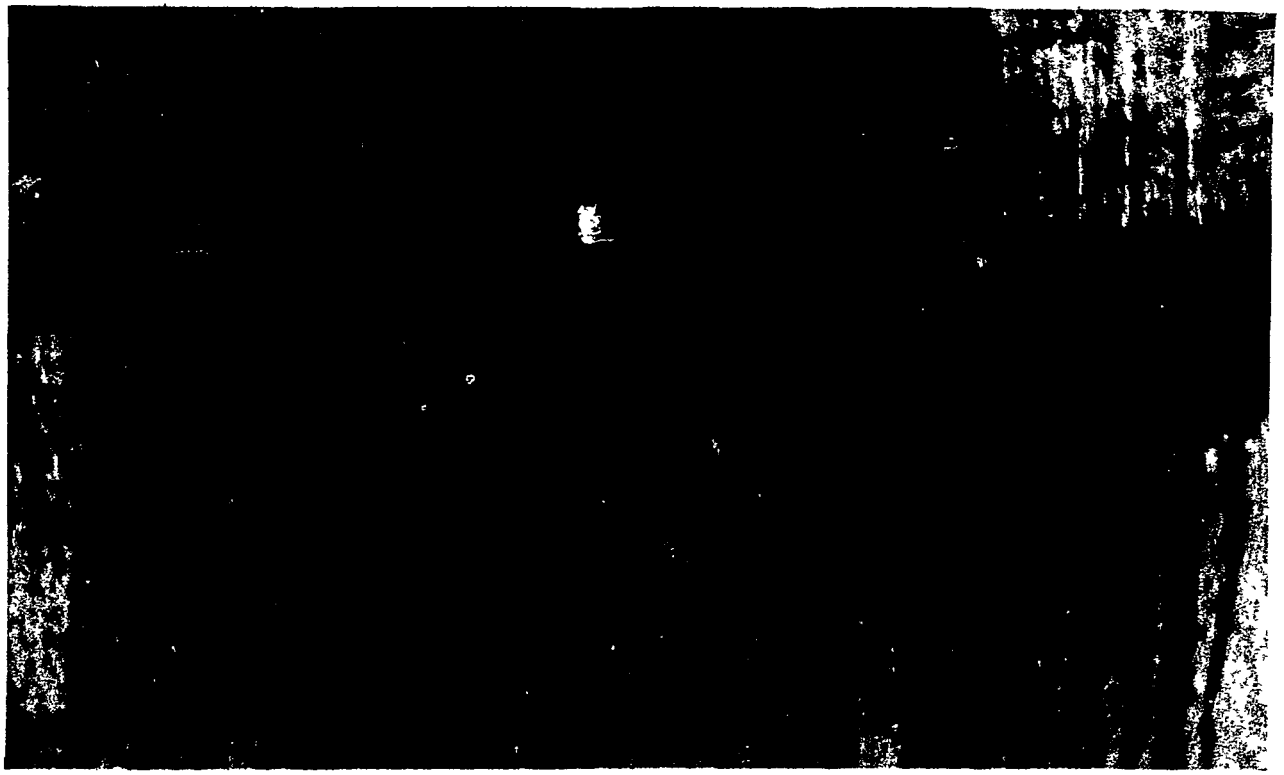


Fig. 13. Type II(b) failure in common persimmon at 5 per cent moisture content. Cutting angle 40 deg., nominal chip thickness 0.030 in.

x 10



Fig. 14. Transition from type I(a), through types I(b) and II(a), to type II(b) failure in sugar maple at 5 per cent moisture content, as cutter emerges from a zone lubricated with oil.

that of the first cut, after which the cycle repeats itself. (See Fig. 15). Both of these failure types result in a very poor surface, and cutting efficiency is low since the load on the cutter in successive cuts varies greatly, and in some passes there would be rubbing rather than cutting. Naturally there occur transitions between failure types I and II, and under certain conditions both types may occur in the one work-piece due to a variation in properties from point to point.

(c) Summary of Effects

All of the variables chosen were influential and the various effects will now be discussed in terms of the failure types described, for the higher cutting angles.

With increasing species density the failure tended to vary from type I(a) through type II(b), and cutting forces increased.

Moisture content had a great effect. In saturated wood the predominant failure type was I(a) with slight splitting, and low steady cutting forces. This was in marked contrast to the cutting at 5 per cent moisture content, for which failures below the cutting plane were always deeper than the nominal chip thickness, and the predominant failure type was type II. Cutting forces were high and the normal force, especially, showed oscillation.

At very high cutting angles failure tended to be either type I or type II(b) depending on moisture content and density, severance at the cutting edge producing a

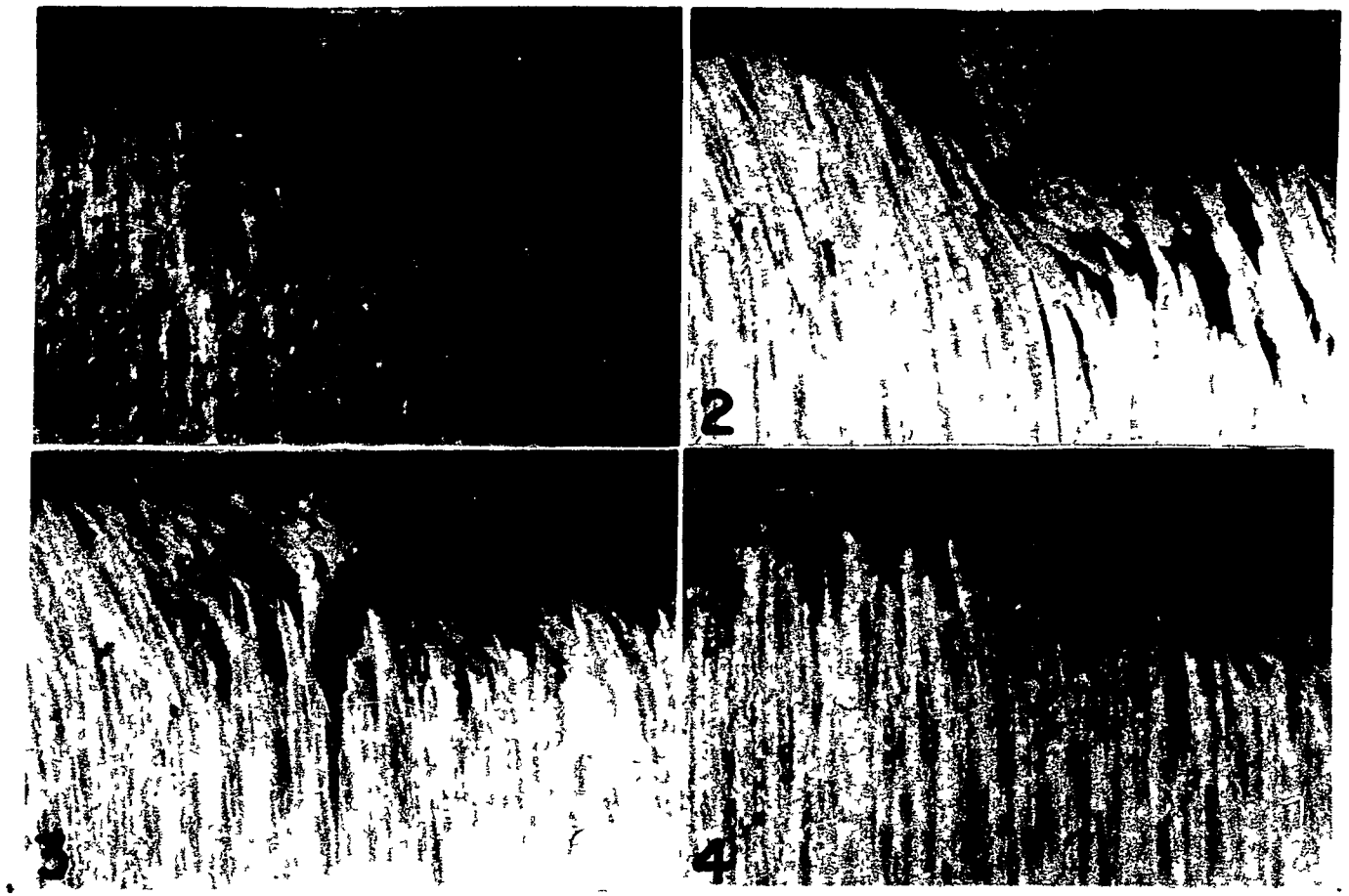


Fig. 15. Sequence of four cuts in sugar maple at 8 per cent, associated with type II(a) failure. Cutting angle 30 deg., nominal chip thickness 0.030 in.

x15

continuous chip in either case. Cutting force increased and the normal force on the cutter changed from negative (into the work) to positive (away from the work) with decreasing cutting angle. At cutting angles below about 20 deg. irregular types of failure developed.

With increasing chip thickness the usual trend appeared to be from type I(a) through I(b) for all saturated woods, and low to medium-density species, and from a crumbling action to type II(b) in dense species at 5 per cent moisture content.

This brief study of observed effects served as a guide to what was required of an analytical model on which to base predictions concerning the effects of the various factors, when cutting in or near the 90°-90° cutting situation. Since type I failure was associated with a better finished surface and more efficient cutting, it was considered that the principal purpose of an analytical model should be to aid in predicting the probable occurrence of the two failure types and the associated cutting forces, for a given set of cutting conditions and wood properties.

(d) Zones of Failure

The incidence of the two failure types depends on the order in which the stresses reach the ultimate strength of the wood in the various zones where failure may occur. The zones where failure may appear are indicated in Fig. 16. For the range of conditions under consideration, they are:-

(1) At the edge of the cutter. In the first cut,

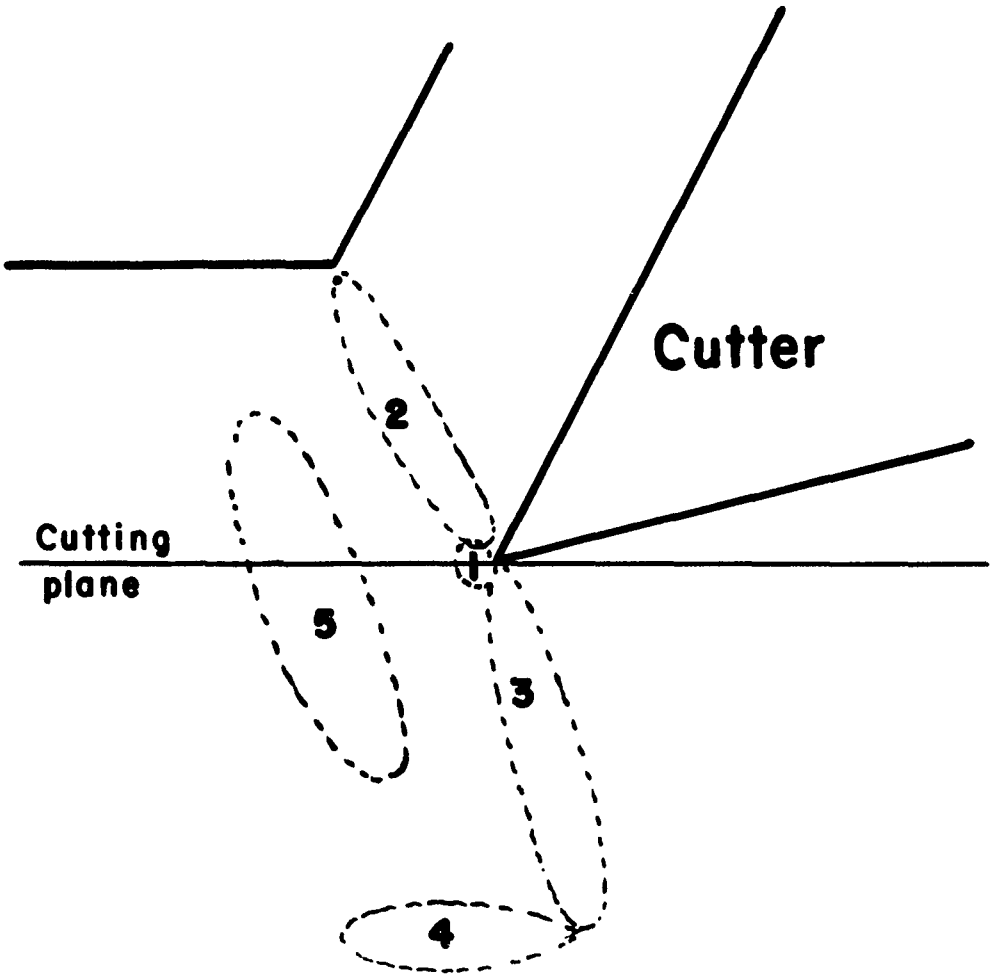


Fig. 16. Zones of failure in 90°-90° cutting.

under the restricted range of conditions, this is inevitable.

(2) In a zone containing the cutting edge and running along the grain up to the surface of the workpiece.

(3) In a plane containing the edge and the longitudinal axis, below the cutting edge. This failure always occurred in the preliminary experiment and might always be expected under practical conditions, where the edge is not ideally sharp and the cutting angle cannot be very great.

(4) In a zone parallel to the cutting plane, and a distance below it of the same order of magnitude as the nominal chip thickness. Failure may be intermittent or continuous.

The essential problem is to estimate the forces associated with each of these failures as the cutter advances, in order to predict the sequence in which they may occur, and hence whether certain failures may occur before those necessary to separate the chip. In the present context, failures in zones (1) and (2) are considered necessary to separate the chip, and the question is whether failures in zones (3) and (4) occur before separation. (Outside the considered range of conditions, failures in zones (3) and (4), rather than (1) and (2), could be associated with chip separation).

The obstacles to the application of exact analytical methods, even to the situation before the first

failure, were discussed earlier in regard to the general cutting situation, and apply equally to the one under consideration. In view of this, resort must be had to approximate or empirical methods, in order to relate cutting forces to the stresses in zones of interest.

CHAPTER 6

SHEAR ABOVE THE CUTTING PLANE - VOSKRESENSKI'S ANALYSIS

The only reported attempts to analyse the 90°-90° cutting situation are described by Voskresenski (6), beginning with the work of Time and Deshevoi, from which he developed his own analysis. This will be discussed as part of the development of the subject.

In order to separate analytically the effects of the face of the cutter, and of an edge of finite radius, the cutter may, in the first instance, be considered as being ideally sharp. (To be rigorous, ideal sharpness could be defined to mean that the mean radius of the edge is of atomic order of magnitude). In this case, the force required for the edge to penetrate and sever a cell wall, and the deflection due to this action, become negligibly small. Then if the chip were sufficiently flexible (for instance, very thin) it could be removed continuously without further failure, but normally it yields or fails in a surface running in the deflected grain direction from the edge up to the surface of the work-piece. If this yielding or failure is assumed to be in shear unaffected by normal or bending stresses across this surface, and the latter is assumed to be a plane at an angle ϕ to the cutting plane, (Fig. 17) then

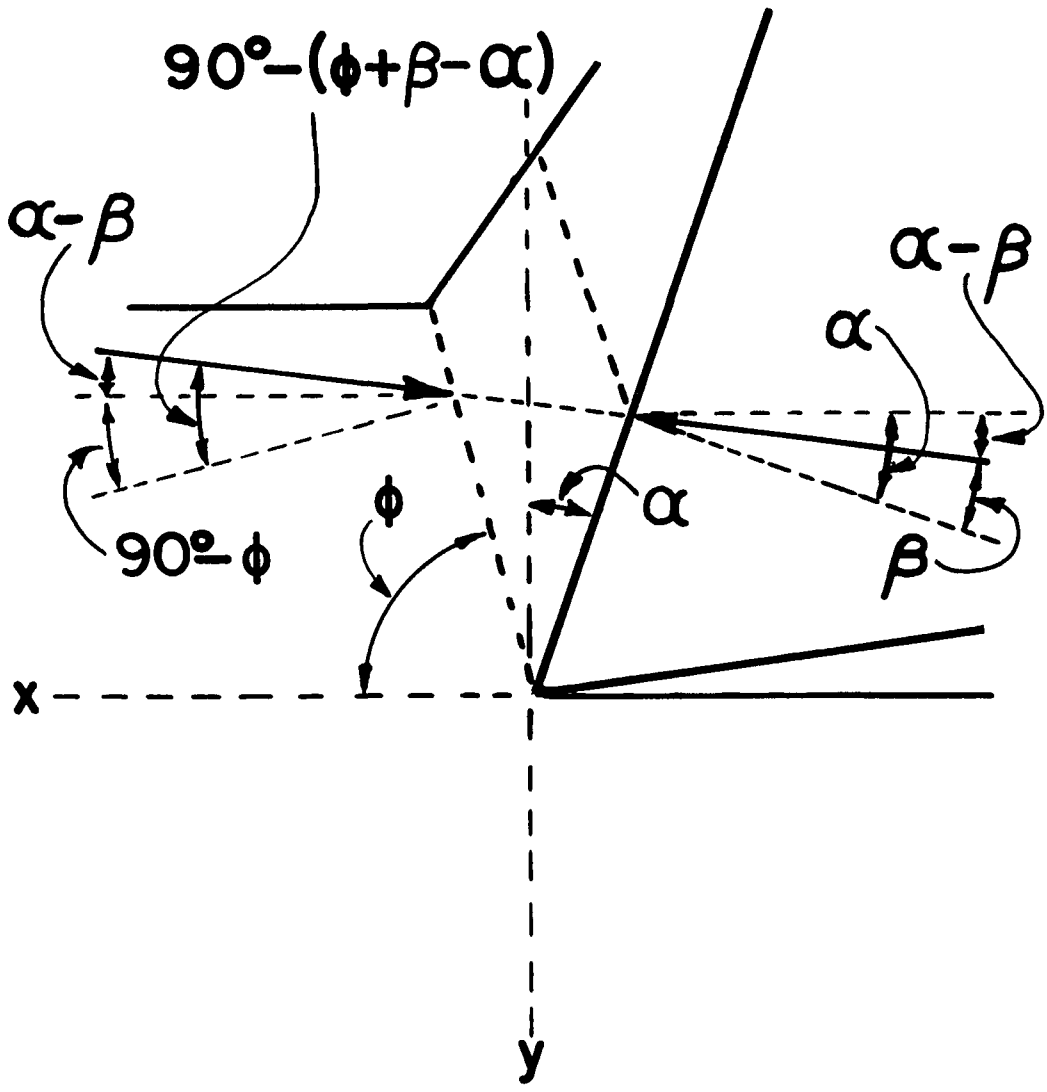


Fig. 17. Diagram for deriving friction angle at the shear plane.

the equation familiar in metal cutting research (20) may be applied. The force component (P_x) parallel to the velocity vector or x axis is given by :-

$$P_x = \frac{\tau_o b t \cos(\beta - \alpha)}{\sin\phi \cos(\phi + \beta - \alpha)} \qquad (3)$$

where

τ_o = shear stress at failure, p.s.i.

β = friction angle = arctan μ

α = cutting angle

ϕ = angle between x axis and the shear plane

b = width of work-piece

t = nominal chip thickness

The normal force component (P_y) is related to P_x by

$$P_y = P_x \tan(\beta - \alpha) \qquad (4)$$

In order to assess the extent to which shear failure accounts for the cutting forces, these equations were applied to the conditions of the cutting tests described earlier. Values for the shear angle ϕ were obtained by measurement made on photographs, and friction values were obtained from cutting tests (Franz (1)) in the case of the matched material, and from Kollmann (9) in the case of the preliminary tests. The theoretical values are compared with observed values in Table 1.

It is evident from Table 1 that especially for the matched material, the calculated force components were considerably below the observed values. This might

TABLE 1

COMPARISON OF OBSERVED CUTTING FORCES WITH VALUES COMPUTED FROM EQUATIONS (3) AND (4)

Width of work-piece 0.25 in., nominal chip thickness 0.030 in.

Species	Moisture Content	Cutting Angle, deg.	Parallel Force, lb.			Normal Force, lb.		Failure Type
			Calc.	Observ.		Calc.	Observ.	
				Min.	Max.			
Eastern white pine *	Sat.	40	14	18	20	-3.2	-2.5	I(a)
	5%	"	23	25	34	-5.3	-6.5	I(b)-II(a)
Yellow-poplar *	Sat.	"	17	22	24	-3.9	-1.8	I(a)
	5%	"	31	27	33	-7.2	-7.0	II(a)
Sugar maple *	Sat.	"	36	36	40	-7.4	-6.8	I(a)
	5%	"	60	80	100	-13.9	-5.0	II
Sugar pine +	Sat.	40	11	15	19	-1.0	-3.8	I(a)
	4%	30	25	40	43	-4.8	-5.0	I(a)
	"	40	23	30	35	-6.3	-7.3	I(b)
Yellow birch +	Sat.	30	15	40	44	-1.1	-4.7	I(a)
	"	40	14	26	31	-3.7	-8.7	I(a)
	4%	30	67	106	116	-7.1	-10.0	I(b)
	"	40	44	69	78	-12.6	-19	I
White ash +	Sat.	30	19	39	43	-2.3	-4.6	I(a)
	"	40	18	26	29	-5.5	-8.3	I(a)
	4%	30	40	79	88	-4.1	+12.0	II(b)
	"	40	30	44	67	-6.9	-2.7	II

* Mechanical properties used were mean values for species

+ Mechanical properties used were obtained from matched material

conceivably be explained on the basis of increased strength associated with high strain rates as discussed in Part I, and the possibility is not eliminated by what follows, but this explanation was rejected for the time being, in order to follow up other possible explanations suggested by the preliminary observations. But before discussing these, it is relevant at this point to refer to the solution of Voskresenski (6). He associates the maximum cutting forces with shear failure above the cutting plane and gives an equation for P_x embodying equation (3), with three additional terms which appear to be introduced to account for the discrepancy noted above. One of these is represented by the equation

$$\frac{P_y}{P_x} = \tan(\beta - \alpha) + \delta$$

Here δ is a term intended to represent an increase in P_y due to a tendency for the chip to expand in the y direction under compression in the x direction, which is restrained by the work-piece on the lower side. If this were valid it appears that δ should be equal to Poisson's ratio, which in this case is about 0.03 (12). This is close to the value for δ given by Voskresenski. However, it is difficult to see that this concept is valid, because the chip is not, in fact, restrained from expanding upwards, except possibly at the cutter face, where the frictional resistance is fully accounted for by the use of $\beta = \arctan \mu$. The only possible effect is an increase of the chip thickness t by approximately

3 per cent.

The second term tending to increase the cutting force is a friction component at the shear plane, acting in addition to the shear resistance of the wood both before and after failure. The difficulty introduced here is that the analysis is based on equilibrium of the chip as a particle, ignoring moment equilibrium. In this case it has been shown (20), and is evident from Fig. 17, that for given values of β and ϕ, the friction coefficient at the shear plane is a fixed value given by

$$\arctan \mu_s = \beta_s = \frac{1}{\tan(\phi+\beta-\alpha)} \qquad (5)$$

Therefore, unless a more complex analysis, treating the chip as a rigid body and involving moment equilibrium, is considered, the introduction of an arbitrary value of β_s is not strictly valid. This objection is overcome in Voskresenski's analysis by allowing ϕ to be variable. This means that the shear plane may rotate so that equilibrium conditions are met at the point of chip separation.

But ϕ is thus fixed for any given value of β_s, as equation (5) shows, and hence, from equation (3), P_x is also fixed. The cutting force is then dependent only on the shear strength, and the coefficients of friction at the shear plane and at the face of the cutter. From equations (3) and (5)

$$P_x = \frac{\tau_o\, b\, t \cos(\beta-\alpha)}{\cos(\beta_s+\beta-\alpha)\sin\beta_s}. \qquad (6)$$

Since cos ($\beta_s + \beta - \alpha$) and cos ($\beta - \alpha$) are approximately equal to 1, it is seen that P_x will be inversely affected by β_s, which is probably not as intended. In any case, the values for P_x calculated from equation (6) are very low, lower than those from equation (3) given in Table 1.

This problem of the effect of normal stress on the shear strength has not been satisfactorily investigated. If friction does play a part, it could be in manner similar to the Coulomb yield criterion (27) for soil, based on the postulate that slip occurs at a plane when the shear stress reaches the value

$$\tau_o = C - \sigma \tan \psi \qquad (7)$$

where C is the cohesion, σ the normal (tensile) stress on the plane and ψ a second empirical constant called the angle of internal friction. The limit theorems of plasticity have been applied (27) to obtain approximate solutions for such problems as the grouser plate of a tractor biting into the ground, but the plate was considered to be perfectly rough, and anisotropy was not involved. However, it appears that an approach of this type as an essay in the comparatively new field of plasticity theory might be fruitful in clarifying the shearing stage of cutting.

Voskresenski also introduces into his computation, without explanation, the shear strength of the wood at 45 deg. to the grain angle. This, of course, would raise his values for P_x considerably, since in the example given the value at 45 deg. is 4.3 times that for shear parallel to the

grain. Perhaps the most significant of his additional terms is the constant force P_o, added to account for the effect of an edge of finite radius. The value used in his computations was obtained experimentally by methods not explained. Voskresenski notes the special importance of the edge in cutting at 90^o-90^o, but does not attribute to it the significance which became apparent during the preliminary observations described earlier. Microscopic study of cutting in process, and interpretation of the force component recordings, suggested that maximum forces do not always occur at the instant of failure in shear along the grain. Rather, they occur before this at the end of what will be termed an indentation phase, which will now be discussed in detail.

CHAPTER 7

THE INDENTATION PHASE OF CUTTING

The term "indentation phase" refers to the penetration of the cutter into the wood, and the action of the cutter edge in the vicinity of the cutting plane. Other phases might concern failure above or below the cutting plane, accompanying or following the indentation phase.

In non-steady chip formation, such as is very common in wood cutting, two stages of indentation may be distinguished. In the first stage the wood is deflected or deformed before the edge without apparent rupture, and in the second, rupture occurs to separate the chip from the work-piece along the cutting plane. The latter stage is known to Russian workers (6) as the "incision stage" and their term will be used in this connotation. The course of the indentation phase, as it appears in the 90°-90° cutting action will now be described.

At first contact of the cutter with the side of a virgin work-piece, the wood at the cutter edge is deflected without apparent rupture. This deflection stage has usually been ignored on the assumption that a work-sharp cutting edge produces a stress intensity much in excess of the strength of the material. But observation has shown that

this stage is negligible only with very sharp cutters and high rake angles. This is understandable if the edge radius of actual cutters is compared with the thickness of typical cell walls. Values given in the literature for the edge radius of sharp cutters are 0.002 mm (6) and 0.0025 mm (21), and measurements made on the work-sharp cutters used in the present study, using a Filar eyepiece at 500x, gave values of 0.0015 to 0.0020 mm. Measurement of the double thickness of typical wood cell walls showed an approximate range of 0.002 to 0.015 mm, only one to ten times greater. Thus, normally, wood deflection becomes considerable before fibre severance commences, as is evident from Figs. 10-13. The wood immediately in front of the cutting edge is densified, frequently to the point where it appears solid and transparent, before fibre severance begins. The surfaces on either side of the edge become convex, and it is apparent from the deflection that, especially below the cutting plane, bending stresses are high. Away from the edge, the surface curvature appears greatest at a point some distance below the cutting plane, suggesting that the failures characteristic of type II are associated with a maximum in the bending stresses in this zone.

If fibre severance commences before type II failure occurs, it takes place rapidly, freeing above and below the cutting plane highly stressed zones of wood. Above the cutting plane, as fibre severance proceeds, shear failures occur in rapid succession to form sub-chips.

Below the cutting plane, as noted by Voskresenski (6), failures in the same plane as the shear failures above, appear to occur simultaneously. This is evident in Fig. 12. Only one such pair of failures above and below the cutting plane may occur before the incision stage ceases and a deflection stage commences, in which case the failure pattern is clearly of type I(a). The oscillations in the recorded forces are small and regular (Fig. 18(a)). Or, the potential energy stored up by the deflection may be such that two or three such pairs of failures occur in rapid succession before a new deflection stage commences. This is typical of type I(b) failure. In accompaniment, the parallel force component usually increases in saw tooth fashion as these failures occur (See Fig. 18(b)). The oscillation of this component is not as great as the normal component, which typically changes in a negative or downward direction during the indentation stage, and then falls in magnitude as incision commences and again slightly as each pair of failures occurs.

In type II(a) failure, the parallel component increases up to the point at which incision begins, then decreases until a deflection stage commences. The normal component usually increases from a low or negative value to positive through the deflection stage, then returns to the low level as incision occurs (Fig. 18(c)).

In type II(b) failure, the parallel component oscillates rather regularly with a long wave length, and the

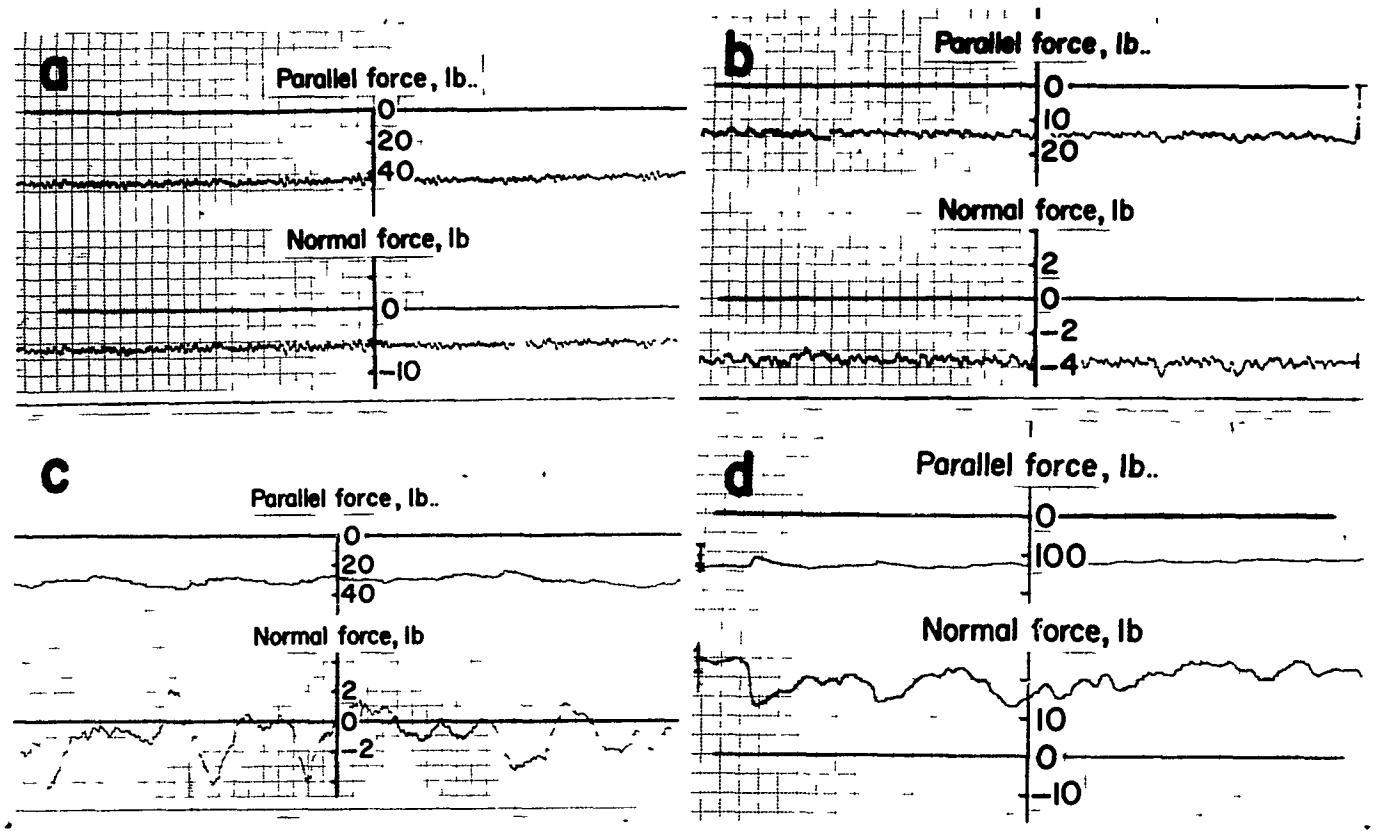


Fig. 18. Recordings of cutting force components associated with the four failure types : (a), type I(a); (b), type I(b); (c), type II(a); (d), type II(b).

normal component, which is commonly negative, oscillates in conjunction with it. This oscillation is presumably correlated with the rhythmic change in depth of the failure zone below the cutting plane which is evident in Fig. 18(d).

Table 1 shows that the minimum values of the parallel force component are yet higher than the values calculated on the basis of shear failure using equation (3). It appears that all the compression built up during the deflection stage is not lost during the incision and shear stages, and that this may be due to friction in the shear plane and at the cutter face. Some evidence concerning this is presented later. It is evident from this study of the cutting process that the indentation phase may be associated with cutting forces greatly in excess of those required to cause shear above the cutting plane to form sub-chips.

This build-up of force is not explicable in terms of elastic or plastic theory, but is a problem which is peculiar to cellular materials. It appears to involve local compression of the wood ahead of the cutting edge, often to the point where a solid transparent zone is formed. This is considered to be an unstable process, occurring as follows. Referring to Fig. 19, the first row of cell walls met by the cutter edge may be pierced or severed, if the edge is sharp enough and the cutting angle large enough, before it is deflected sufficiently to bear against the adjacent walls. In this case fibre severance and cutting are continuous. However, in the case of a cutter of normal sharpness, and with

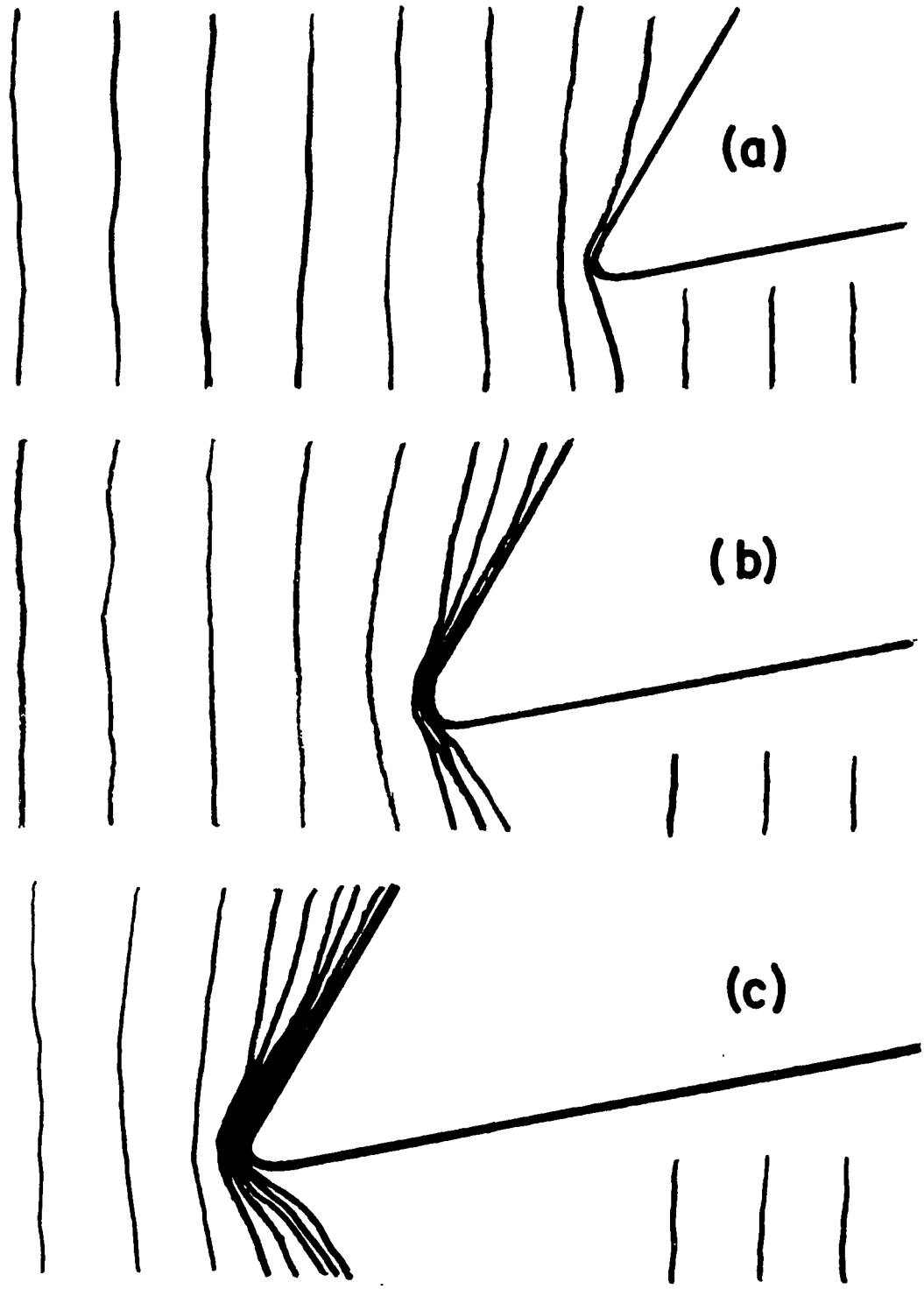


Fig. 19. Indentation by cutter edge, with deflection of cell walls.

a cutting angle within the practical range, the first row of cell walls will probably be deflected against the adjacent row, thus gaining normal and frictional resistance to penetration by the cutter edge. This increases the probability that these two sets of walls will be deflected another cell space before bearing against the next set, and gaining further support, and so on. Hence the situation is unstable, and the formation of a densified zone in front of the cutter has an effect of distributing the stress to a widening base. If type II failure does not intervene, deflection is terminated by fibre severance at the cutter edge, and the incision stage commences.

In contemplating the nature and significance of the indentation phase, thought was given to methods of modifying it, in order to reveal some of the factors involved. Brief tests involving two such methods are discussed in the following.

CHAPTER 8

THE EFFECT OF LATERAL VIBRATION ON THE INDENTATION PHASE

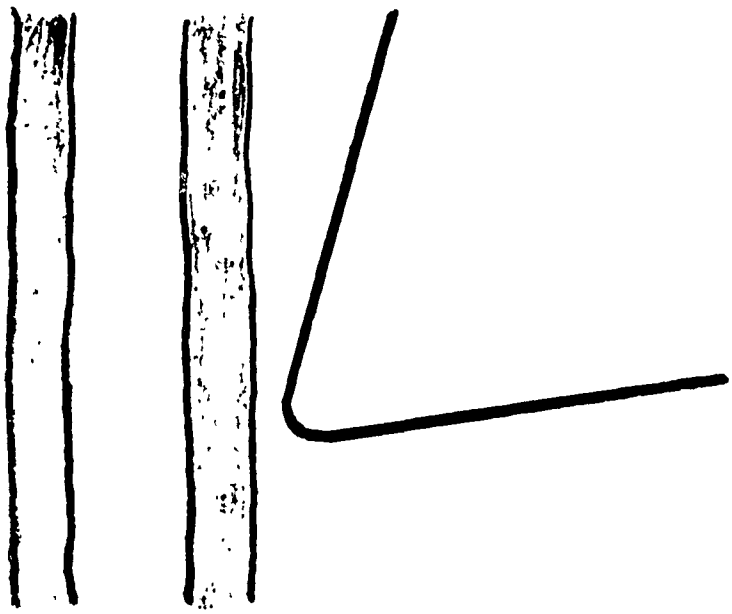
It is to be expected that a fundamental situation in the cutting of one material might have analogies in the cutting of other materials, and thought on these lines led to comparison of the 90^{o}-90^{o} situation in cutting wood with the cutting of other fibrous or cellular materials such as grass, meat and bread. These materials yield greatly before the direct advance of a cutter and develop considerable resistance to incision. Therefore, in practice, cutters for these materials are given a lateral motion or "draw" and are frequently used with a "sawing" action. The beneficial effects, involving modification of edge action, are possibly as follow :-

(1) Considering a section of the cutter and wood work-piece taken in a vertical plane containing the velocity vector, the cutting angle and the angle included between the faces would be respectively higher and lower. This would, of course, have an important effect on phases other than indentation, such as shear above the cutting plane or bending of a continuous chip. But it should be noted that in the range of cutting angles studied (up to 45 deg.) increasing the angle was not very beneficial. However, of more

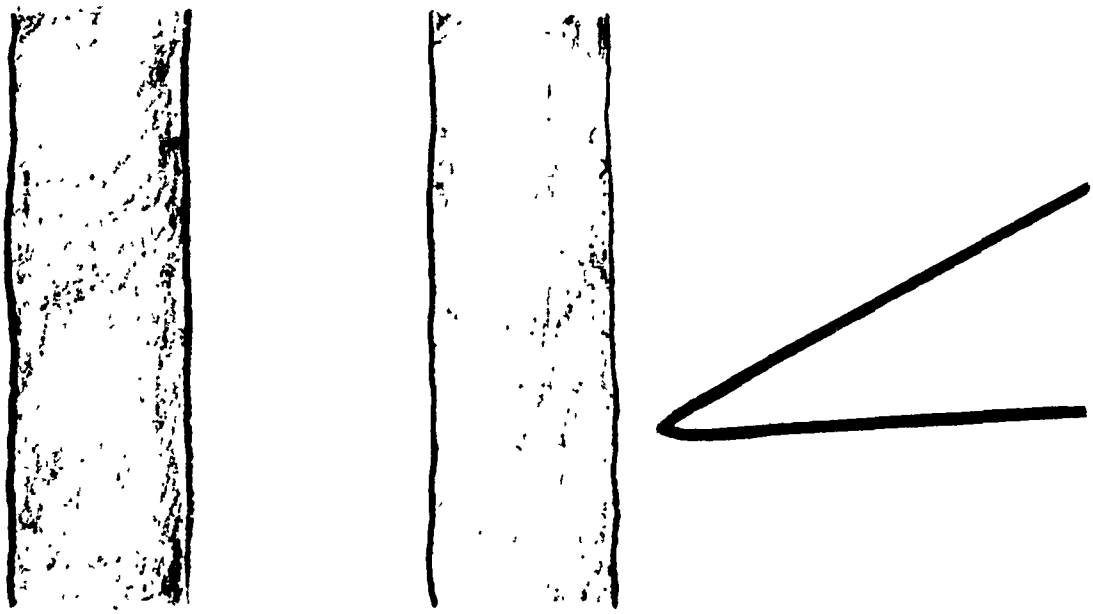
immediate interest is the effect on action of an edge with finite curvature. The mean radius of curvature of the intersection boundary of the cutter edge would be lowered, and the apparent thickness of the cell wall increased as suggested in Fig. 20. This would be expected to simultaneously reduce the force required to indent the cell wall, and increase the stiffness of the wall, thus reducing deflection.

(2) As an alternative to the impractical task of maintaining a near-perfect edge for cutting grass and meat, it is common practice to sharpen frequently with a rough stone. This would produce small serrations on the edge which, with a lateral edge motion, would act like a minute "saw" in tearing the cell walls without deflecting them unduly. Even a comparatively fine edge such as is produced by good sharpening practice would possess some serrations which, to a lesser extent, would have this tearing effect. In the absence of conspicuous serrations, the friction of the laterally moving edge might be expected to result in the wearing or abrading of a groove in the cell wall.

(3) The effect of a "sawing" motion or lateral oscillation of the edge might be to allow indentation of the wall, without building up excessive deflection in one direction, by changing the sense of motion. This would possibly be a dynamic effect, due to inertia of a zone of wood preventing it from responding instantaneously to a change in direction of force. However, in view of the



(a) Section perpendicular to edge



(b) Section highly oblique to edge

Fig. 20. Effect of taking section in resultant cutting direction on apparent cutting angle and apparent wall thickness.

discussion on the effect of cutting speed in Part I, this is not considered an important effect.

It appeared possible that the introduction of a lateral velocity component might produce some of these suggested benefits in cutting at 90°-90° in wood. Therefore, using the equipment described earlier, cutting tests were carried out in which the work-piece was given a lateral motion by vibrating it at 60 c.p.s. using a solenoid. Cutting in various species, at various moisture contents, cutting angles and cutting speeds (up to 21.5 in. per min.), the effect of vibration in every case was to replace the ruling failure type by type I(a), with very little delamination as discernible using a 10x lens. Fraying at the edges, which is characteristic of cutting in this situation, was absent. The improvement in surface quality is illustrated in Fig. 21. It was not possible to observe the cutting action underneath the microscope.

The force component parallel to the third (z) axis could not be measured, but the components in the other two directions were recorded and are shown in Table 2. However, the significant result was the highly beneficial effect on the surface produced. This is attributed to almost complete elimination of the deflection stage, and is therefore regarded as evidence as to the importance of the cutter edge.

It is evident from Table 2 that the forces and friction coefficient are reduced less at the higher forward cutting speeds, and it was observed that the surface

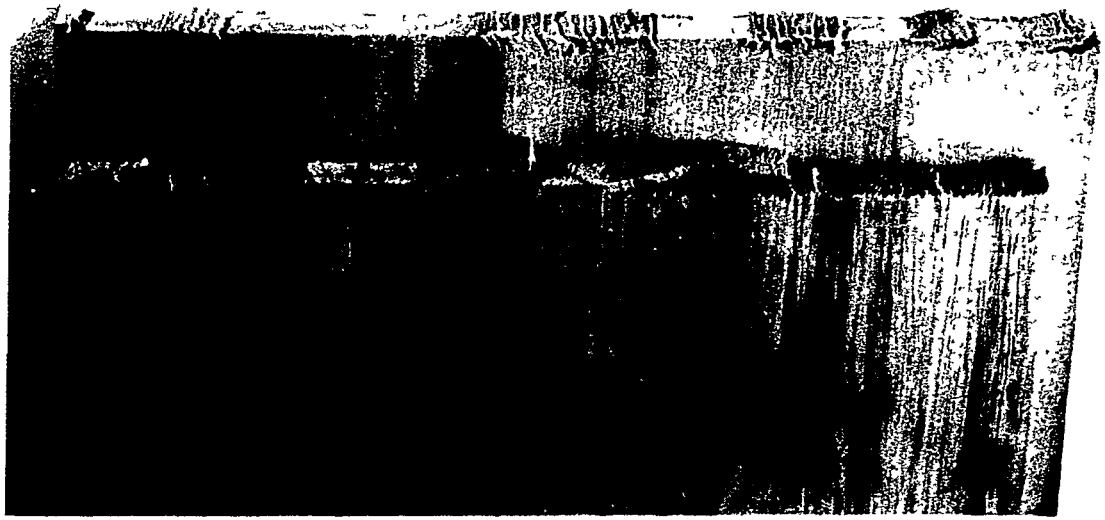


Fig. 21. Lateral vibration at 60 c.p.s. prevented type II failure and improved surface quality in cutting yellow-poplar (top) and common persimmon (bottom) at 0.5 in. per min. Vibration was alternately applied and removed. Cutting angle 25 deg., nominal chip thickness 0.030 in.

TABLE 2

THE EFFECT OF INDUCED LATERAL VIBRATIONS AT 60 C.P.S.
ON CUTTING FORCES AND APPARENT FRICTION COEFFICIENTS IN CUTTING AT 90°-90°

Width of cut 0.25 in., nominal chip thickness 0.030 in.

Species and Moisture Content	Rake Angle, deg.	Cutting Speed, inches per minute	Maximum Parallel Force, lb.		Normal Force, lb.		Apparent Cutting Friction Coefficient *	
			Without Vibration	With Vibration	Without Vibration	With Vibration	Without Vibration	With Vibration
Sugar pine, saturated	20	3.0	32	12	+1.1	-0.9	0.40	0.28
	40	3.0	19.6	4.8	-4.3	-3.0	0.52	0.14
Yellow birch, saturated	20	3.0	65	36	-1.5	-7.0	0.33	0.16
	40	3.0	39	20	-12.0	-11.0	0.42	0.20
White ash, saturated	20	3.0	47	20	+2.2	-4.9	0.42	0.11
	40	3.0	25	9.2	-7.5	-7.4	0.43	0.02
Yellow-poplar, saturated	25	3.0	33	13	+1.1	-3.4	0.53	0.18
	40	3.0	22	9.3	-4.5	-4.6	0.52	0.24
Yellow-poplar, at 5%	25	0.5	39	13	+2.7	-4.5	0.55	0.10
		3.0	36	15	+0.5	-5.1	0.48	0.11
		21.5	37	23	+0.5	-5.0	0.48	0.23
Common persimmon, at 5%	25	0.5	145	25	+2.7	-10.0	0.49	0.05

* from equation (8)

improvement was not so marked. This indicates that a certain minimum ratio of lateral velocity component to forward component is necessary to eliminate the deflection stage under any given set of conditions.

It was thought that similar effects might be apparent to a lesser extent in other cutting directions, and a similar procedure was followed for cuts at 90^{o}-0^{o} (planing action) in eastern white pine and yellow birch at 5 per cent, and at 0^{o}-90^{o} (veneer cutting) in saturated yellow birch, the other cutting conditions being as shown in Table 3, in which the force components and friction coefficients are also given. The effect of vibration on the surface quality of eastern white pine at 5 per cent moisture content, cut with 5 deg. cutting angle is shown in Fig. 22. The improvement in surface quality is apparent and is attributed to elimination of a deflection stage in the vicinity of the edge. The surface cut without vibration was of the type normally associated with the compression type of chip (1) and commonly termed fuzzy grain. Where vibration was applied, the cut surface was relatively smooth, without raised grain, although the chip type was similar. In cutting yellow birch at 15 deg. cutting angle, the chip type was changed by vibration from the "shear failure" type (Franz type II (1)) to the "beam failure" type (Franz type I (1)) due probably to a reduced friction component in the x,y plane.

The effect of vibration on surface quality and chip form, cutting at 0^{o}-90^{o} with 45 deg. cutting angle and

TABLE 3

THE EFFECT OF INDUCED LATERAL VIBRATION AT 60 C.P.S. ON CUTTING FORCES AND APPARENT FRICTION COEFFICIENTS IN ORTHOGONAL CUTTING AT 90°-0° AND 0°-90°.

Cutting speed 3 in. per min.

Species and Moisture Content	Cutting Situation	Rake Angle, deg.	Nom. chip thickness, mils	Maximum Parallel Force, lb.		Normal Force, lb.		Apparent Cutting Friction Coefficient *	
				Without Vibration	With Vibration	Without Vibration	With Vibration	Without Vibration	With Vibration
Eastern white pine at 5%	90°-0° (e.g. planing)	5	0.030	66	53	+10	+5.3	0.24	0.19
			0.050	100	68	+10	+6.3	0.19	0.18
Yellow birch at 5%	90°-0°	15	0.010	43	4.5	+6.5	-0.4	0.44	0.26
			0.015	62	5.0	+18.5	-1.0	0.62	0.08
Yellow birch saturated	0°-90° (e.g. rotary veneering)	45	0.030	11	4.0	-2.4	-3.0	0.64	0.14
			0.050	21	7.8	-4.1	-4.7	0.67	0.25

* from equation (8)



Fig. 22. Lateral vibration at 60 c.p.s. (centre section) prevented fuzzy grain in cutting at 90° -0° (planing) in eastern white pine at 5 percent moisture content. Cutting angle 5 deg., nominal chip thickness 0.015 in.

0.050 in. chip thickness in saturated yellow birch is shown in Fig. 23 and the cutting forces and friction coefficient are given in Table 3. Fig. 23 shows that the surface and chip form produced without vibration is characteristic of veneer cutting without a pressure bar. The surface is very rough due to failures occurring below the cutting plane, and the chip is very uneven in thickness with checks at uneven intervals, and is weak in places. Application of vibration resulted in a much smoother surface with little tear out. The lathe checks were more closely and evenly spaced (0.075 in. as against 0.170 in.) and more even in depth, so that the chip was stronger. Since, without vibration, the normal force component was in this case negative, the beneficial effect of vibration is not attributed to reduction of friction at the face, but to reduction of deflections at the edge.

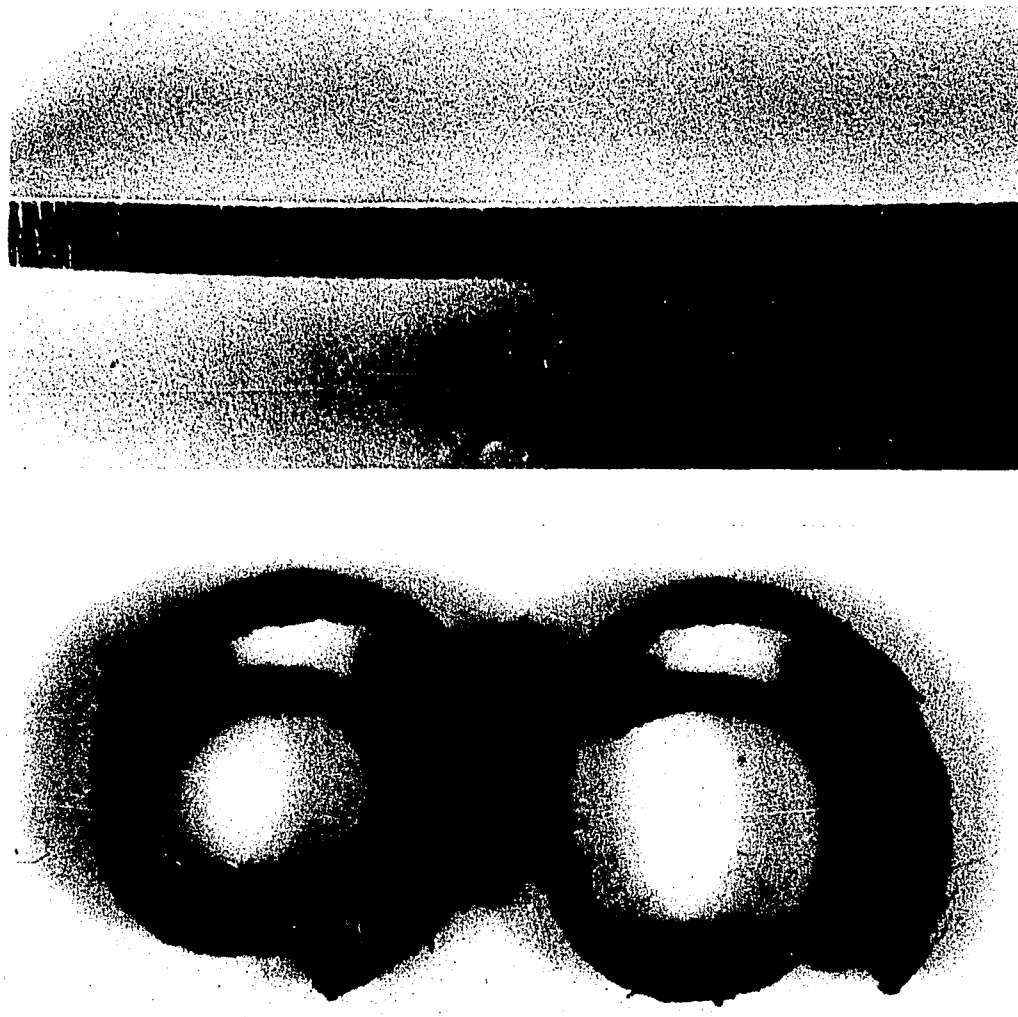


Fig. 23. The effect of lateral vibration in cutting at 0° -90° (veneer cutting) in saturated yellow birch. Cutting angle 45 deg., nominal chip thickness 0.050 in. Surface cut with vibration is at left. Inner portion of curled chip was cut with vibration.

CHAPTER 9

THE EFFECTS OF LUBRICATION ON THE INDENTATION PHASE

Early metal cutting theory assumed an ideally sharp edge and the friction coefficient was obtained from the force components by the relation (20)

$$\mu_c = \tan\left(\arctan\frac{P_y}{P_x} + \alpha\right) \tag{8}$$

As has most recently been emphasised by Albrecht (21), the edge actually has a finite radius, and μ_c involves not only the friction at the cutter face, but also forces exerted around the edge. For this reason the friction coefficient and the friction angle obtained by means of equation (8) will be termed "cutting" values.

Thus the cutting friction coefficient μ_c is not, as is assumed in the simple shear theory, identical to the friction coefficient according to the physical definition

$$\mu = \frac{F}{N} = \tan\beta \tag{9}$$

where N and F are the forces respectively normal and parallel to the direction of slip between two surfaces. As Albrecht points out, μ_c is given by

$$\mu_c = \frac{P_y'' + P'\sin(\beta-\alpha)}{P_x'' + P'\cos(\beta-\alpha)} \tag{10}$$

where P' and P'' are the resultant forces associated respectively with the face and the edge, and β is the true or physical friction angle for the face.

Therefore the effect of varying friction between the wood and the cutter may be complex.

This is illustrated by the results of cutting tests which were made to investigate briefly the role of friction in the indentation phase of cutting. Using the same equipment as previously, cuts were made in specimens of yellow-poplar, yellow birch and sugar maple at 5 per cent moisture content. S.A.E. 30 lubricating oil was applied at intervals along the work-piece. Cutting conditions, force components and cutting friction coefficients are shown in Table 4. It is apparent that the relationship between forces, cutting friction coefficients and failure type is not simple. Forces were reduced considerably by lubrication in each case, but only in the case of sugar maple was the failure type changed so that surface quality was substantially improved (See Fig. 24). It is noted that this is the only case in which cutting friction was substantially decreased. In the case of yellow-poplar, with 20 deg. cutting angle, the cutting friction coefficient was actually increased. In interpreting these results it will be assumed that the oil did not change the wood properties, on the grounds that no swelling was detected by thickness measured with a micrometer. Then the reduction in both force components is attributable to a reduction in the true

TABLE 4

THE EFFECT OF LUBRICATION WITH S.A.E. 30 OIL
ON MAXIMUM PARALLEL CUTTING FORCE
AND THE CUTTING FRICTION COEFFICIENT

Cutting at 90°-90°, with a cutting speed of 0.5 in. per min.
Moisture content 5 per cent, Width of cut 0.25 in.,
Nominal chip thickness 0.030 in.

Species	Cutting Angle deg.	Parallel Cutting Force, lb.		Cutting Friction Coefficient,* Maximum		Failure Type	
		Dry	Lubricated	Dry	Lubricated	Dry	Lubricated
Yellow-poplar	20	64	43	0.39	0.56	II(a)	II(a)
	40	33	24	0.56	0.46	II(a)	II(a)
Yellow birch	40	75	30	0.59	0.60	I(b)	I(b)
Sugar maple	30	111	79	0.68	0.52	II(b)	I(a)
	40	83	53	0.78	0.58	II(b)	I(a)

* From equation (8)

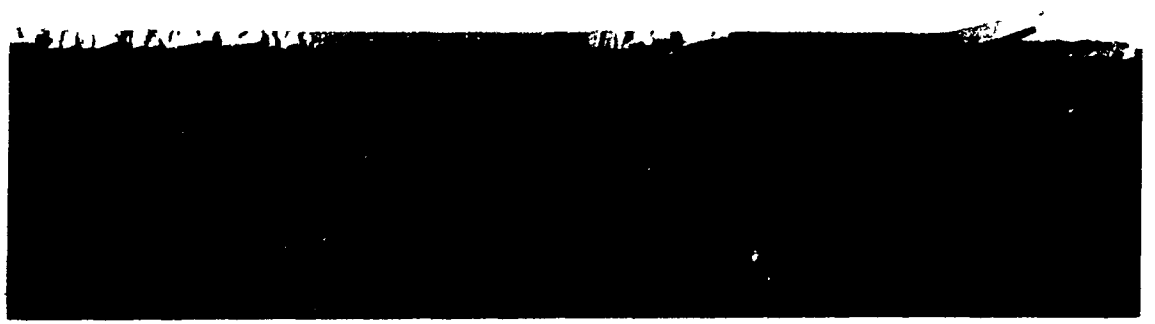


Fig. 24. The effect of applying S.A.E. 30 lubricating oil (dark-stained areas) on failure type in sugar maple at 5 per cent moisture content. Cutting angle 40 deg., nominal chip thickness 0.030 in.

friction coefficient, additional evidence, in the case of yellow birch and hard maple, being that the sub-chips tended to jump out from between the shear plane and the cutter face.

On this assumption, the maintenance of a comparable or higher cutting friction coefficient with lubrication must be attributed to unfavourable effects at the cutter edge. For instance, a lower true friction coefficient might result in a greater tendency for the fibres in contact with the edge to pull around it, creating an upward pressure beneath the cutter, somewhat as in Fig. 9 (a - c). This would offset the reduction in the normal forces on the face to an extent depending on the stiffness of the wood. A wood with a high transverse Young's modulus would be less affected, and this suggests a possible explanation for the different results obtained.

CHAPTER 10

CONCLUSIONS PROVIDING THE BASIS FOR AN ANALYSIS

The foregoing considerations led to these conclusions:-

(1) The discrepancy between force values calculated on the basis of shear failure and the observed maximum values is explicable in terms of the indentation phase.

(2) The maximum force values recorded occur at the instant where the deflection stage of indentation ends and incision by fibre severance begins.

(3) Failures below the cutting plane, in zones (3) and (4) indicated in Fig. 16, occur during the deflection stage. Therefore the force required to initiate incision must exceed that required to raise the stresses in these zones.

(4) Failure by shear above the cutting plane (zone (2) Fig. 16) occurs after the maximum force is attained at the commencement of incision, actually at a force level higher than that calculated from equation (3), because there is continued resistance to the edge, and possibly because of friction effects at the shear plane.

As discussed in Part II a detailed relationship

between cutter displacement, cutting force and stress distribution seemed unattainable. However, it appeared feasible to attempt to predict the value of the cutting force at onset of incision and then compare the associated stress in each zone of potential failure with the strength of the wood, in order to estimate the likelihood of failure having occurred there. For this purpose, it was necessary to make the best assumptions possible as to the nature of the stress causing failure in each zone, before seeking models capable of registering such failures.

The Nature of the Stresses Causing the Various Failures

The nature of the failure in zone (2) has been discussed previously, and is assumed to be a shear failure along the deflected grain direction.

Considering the cutter edge to have finite radius, there appear to be three possible ways in which failure can occur in the compacted zone (1) at the cutter edge. One possibility is a failure in shear, in a plane containing the cutting edge and extending ahead of the cutter. This is the type of failure usually considered for practically isotropic materials such as metals, and can be considered for wood in cutting situations in which the weak plane is approximately in this direction. But in the 90°-90° situation under consideration, such a plane is approximately perpendicular to the grain direction, and it is generally considered impossible to fail wood by shear in this plane. Deflection occurs due to the low Young's modulus perpendicular

to the grain, distributing the load, and introducing other types of stress.

The possibility of a bending failure is suggested by the curvature of fibres around the cutter edge, but it is apparent that such curvature is not generally sufficient to cause bending failure of a wall, or this would occur very early, before the wall could be collapsed against an adjacent one. Further, there is no apparent reason why the force required to cause a bending failure would be dependent on the rake angle, coefficient of friction, or chip thickness.

The remaining possibility appears to be separation by failure in tension parallel to the grain, since it is apparent from Fig. 25 that a separation must occur in the axial direction of a fibre to enable parts to pass respectively above and below the cutter edge. The question as to how such a tension might be applied to the fibres at this point is deferred until discussion of analytical models.

Concerning the failures in zone (3), Voskresenski (6) postulated that they were caused by tension perpendicular to the grain just behind the cutting edge. A difficulty here is that this zone is isolated from the work-piece to the rear by existing failures of the same type. There are grounds for concluding that these failures are more probably due to shear along the grain. Firstly, the shear strain in the vicinity of the cutter edge, except in the case of type II failure, appears to be much higher than the failing strain of wood. Taking, from the Wood Handbook (12), the modulus

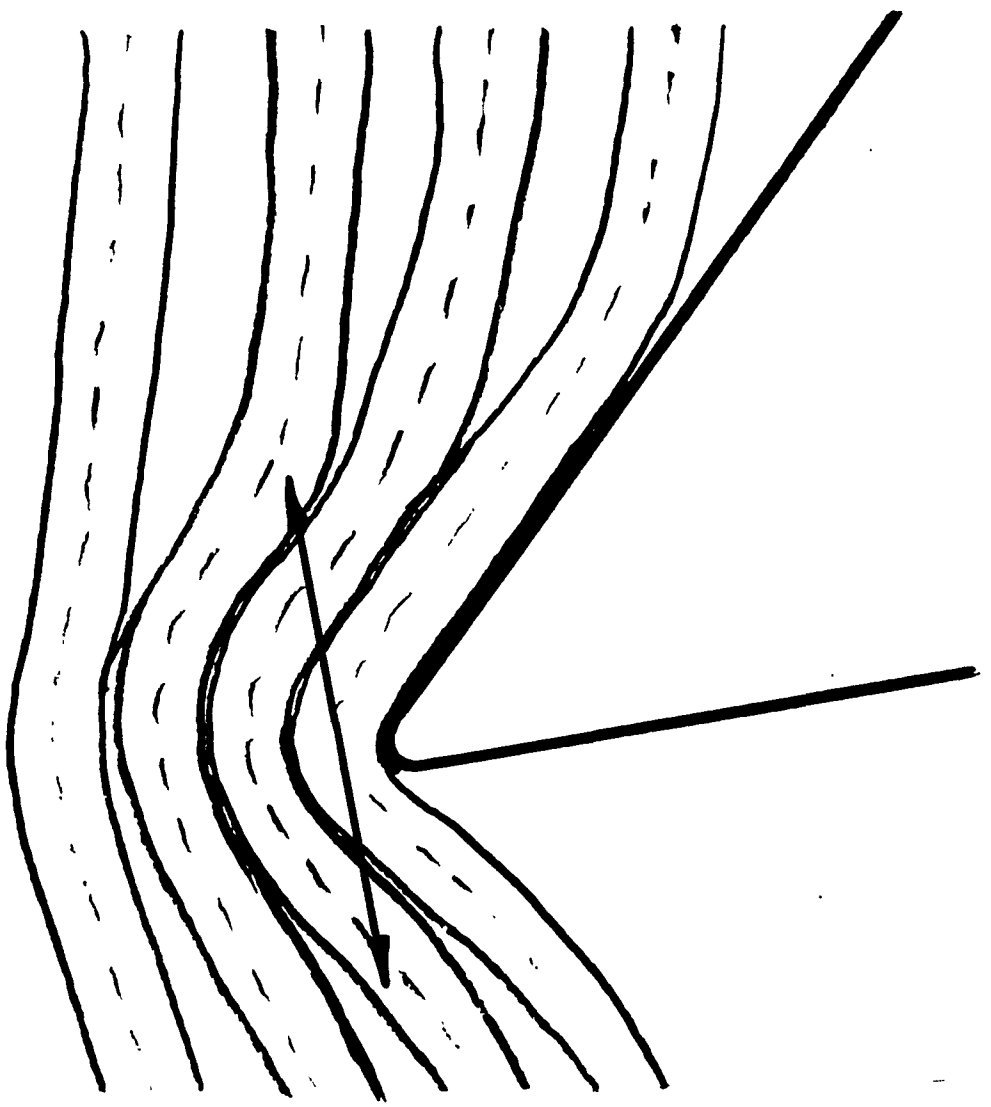


Fig. 25. Basic postulate concerning incision. Failure in tension.

of rigidity and shear strength of dry yellow-poplar to be 1.2×10^5 p.s.i. and 1,170 p.s.i. respectively, the strain at shear failure is 0.01, corresponding to a deflection angle of approximately 0.1 deg. Even if the strain at failure were equivalent to a deflection angle of 1 deg., the deflections in the vicinity of the cutter edge greatly exceed this, and in most cases would do so some distance ahead of the cutter edge. It is therefore concluded that, not only are the failures appearing in zone (3) due to shear, but that in most cases they actually occur at a distance ahead of the cutter edge (zone (5) Fig. 16) while the wood is still being compressed, at which stage they are not readily visible. It is suggested that the difference between type II(a) and type II(b) failures is that, in the former case, a shear failure occurs at a distance ahead of the cutter to form a lamina distinct from the remainder of the work-piece for some distance down from the surface, whereas in type II(b) failure, in which the deflections are much less, no such shear failure forms. This would account for the continuity of the chip and the detached portion below the cutting plane in type II(b) failure.

As suggested earlier, the failures in zone (4) appear to be associated with bending of a region ahead of the cutter edge, extending an indefinite distance down into the work-piece. In view of the discussion concerning failures in zone (5) above, in type II(a) failure the shear stresses due to bending would be relieved at some distance x ahead

of the cutter, whereas in type II(b) the x dimension of the zone under bending stress and the position of the neutral plane may be indefinite. In either case the position of the neutral plane may be affected by axial stresses acting in this region, due to the normal component of the cutting force.

Since wooden beams frequently fail in compression on the concave side, the question arises as to whether this might be so in the present case. However, there is no visual evidence of crumpling in the compression zone at magnifications up to 60x, and the support offered by the work-piece ahead of the cutter would be a factor in preventing compression failure. Further in type II(a) failure the fracture in zone (3) is typical of tension, and in type II(b) failure the normal force component is frequently negative, representing tension on the wood beneath the edge. Therefore, it seems clear that failures in zone (3) are the result of tension stresses. This being so, it is necessary to consider the relationship between the tension stresses presumed to develop to failure point at the cutter edge, and those also presumed to cause failure in the same fibre line at a lower point. A possible explanation seems to be that the tension stress is highly concentrated at the cutter edge, but below the cutting plane is distributed to a much wider zone of wood. Thus some stress due to axial force would be superimposed on bending stresses in zone (3). Therefore, in a curve representing stress in

the fibre line against distance below the cutter edge, there would be two maxima, one near zero and one at the point of maximum curvature at a distance below it (Fig. 26). In type II(b) failure, it would be required that the maximum at zone (3) be higher than that at the edge, to account for the occurrence of failure there before it occurs at the cutter edge, as is evident in Fig. 13.

Having set up postulates as to the types of stress causing failures in the various zones, there is again the problem of how the cutting forces may be related to these stresses. The intervening discussion has indicated some of the requirements which a model or models must meet, in order to account for the influence of the important variables on the occurrence of failures in the various zones. All such models involve simplifying assumptions and are hence unsatisfactory in some respects, but the hope is that the effects of such simplifications are small compared with those due to the important variables, and to the variability of the material.

Two possible models to account for the cutting force at the commencement of the incision stage of indentation will be described. In the first one, consideration is given to an analogy with the reactions of a string on an elastic foundation, acted on by a lateral load. In the second, an analogy with an elastically supported beam is drawn.

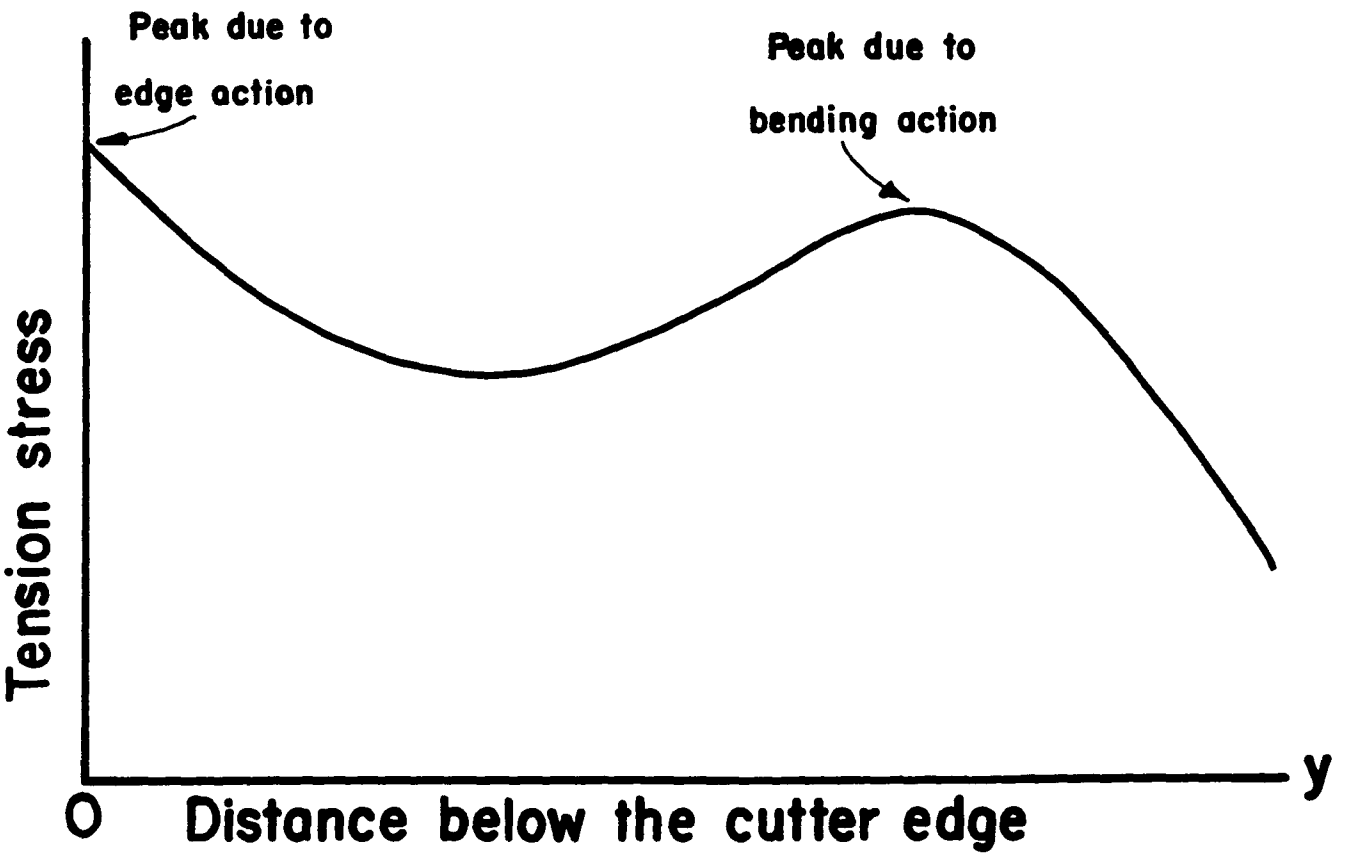


Fig. 26. Hypothetical distribution of tension stress along the fibre below cutter edge.

PART IV

ANALYTICAL MODELS FOR THE 90°-90° CUTTING SITUATION

CHAPTER 11

STRING ON ELASTIC FOUNDATION

In view of the possibility of shear failures ahead of the cutter there may occur a thin layer of wood with its axis along the grain, isolated from the remainder of the work-piece for some distance, but still subject to support by the remainder of the work-piece ahead of the cutter. Since this layer is thin and its deflections are observed to be high, it might be considered as a string, that is to have axial tensile properties but no bending properties. Then the model, illustrated in Fig. 27(a), is that of a weightless string supported normally by an elastic foundation, with a concentrated lateral load at a distance t from one end, the other being at infinity.

The tension stresses in the string are developed purely as a result of its deflection by the lateral load, and the reaction of the foundation. Thus the model represents the direct effect of the edge alone on the tension stresses in its vicinity, without regard to the effects of the cutter face, friction or shear.

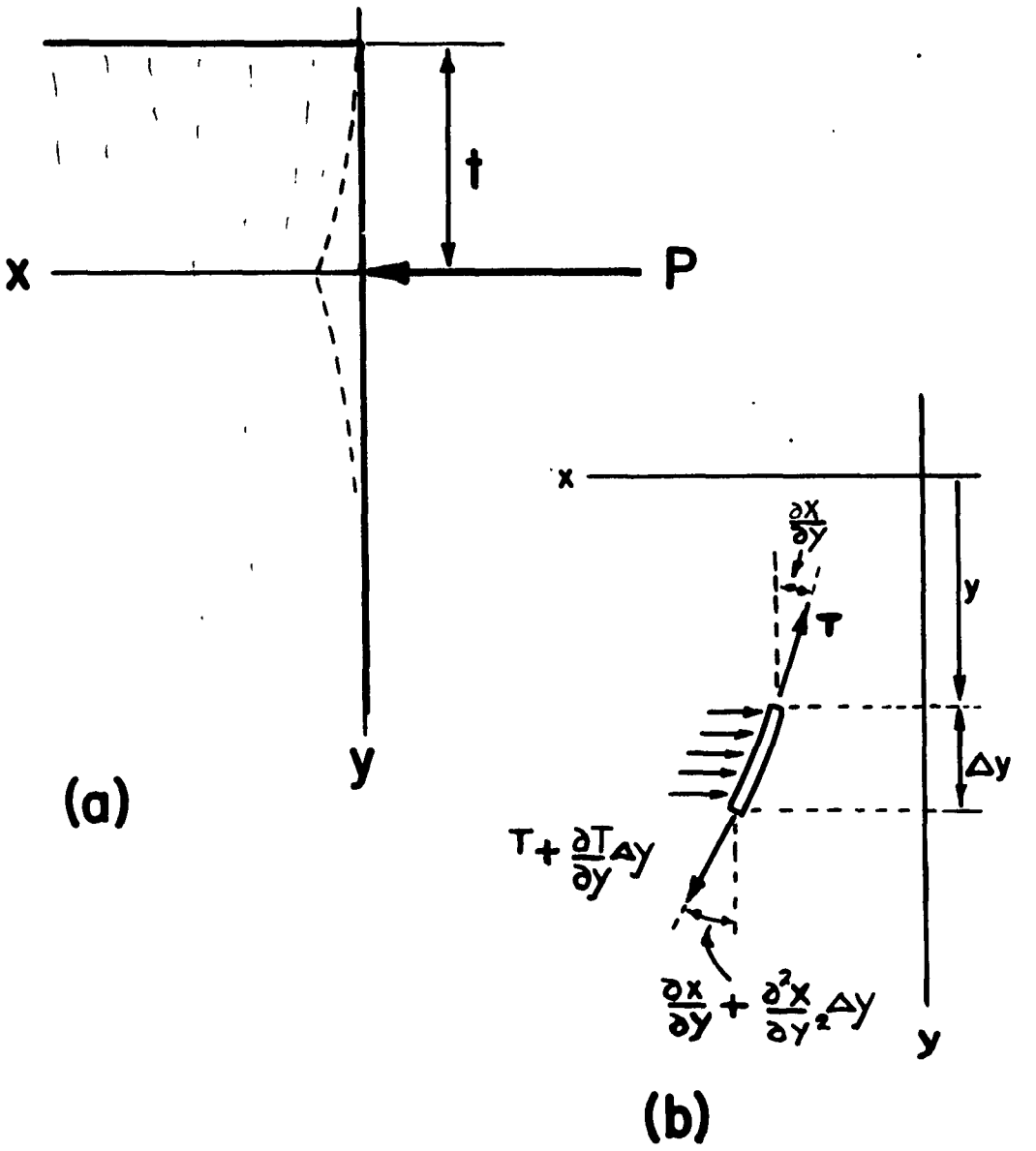


Fig. 27. Model for indentation phase. String on elastic foundation.

It is required to find a relationship between the deflection of the string and its tension, and then to relate these to the load.

To develop a relationship between lateral deflection (x) and tension (T) in the string, consider the equilibrium of an element of length, as in Fig. 27(b)

For $\Sigma F_x \equiv 0$

$$-T\frac{\partial x}{\partial y} + \left(T + \frac{\partial T}{\partial y}dy\right)\left(\frac{\partial x}{\partial y} + \frac{\partial^2 x}{\partial y^2}dy\right) - Kx\,dy = 0$$

where K = foundation modulus.

This simplifies to

$$T\frac{\partial^2 x}{\partial y^2} + \frac{\partial T}{\partial y}.\frac{\partial x}{\partial y} - Kx = 0 \qquad (11)$$

For $\Sigma F_y \equiv 0$

$$T + \frac{\partial T}{\partial y}dy = T + AE\frac{\partial \epsilon}{\partial y}dy \qquad (12)$$

where A and B are respectively the cross-sectional area and the Young's modulus of the string, and ϵ the strain in it. If it is assumed that each point of the string moves parallel to the x axis, placing some limit on deflections in this direction, the strain ϵ in the string is

$$\epsilon = \frac{\Delta y\sqrt{1 + \left(\frac{\partial x}{\partial y}\right)^2} - \Delta y}{\Delta y} \simeq \frac{1}{2}\left(\frac{\partial x}{\partial y}\right)^2$$

using the binomial expansion.

Thus,

$$T = AE\epsilon = AE \cdot \frac{1}{2}\left(\frac{\partial x}{\partial y}\right)^2 \tag{13}$$

where A = cross-section area of the string

E = Young's modulus in tension of the string

Use of this expression in (12) gives

$$\frac{\partial T}{\partial y} = AE \frac{\partial}{\partial y}\left[\frac{1}{2}\left(\frac{\partial x}{\partial y}\right)^2\right] = AE \frac{\partial x}{\partial y} \frac{\partial^2 x}{\partial y^2} \tag{14}$$

Substituting from (13) and (14) in (11),

$$\frac{AE}{2}\left(\frac{\partial^2 x}{\partial y^2}\right)\left(\frac{\partial x}{\partial y}\right)^2 + AE\left(\frac{\partial^2 x}{\partial y^2}\right)\left(\frac{\partial x}{\partial y}\right)^2 - Kx = 0$$

or

$$\frac{d^2x}{dy^2} - \frac{2K}{3AE}\frac{x}{\left(\frac{dx}{dy}\right)^2} = 0 \tag{15}$$

Then the important parameter governing the behaviour of the string is $\frac{K}{E}$, the ratio between the foundation modulus and the Young's modulus in tension of the string.

This equation may be written

$$\left.\begin{aligned} &\left(\frac{dx}{dy}\right)^2 \frac{d^2x}{dy^2} - p^2 x = 0 \\ &\text{where} \quad p^2 = \frac{2K}{3AE} \end{aligned}\right\} \tag{16}$$

To obtain the first integral of the differential equation, it may be written

$$\left(\frac{dx}{dy}\right)^3 \frac{d^2x}{dy^2} - p^2 x \frac{dx}{dy} = 0$$

or

$$\frac{d}{dy}\left[\frac{1}{4}\left(\frac{dx}{dy}\right)^4 - \rho^2\frac{x^2}{2}\right] = 0$$

so that

$$\left(\frac{dx}{dy}\right)^4 - 2\rho^2x^2 = C \qquad (17)$$

Since from equation (13), T is proportional to $\left(\frac{dx}{dy}\right)^2$, this equation shows that the relationship between the tension and the deflection in the string is hyperbolic.

There are two sets of boundary conditions, one for the region above the cutting plane (y negative) and one for the region below it (y positive) :-

$$\left.\begin{aligned} y<0,\ \omega(0)=\omega_0\ ;\ T_{y=-t}=0 \text{ or } \left(\frac{\partial x}{\partial y}\right)_{y=-t}=0 \\ y>0,\ \omega(0)=\omega_0\ ;\ T_{y\to\infty}=0 \text{ or } \left(\frac{\partial x}{\partial y}\right)_{y\to\infty}=0 \end{aligned}\right\} \qquad (18)$$

Determination of C in equation (17) depends on these conditions, but unfortunately there is no analytical solution of this equation to enable them to be applied directly, and a numerical or graphical solution would be required. In view of this, and the factors not taken into account by this model, it did not appear profitable to carry this approach further.

However, a significant implication of this analysis is the importance of the parameter $\frac{K}{B}$, which depends, in this case, on the ratio of the Young's moduli respectively

perpendicular and parallel to the grain. Since a similar parameter occurs in the analysis developed in the next chapter, this is regarded as confirmatory evidence as to the importance of this ratio.

CHAPTER 12

BEAM ON ELASTIC FOUNDATION

In the string model, the tension at the edge was supposed to be developed due to lateral deflection. The new postulate is that this tension is developed by an axial force in the fibres, imposed principally by the face of the cutter, but partly by the rounded edge. This axial force is assumed to correspond to the component of the resultant cutting force in the average direction of the fibres, close to some point on the rounded cutter edge, where maximum tension stress is supposed to occur (See Fig. 28).

The problem is now to relate the tension stress in the fibres at the cutting edge, and their deflected direction, to the cutting forces.

The tensile stress across the cutting plane is assumed to diminish ahead of the cutter, from a maximum at the edge, in some fashion related to decreasing deflection of the surrounding wood. For such stress concentrations Green's analysis for aeolotropic plates (22) gives a hyperbolic relation between stress and distance along a radius originating at the load point, but implies infinite stresses at this point. To keep the stresses finite as they must be in reality, it is assumed that the hyperbolic

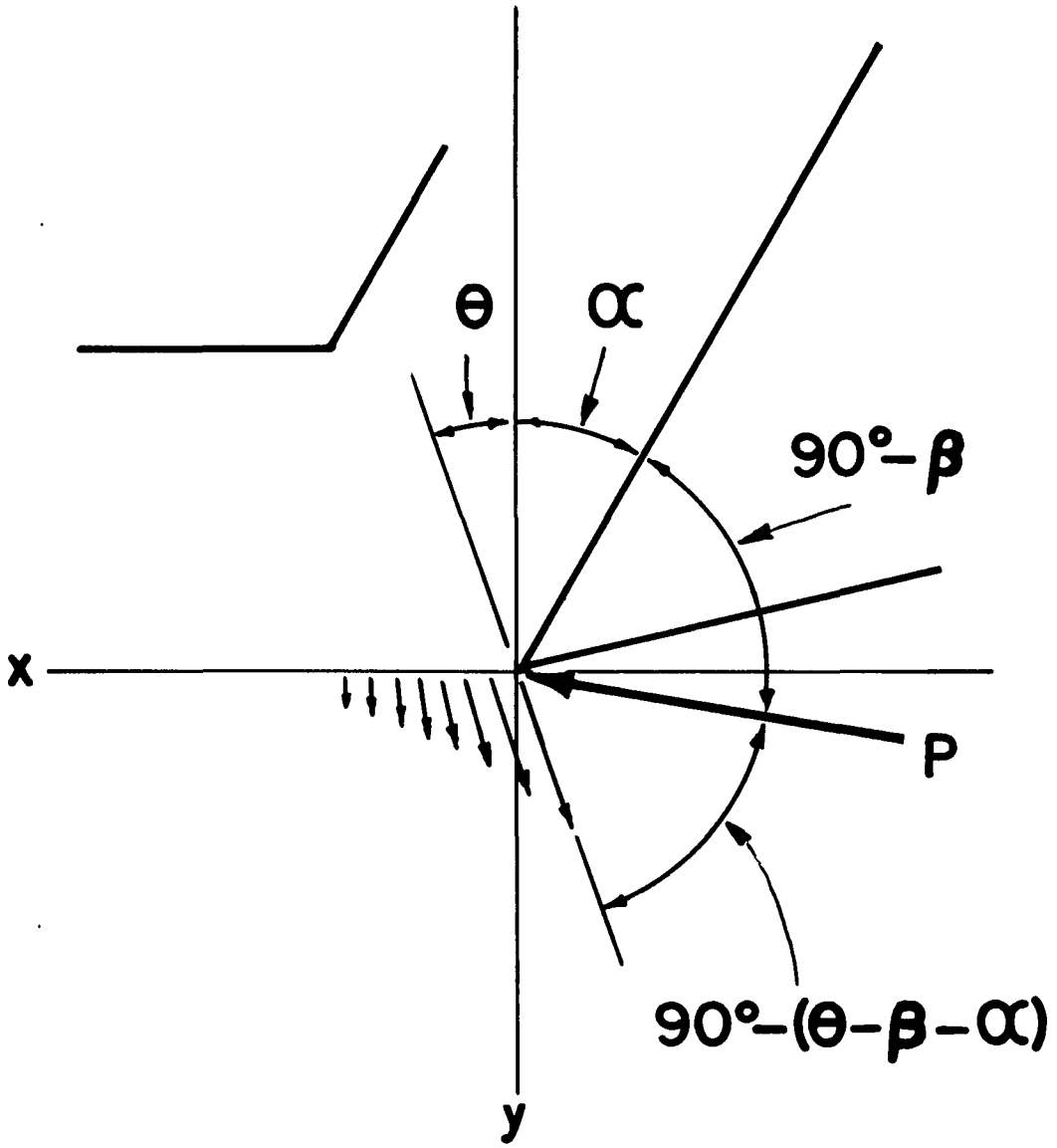


Fig. 28. Relation between cutting force and assumed stress distribution along cutting plane.

relation may be approximated by a curve of exponential form with suitable decay constant, as follows :-

$$\sigma = \sigma_{(0)} e^{-\varphi x}$$

where σ is the tension stress along the fibres, and φ is the constant giving the rate of decay (See Fig. 28).

These tensile stresses across the cutting plane will have a resultant that is not quite parallel to the y axis, because, close to the cutting edge, the fibres are deflected by the horizontal component of the cutting force through an angle θ from the y axis. Since the stresses near the edge are dominant, the resultant of the tensile stresses is considered to be approximately in this direction. If these stresses are considered to be in equilibrium with a component P_θ of the cutting force P in this direction, located at the cutting edge, the following relation applies, for unit width:-

$$P_\theta = \int_0^\infty \sigma_{(0)} e^{-\varphi x} dx$$

Performing the integration,

$$P_\theta = \frac{\sigma_{(0)}}{\varphi} \qquad (19)$$

From Fig. 28 the acute angle between P and P_θ is $90^\circ - (\theta - \beta + \alpha)$, where β is the angle of friction.

Hence,

$$P_\theta = \frac{\sigma_{(0)}}{\varphi} \cdot \frac{1}{\sin[\theta - (\beta - \alpha)]}$$

which, if Θ and $|\beta-\alpha|$ are small, approximates to

$$P_\theta = \frac{\sigma_{(o)}}{\varphi[\theta - \sin(\beta-\alpha)]} \qquad (20)$$

It is now necessary to determine Θ, which represents only the local deflection of the fibres at the cutter edge. It could be measured only with some difficulty and inaccuracy, and in any case experimental determination is to be avoided if possible, since causal relationships would then remain hidden.

The determination of Θ analytically demands expressions for the stresses and strains across the y, z plane at the origin, and stresses and strains elsewhere in this plane are also of interest, as discussed later. The situation might be simplified to that of a concentrated load acting parallel to the surface of an anisotropic half-plane. There are solutions in theory of elasticity for this problem, but they give infinite stresses and deflections at this load point. Further, in the 90°-90° situation, failure occurs in other ways before incision begins, so that the half-plane does not persist intact. Since no analysis is available to cope with failure due to a concentrated load, some manner of distribution of this load to the surrounding wood must be considered.

It is postulated that in the y, z plane, at a certain small distance (h) ahead of the edge, the distribution of lateral deflections and stresses which is again probably of a modified hyperbolic type, may be approximated by an

exponential relationship, with a maximum at the cutting plane, if the appropriate decay constant can be found. Thus

$$x = x(0)e^{-\xi y} \tag{21}$$

where ξ is the decay constant.

If the stress in the wood in the x direction is related to this deflection by a proportionality constant K, and the force P_x is assumed to be in equilibrium with the resultant of these stresses

$$P_x = \int_0^\infty Kx\,dy$$

$$= \int_0^\infty K x(0) e^{-\xi y} dy$$

$$= \frac{K x(0)}{\xi} \tag{22}$$

The deflection angle Θ is given approximately by differentiating equation (21) with respect to y, Thus

$$\frac{dx}{dy} = -\xi x(0) e^{-\xi y}$$

and at y = 0,

$$\Theta = \xi x(0)$$

$$= \frac{\xi^2 P_x}{K}$$

in view of equation (22).

From equation (4) it can be deduced that

$$P_x = P\cos(\beta-\alpha)$$

so that

$$\theta = \frac{\xi^2 P}{K}\cos(\beta-\alpha) \qquad (23)$$

P can be obtained simply by eliminating θ from equations (20) and (23).

There is then the question of determining ζ and ξ.

They could presumably be obtained as empirical constants by solution of simultaneous equations using experimental results for each set of cutting conditions, but it appeared much preferable to obtain them as functions of wood properties and cutting conditions, even if only approximately. This involves the creation of models, the behaviour of which is represented by equations similar to (20) and (23).

Considering equations (20) and (23), it is noted that they have the same form as those representing the behaviour of an elastically supported semi-infinite beam, subject to simple bending by a concentrated load at the free end. The theory of elastically supported beams is fully treated in a book by Hetényi (23), to which frequent reference will be made, and only special developments of the theory necessary for the present purpose will be set out here.

It is asserted that, just as observed wave forms

may be approximated by Fourier series after determination of the constants involved, the stress distributions referred to above could be approximated by the stress distribution in an elastic foundation beneath a beam, by proper choice of the attributes of the beam and foundation. Thus it is not maintained that the model beams which will be discussed necessarily have physical reality, even if there may be some semblance.

Since the deflections occurring at the cutter edge in some situations are greater than are usually considered in beam theory, it is evident that a single equation of the form given in (22) may not apply over this large range of deflection. However, it is asserted that an equation of this form may approximate the stress distribution over a limited range of large deflections, and since this is the way in which it will be used, the beam model must be considered in this light.

An advantage of the elastically supported beam model is that it involves elastic properties of the beam and the foundation which are measured in perpendicular directions. This allows the introduction of the different elastic properties of wood in the two directions, thus providing to some extent for its anisotropy. Further, the model overcomes the difficulty of using elasticity theory with a concentrated load, since the beam in effect distributes the load to the bulk of the wood in a defined manner.

The first of the imaginary beams in the double-beam model to represent equations (19) and (22) relates to equation (19) and the constant ξ. It is illustrated in Fig. 29. In this case the cutting plane suggests an obvious lower boundary for the beam, especially as the chip thickness is known to affect the cutting force. Hence, the unseparated chip is seen as constituting a semi-infinite beam with a concentrated load at its free end (x = 0). However, in 90°- 90° cutting the grain direction is perpendicular to the beam axis and across the boundary between the beam and the foundation, and while this has the effect of limiting the deflections and helping to preserve the conditions pertaining to elasticity theory, vertical shear effects are augmented, thus tending to increase the actual beam deflection. However, the parallel component of the cutting force acting approximately along the cutting plane would tend to bend the beam in the opposite direction, as is evident from microscopic study, especially in saturated wood and at higher chip thicknesses. Therefore, in the absence of clear and consistent effects of these departures from orthodox conditions for beam theory, this was applied without modification to Beam I. That is, ξ is identified with the parameter 2λ in the equation for the displacement beneath a concentrated load at the end x = 0 of an elastically supported semi-infinite beam (23) :-

Thus the displacement at the end x = 0 is given by :-

$$y = \frac{2P_y\lambda}{k} \qquad (24)$$

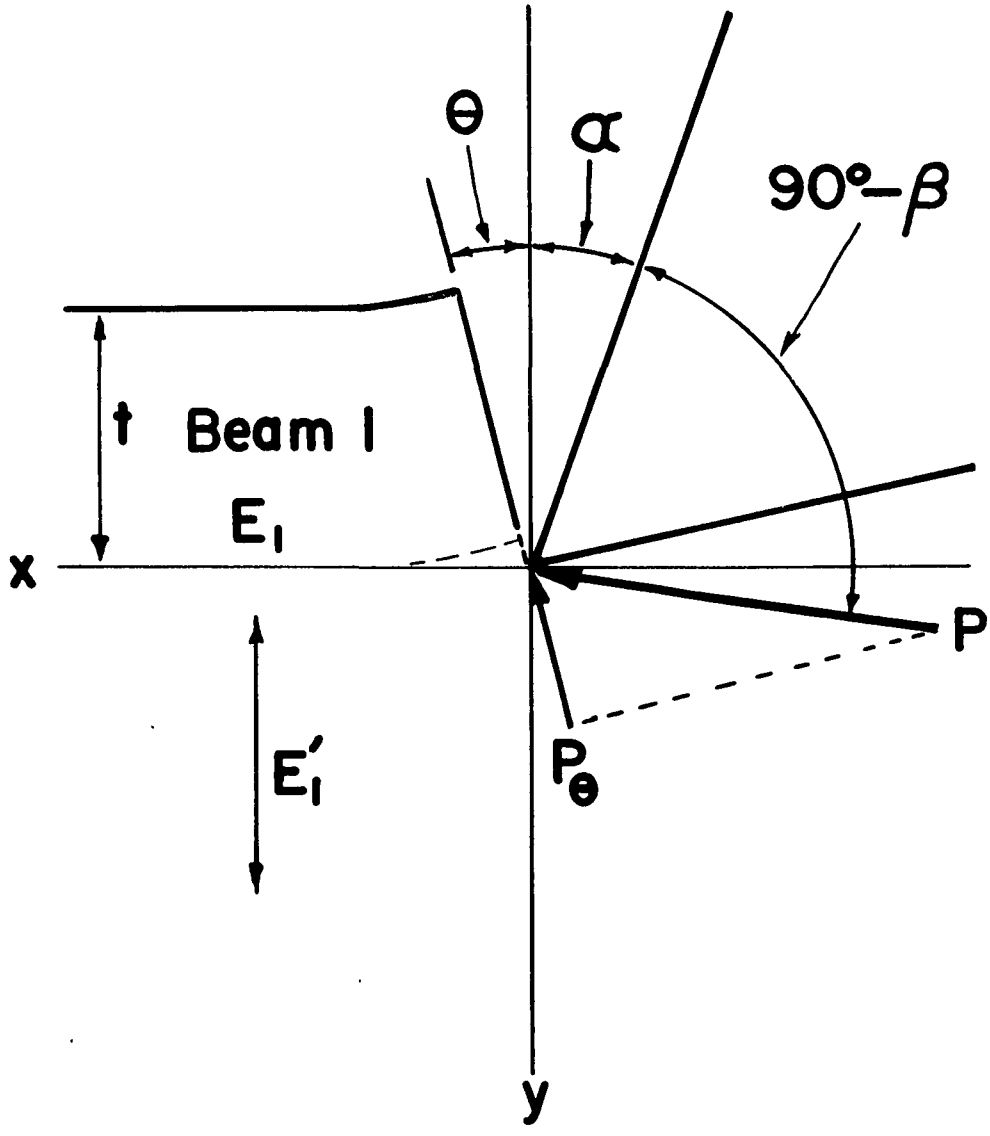


Fig. 29. Double-beam model - Beam 1.

where k is the load imposed on the foundation per unit length of beam for a unit deflection. If Θ is small, the magnitude of P_Θ may be assumed to be equal to that of P_y, and equation (24) may be compared with equation (19), since the stress in the foundation is given by

$$\sigma = ky \tag{25}$$

Considering the foundation as an isotropic elastic solid Biot (24) provides an expression for k so that the convenient Winkler theory (23) can be used as an approximation to the more exact theory, which requires numerical integration. He gives :-

$$k = 0{\cdot}645\frac{bE'}{h}\left(\frac{E'}{E}\right)^{\frac{1}{3}} \tag{26}$$

for a beam of width b and depth h.
Since in the Winkler theory (23),

$$\lambda = \sqrt[4]{\frac{k}{4EI}} \tag{27}$$

where E and I are respectively the Young's modulus and moment of inertia of the beam, use of Biot's expression for k gives

$$\lambda = \frac{1{\cdot}18}{h}\left(\frac{E'}{E}\right)^{\frac{1}{3}} \tag{28}$$

Here E' and E are respectively the foundation modulus and the beam modulus, and t is the nominal chip thickness. E' does not necessarily equal E_T the Young's modulus

of the material, but represents the stress developed at a point of the foundation by a unit deflection. Since the foundation in the present case is highly anisotropic the foundation modulus requires correction for this. It is possible to do this approximately by using the theory developed by Green (22) for the stress distribution in an orthotropic half-plane due to an isolated force applied normally to the straight boundary. For the longitudinal-tangential (L, T) plane (Fig. 6) where the grain is perpendicular to the straight boundary, and parallel to the force, the stress at depth t is given by,

$$\frac{t}{P_n}\sigma_x = \frac{2}{\pi\left(\gamma_1^{\frac{1}{2}} - \gamma_2^{\frac{1}{2}}\right)}\left(\frac{\gamma_2 - 1}{2} - \frac{\gamma_1 - 1}{2}\right) \qquad (29)$$

Here γ_1 and γ_2 are given by the relationships

$$\gamma_1 \gamma_2 = \frac{S_{11}}{S_{22}}$$

$$\gamma_1 + \gamma_2 = \frac{S_{66} + 2S_{12}}{S_{22}}$$

where

$$S_{11} = \frac{1}{E_T}\ ; \qquad S_{22} = \frac{1}{E_L}$$

$$S_{12} = \frac{\mu_{LT}}{E_L}\ ; \qquad S_{66} = \frac{1}{G_{LT}}$$

E_L, E_T, G_{LT} and μ_{LT} are the elastic moduli in the L, T plane of wood. The equation for an infinite beam supported on an elastic half-plane and subject to a concentrated load is

$$y = \frac{P_n \lambda}{2k} \tag{30}$$

and using (25) and (28) with this,

$$\sigma_x = \frac{P_n \lambda}{2} = \frac{P_n}{t} \frac{1.18}{2} \left(\frac{E'}{E}\right)^{\frac{1}{3}} \tag{31}$$

Comparing (29) and (31), it is seen that

$$\left(\frac{E'}{E}\right)^{\frac{1}{3}} = \frac{4}{1.18\pi\left(\gamma_1^{\frac{1}{2}} - \gamma_2^{\frac{1}{2}}\right)} \left(\frac{\gamma_2 - 1}{2} - \frac{\gamma_1 - 1}{2}\right) \tag{32}$$

and this may be applied to equation (24), to take account of the anisotropy of the foundation, for a limited range of the ratio E_T/E_L.

Using equations (20), (24), (25) and (28) for Beam 1, with σ_x equal to σ_o, the tensile strength parallel to the grain,

$$P = \frac{0.424 \dfrac{bt\sigma_o}{\left(\dfrac{E_1'}{E_1}\right)^{\frac{1}{3}}}}{\theta - \sin(\beta - \alpha)} \tag{33}$$

The second "beam" in the double-beam model, to represent equation (22), is sketched in Fig. 30. Again the model beam is envisaged as a semi-infinite beam elastically supported by a foundation of infinite depth. In reality, support may be on one or both sides of the beam.

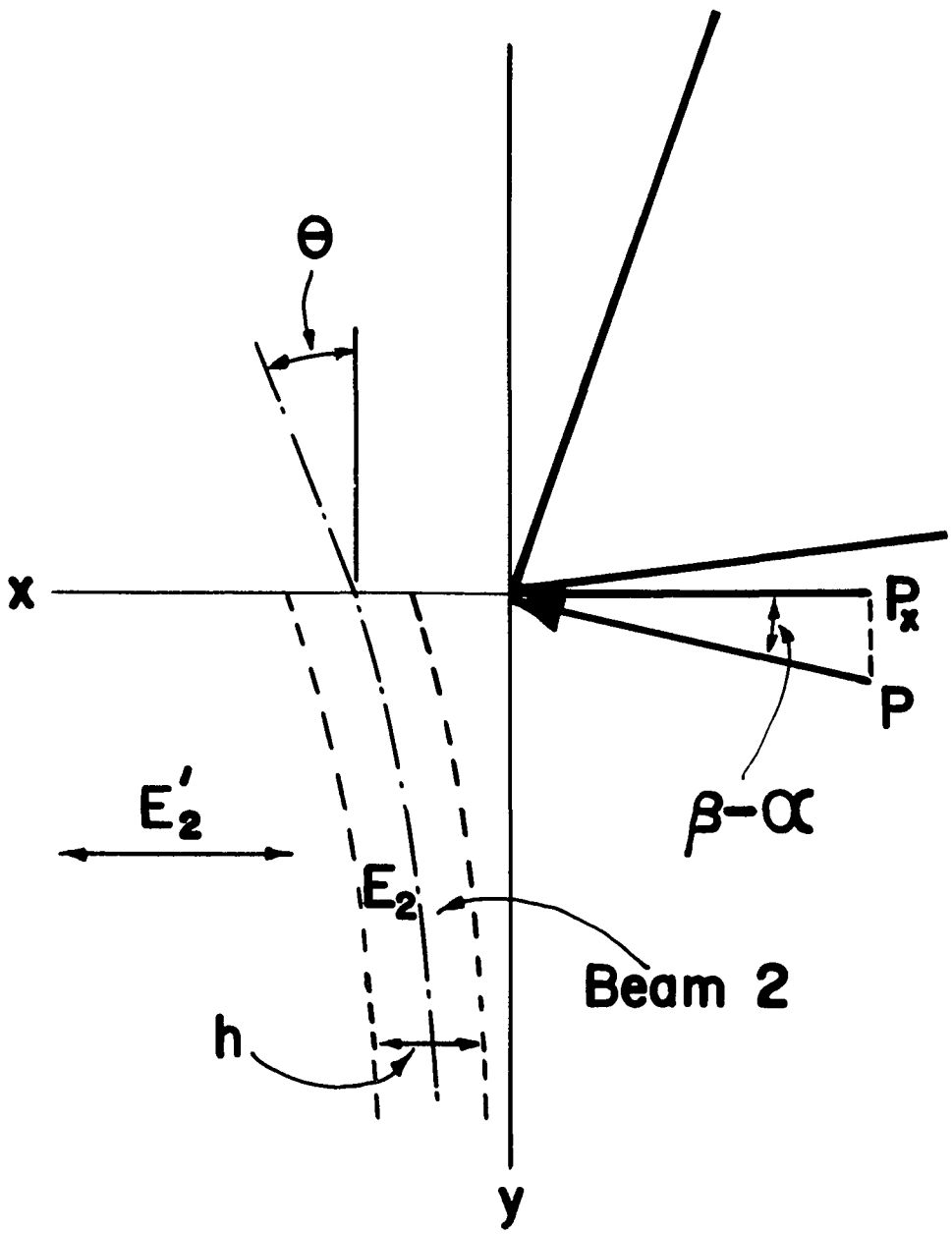


Fig. 30. Double-beam Model - Beam 2.

But with a foundation of infinite depth, this is considered not to affect equilibrium deflections.

There are several difficulties which arise if it is attempted to relate this beam model directly to reality. In the first cut in a virgin work-piece, as in the present case, the "beam" does not appear to be physically isolated from the remainder of the material, except (usually) at a surface containing the cutter edge and extending down from it some distance. However, it is probable, as discussed earlier, that a failure in shear in a surface parallel to this one, at a short distance ahead of it, isolates a physical lamina and eliminates shear connection with the remainder of the wood, within a short distance of the cutting-plane. Hence, the model beam is envisaged as a semi-infinite shallow strip elastically supported by a foundation of infinite depth, with a concentrated load at its free end ($y = 0$).

This would suggest that the appropriate depth for the beam is that corresponding to closest spacing of splits, which, from Table 5 is seen to vary from 0.003 to 0.007 in. However, there are other considerations which suggest the desirability of letting the height be arbitrary, so that the beam may remain fictitious. Firstly, the deflections are in many cases large, so that they are no longer linearly related to load, and shear may become significant. Further, this may result in the occurrence of load components parallel to the axis of the beam both in the beam and in the

TABLE 5

MEAN WAVELENGTHS OF RECORDED CUTTING FORCES

Species	Moisture Content	Mean Wave Length of Cutting Forces, mils		
		Major	Intermediate	Minor
Sugar pine	4%	37	29	7.0
	Sat.	45	19	5.0
Yellow birch	4%	(28)*	(12)*	7.0
	Sat.	-	12	3.8
White ash	4%	44	17	5.1
	Sat.	39	11	3.0

* Not very distinct.

foundation, although in the present case, in which the grain is parallel to the beam, these effects may be opposed. There is also a source of error due to the load not being concentrated at the end, but distributed in some fashion. For instance, it would be possible to consider a concentrated force applied at a distance t from the end of the semi-infinite beam. Simplifying the general solution for this situation given by Hetenyi (23), the beam slope at the point t is given by

$$\theta_t = \frac{2P_x\lambda^2}{k} e^{-2\lambda t} \cos^2 \lambda t \qquad (34)$$

In this equation λ (and therefore the height of the beam, h) and t are involved in exponential and trigonometrical expressions complicating the analysis. Other assumed distributions such as a uniform loading, would introduce even greater complications. Further, since θ is small, it is evident from equation (22) that P is very sensitive to θ. Therefore it was considered, that if it should prove necessary to take into account such a factor as the exponential-trigonometrical factor in (34), it should be treated as an arbitrary factor to be determined as discussed later.

If the load is assumed to be concentrated at the free end of the semi-infinite beam, the slope θ at this point is given (23) by the equation

$$\theta = \frac{2\lambda^2 P_x}{k}$$

which compares with equation (23).

Using Biot's expressions (24) for k and λ as applying to Beam 2 of the model,

$$\theta = 4{\cdot}32 \frac{\left(\frac{E_2'}{E_2}\right)^{\frac{1}{3}}}{hbE'} P_x \qquad (35)$$

As discussed above, h was left arbitrary to account for uncertainties as to the effects of large deflections and of an unknown load distribution, in the hope that a single value, determined by comparison with experimental results, could be used thenceforth.

E_2' is obtained in a similar manner to E_1' from Green's expression (22) for an isolated force perpendicular to the grain :-

$$\frac{h}{P_n}\sigma_y = \frac{2\gamma_1^{\frac{1}{2}}\gamma_2^{\frac{1}{2}}}{1{\cdot}18\pi\left(\gamma_1^{\frac{1}{2}}-\gamma_2^{\frac{1}{2}}\right)}\left(\frac{\gamma_2-1}{\gamma_2}-\frac{\gamma_1-1}{\gamma_1}\right) \qquad (36)$$

Comparing this with equation (30) as before

$$\left(\frac{E_2'}{E_2}\right)^{\frac{1}{3}} = \frac{4\gamma_1^{\frac{1}{2}}\gamma_2^{\frac{1}{2}}}{1{\cdot}18\pi\left(\gamma_1^{\frac{1}{2}}-\gamma_2^{\frac{1}{2}}\right)}\left(\frac{\gamma_2-1}{\gamma_2}-\frac{\gamma_1-1}{\gamma_1}\right) \qquad (37)$$

P may now be obtained by eliminating θ from equations (33) and (35), to give a quadratic equation in P of the form

$$aP^2 - bP - c = 0$$

in which the coefficients derived from equations (33) and (35) are

$$a = \frac{4{\cdot}32}{hbE_2'}\left(\frac{E_2'}{E_2}\right)^{\frac{1}{3}}$$

$$b = \sin(\beta - \alpha)$$

$$c = \frac{0{\cdot}424\,bt}{\left(\frac{E_1'}{E_1}\right)^{\frac{1}{3}}}$$

(38)

The positive solution for P is

$$P = \frac{b + \sqrt{b^2 + 4ac}}{2a} \qquad (39)$$

where a, b and c are as given above.

The elastic constants necessary for the application of equations (32) and (37) to find the parameters

$$\left(\frac{E_1'}{E_1}\right)^{\frac{1}{3}} \quad \text{and} \quad \left(\frac{E_2'}{E_2}\right)^{\frac{1}{3}}$$

are difficult to obtain reliably and were not all available for the matched material used earlier. Therefore the few data given in the Wood Handbook (12), were used to obtain

average values for the ratios E_1'/E_1 and E_2'/E_2. Comparison of these with the average ratios E_T/E_L provided the general factors for obtaining E_1' from E_L and E_2' from E_T. These factors were respectively 0.82 and 3.92.

Theoretical results were compared with the two sets of experimental cutting data referred to earlier. For sugar pine, yellow birch and white ash most mechanical properties obtained from matched material were available (1) and these were supplemented by the author. For eastern white pine, yellow-poplar and sugar maple, species-mean properties were taken from the Wood Handbook (12), as a test of the general applicability of the solution given above. It was found that the solution was rather sensitive to the friction angle (β) and that it was necessary to use values derived from the cutting force components, as physical values were not available. This point is discussed later. The friction angles are included in Table 6 together with the values for mechanical properties, for all six species at two moisture contents.

For the matched material theoretical curves for P as a function of cutting angle are compared with plotted experimental values for cutting angles from 20 to 40 deg., and nominal chip thicknesses of 0.010 and 0.030 in. in Figs. 31 and 32. For the other material a similar comparison is made at a nominal chip thickness of 0.030 in. in Fig. 33. Figs. 34 - 36 show, for the matched material, a comparison of theoretical curves for P as a function of

TABLE 6

MECHANICAL AND PHYSICAL PROPERTIES
USED IN COMPUTATIONS BASED ON EQUATIONS (3) AND (39)

Species	Moisture Content	Young's Modulus (10^3 lb. per sq. in.)		Tensile Strength Parallel to Grain lb. per sq. in.	Shear Strength Parallel to Grain lb. per sq. in.	Cutting Friction Angle, deg.
		E_L	E_T			
Sugar pine	4%	1,545	62.45	13,800	850	31.6
	Sat.	1,330	27.4	10,200	530	28.4
Yellow birch	4%	2,050	115.6	27,900	1,600	27.4
	Sat.	1,420	32.0	17,200	710	23.2
White ash	4%	1,440	130.8	21,100	1,940	37.5
	Sat.	1,250	69.0	11,900	1,020	24.6
Eastern white pine	5%	1,240	50.3	13,000	1,090	33.9
	Sat.	1,000	23.0	4,900	680	31.3
Yellow-poplar	5%	1,580	68.0	14,800	1,430	24.6
	Sat.	1,220	28.1	10,000	790	35.9
Sugar maple	5%	1,830	110	16,910	2,820	37.9
	Sat.	1,550	35.6	24,140	1,460	29.6

Fig. 31. Comparison of theoretical relationship between cutting force and cutting angle with experimental points : matched material. Nominal chip thickness 0.030 in., width of cut 0.25 in.

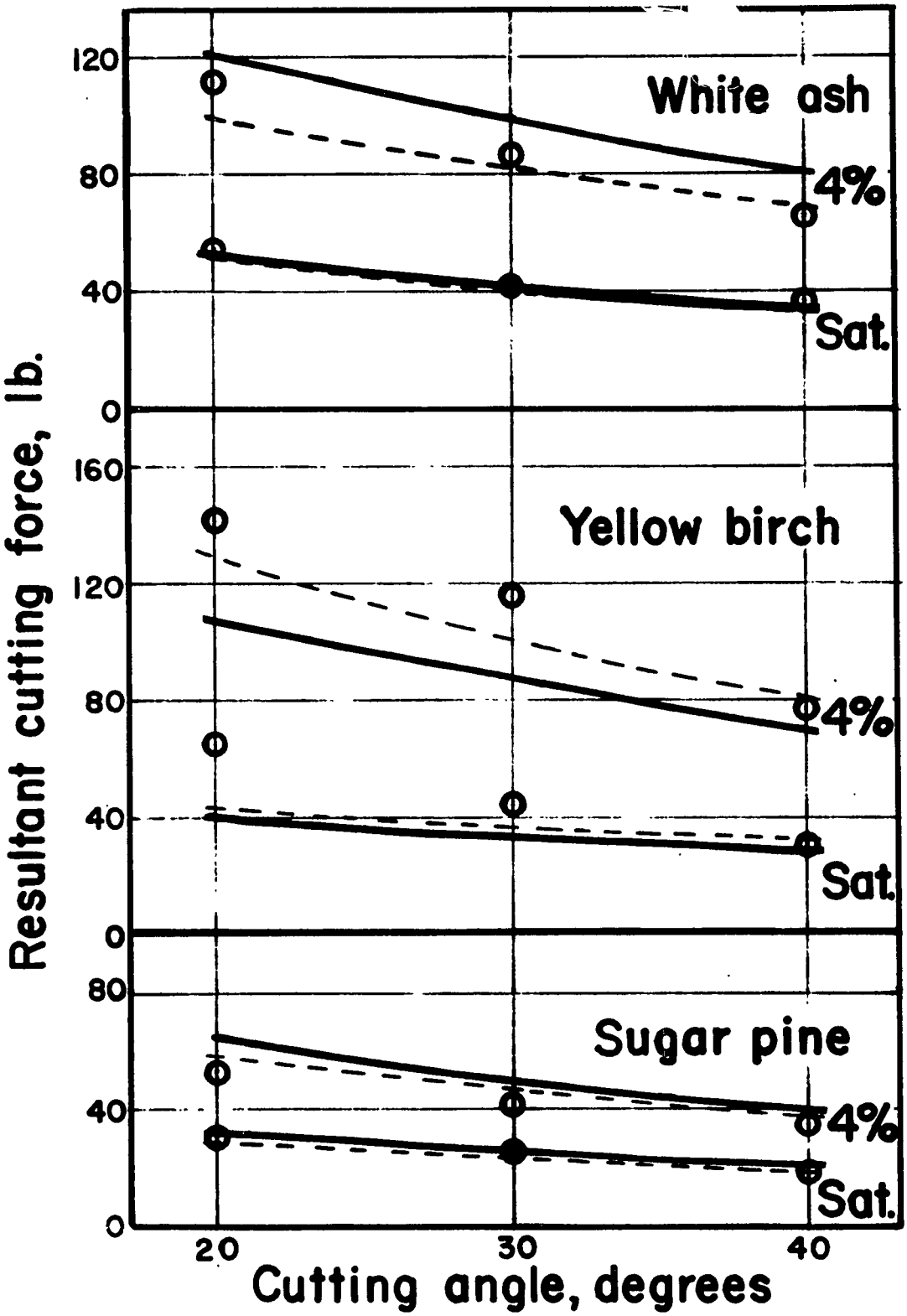

White ash
4%
Sat.
Yellow birch
4%
Sat.
Sugar pine
4%
Sat.
Resultant cutting force, lb.
120
80
40
0
160
120
80
40
0
80
40
0
20
30
40
Cutting angle, degrees
Computed from properties of matched material
" " species—mean properties

Fig. 31

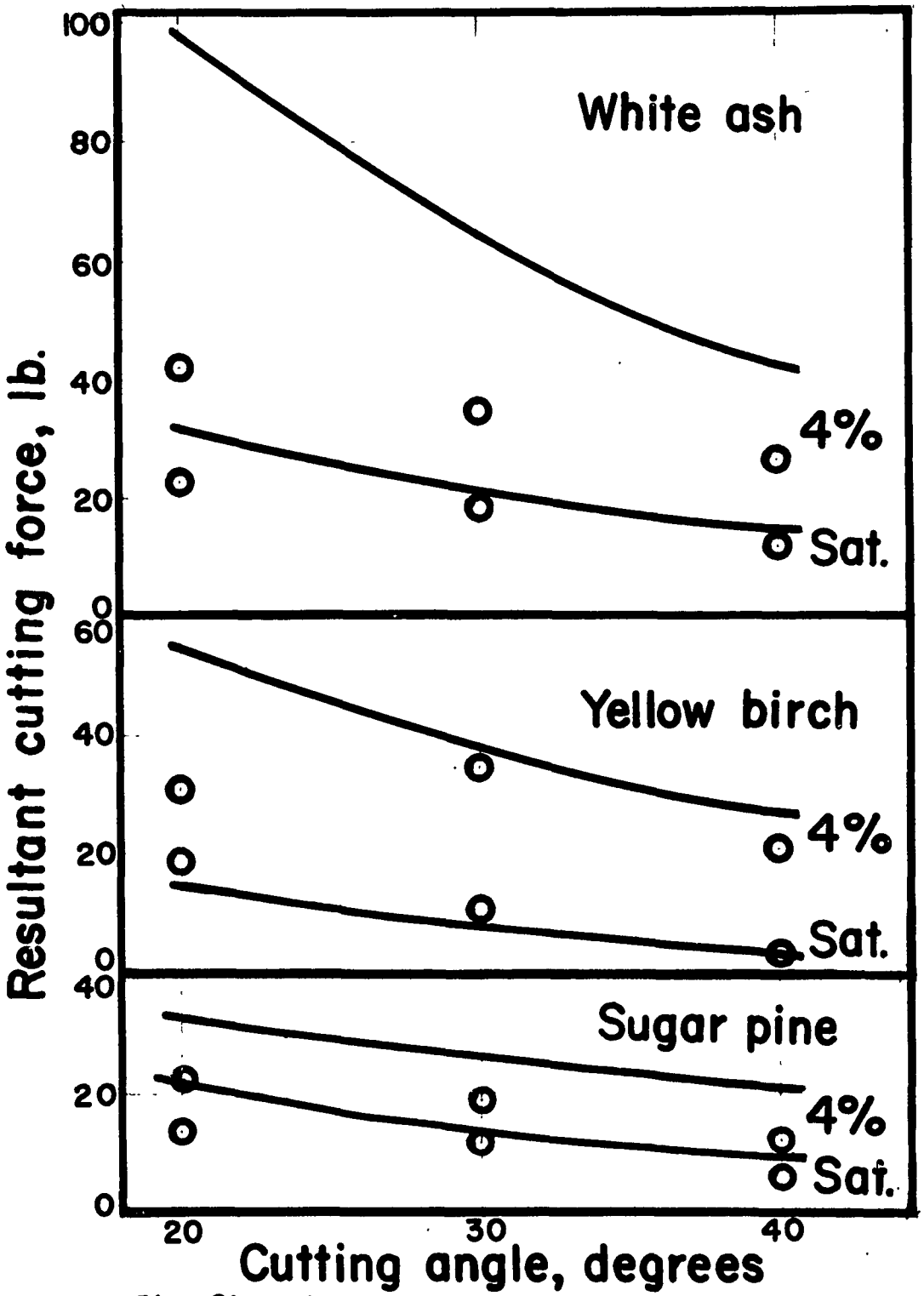


Fig. 32. Comparison of theoretical relationship between cutting force and cutting angle with experimental points : matched material. Nominal chip thickness 0.010 in., width of cut 0.25 in.

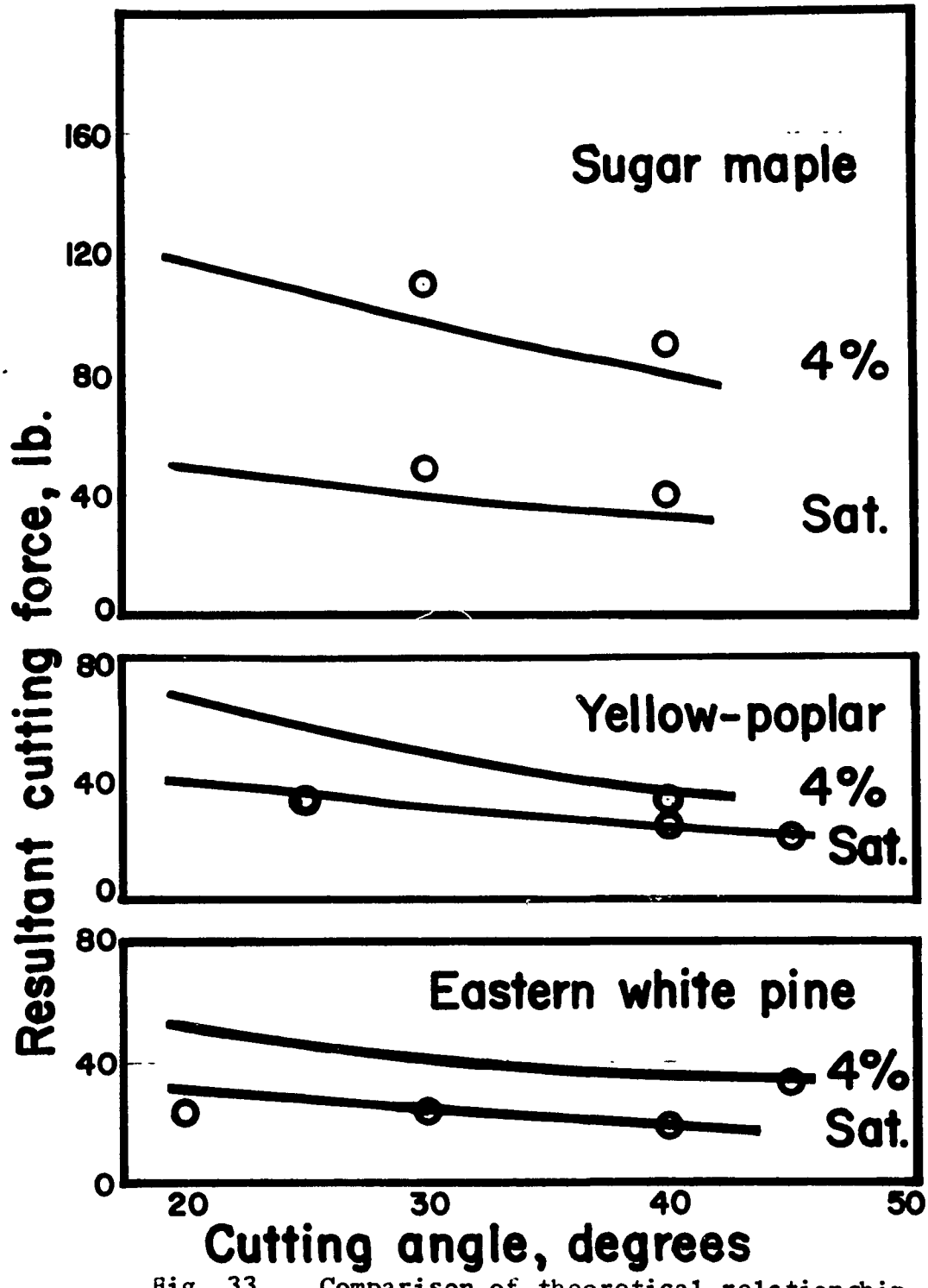


Fig. 33. Comparison of theoretical relationship between cutting force and cutting angle, based on species-mean properties, with experimental points. Nominal chip thickness 0.030 in., width of cut 0.25 in.

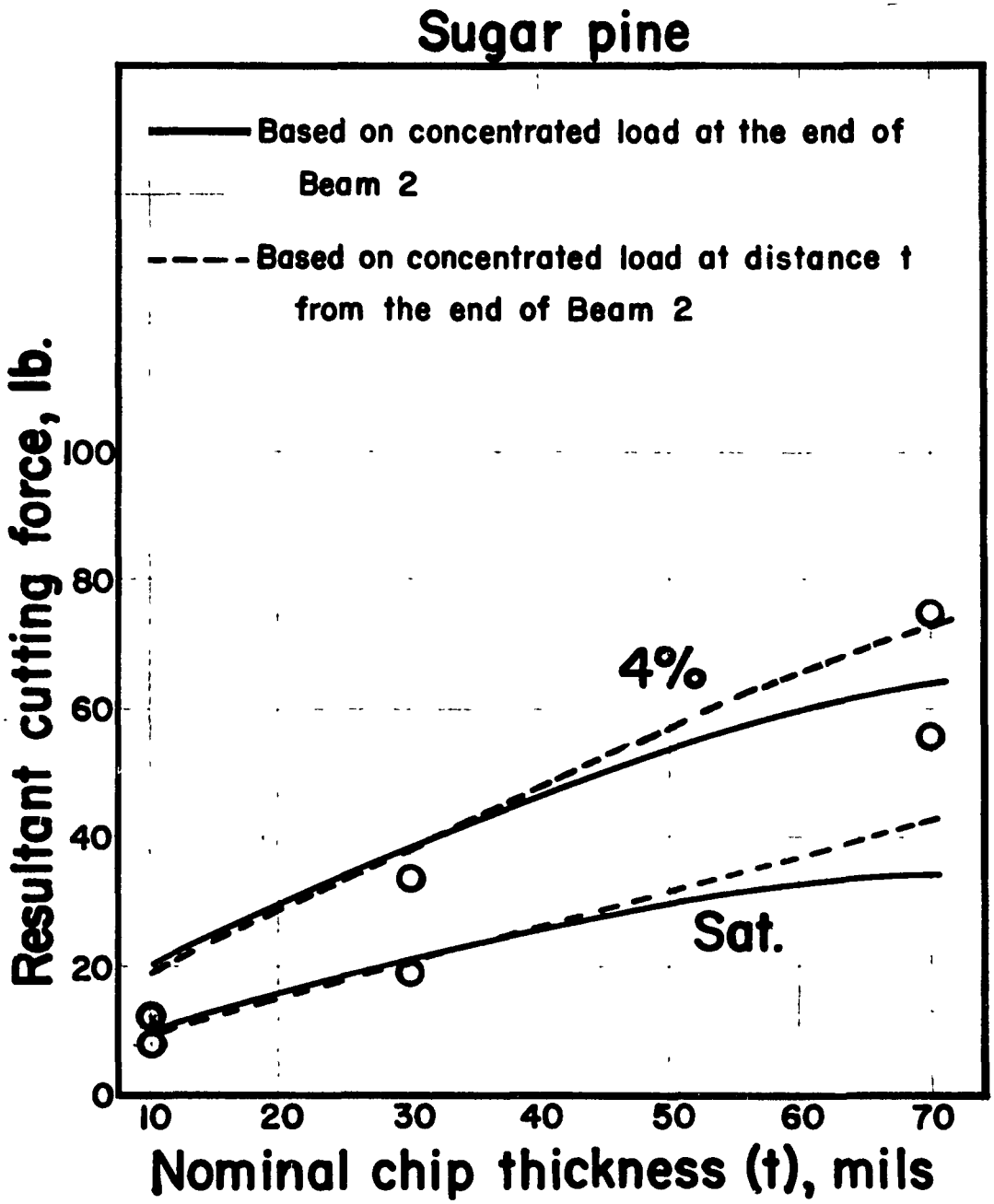


Fig. 34. Comparison of theoretical relationship between cutting force and nominal chip thickness with experimental points : sugar pine. Cutting angle 40 deg., width of cut 0.25 in.

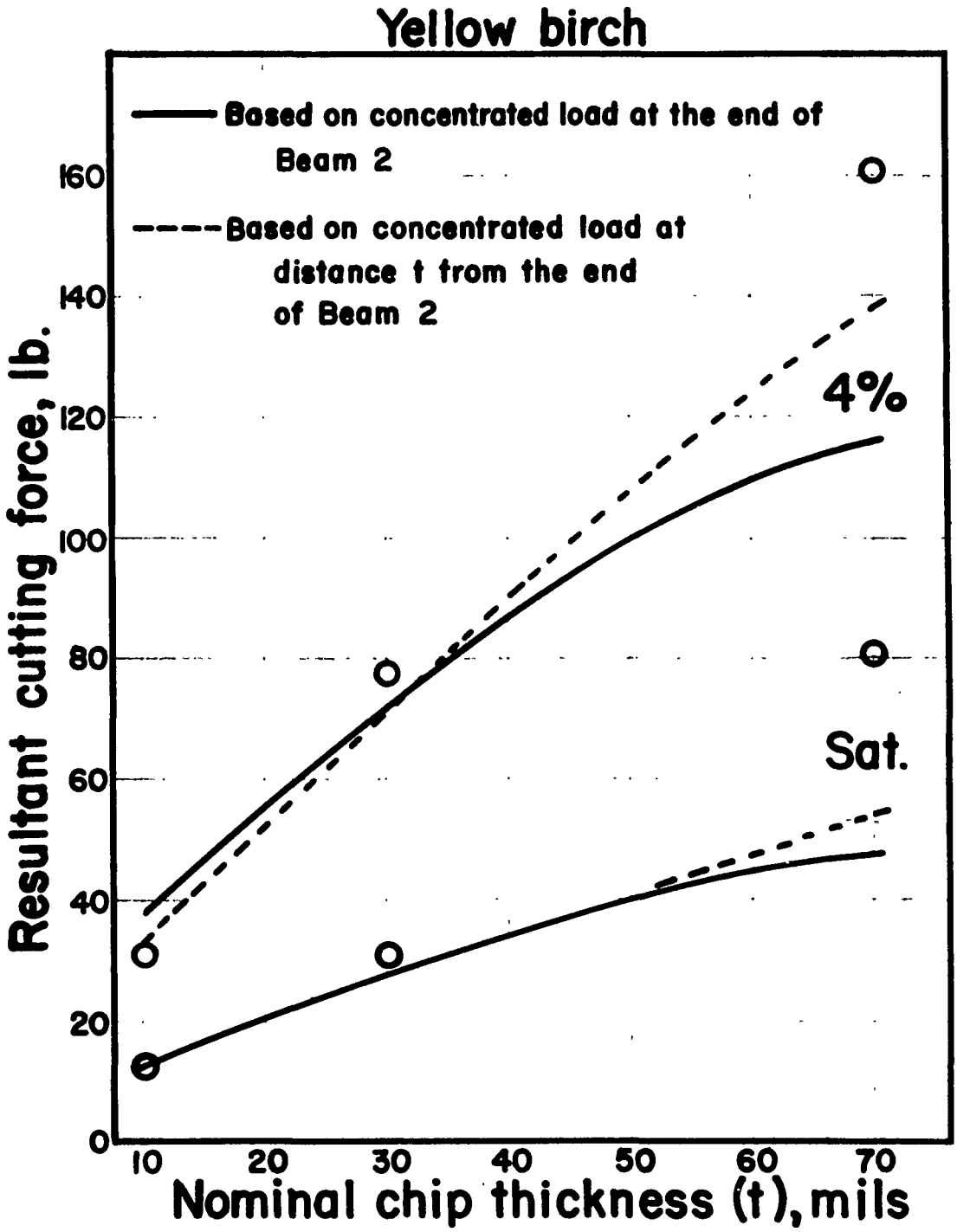


Fig. 35. Comparison of theoretical relationship between cutting force and nominal chip thickness with experimental points : yellow birch. Cutting angle 40 deg., width of cut 0.25 in.

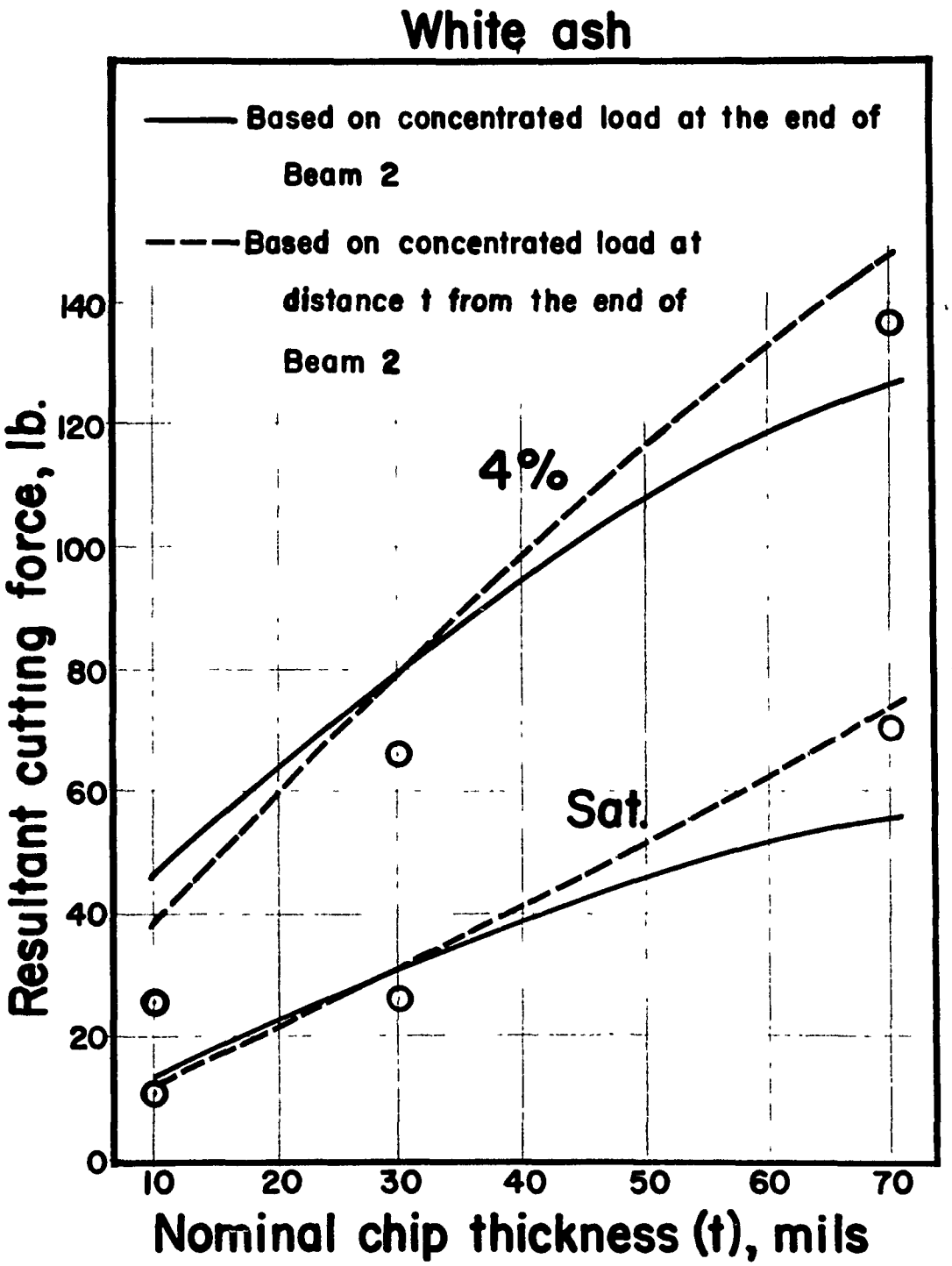


Fig. 36. Comparison of theoretical relationship between cutting force and nominal chip thickness with experimental points.: white ash. Cutting angle 40 deg., width of cut 0.25 in.

nominal chip thickness with plotted experimental values.

Discussion of Double-beam Model

Comparing the theoretical and experimental results for a nominal chip thickness of 0.030 in., in Figs. 31 and 33, there is evidence that the double-beam model responds correctly to variation in cutting angle over the range studied. In all species at both moisture contents, except in the case of yellow birch, the theoretical curves run roughly parallel to the trend of the plotted experimental points. Considering that the material varied over an air-dry specific gravity range of 0.35 to 0.63, a moisture content range of 4 per cent to saturated, a (cutting) friction coefficient range of 0.43 to 0.78, a range of the ratio E_T/E_L from 0.02 to 0.065, and considering the 20 - 30 per cent coefficient of variation of properties within a species, general correspondence is regarded as very good. In the case of the material for which only species-mean values for mechanical properties were available, fit of the theoretical curves to observed values is better than for the matched material. This adds support to an explanation of the discrepancies between theoretical and experimental results, suggested by the following discussion of factors influencing the theoretical curves.

In the solution for P_x (equation (39)) an important factor affecting both the general height and general slope of the theoretical curves of Figs. 31 - 33 is the factor a. This may be seen by considering partial

derivatives.

In equation (39), b^2 is much smaller than $4ac$ so that this equation may be approximated by

$$P = \frac{b}{2a} + \sqrt{\frac{c}{a}} \tag{40}$$

Using this equation the partial derivative of P with respect to a is

$$\frac{\partial P}{\partial a} = -\frac{1}{2a^2}\left(b + \sqrt{ac}\right) \tag{41}$$

Since this has a numerical value of the order 10^3, it is apparent that a is dominant in determining the level of P in Figs. 31 - 33.

The slope of the curves in Figs. 31 - 33 is indicated by the partial derivative of (40) with respect to b, and this is

$$\frac{\partial P}{\partial b} = \frac{1}{2a} \tag{42}$$

Hence the average slope over the range is seen to be dependent mainly on the factor a. Equation (38) shows that a involves principally the ratio E_2'/E_2 and the quantity E_2' expressing the reaction of the foundation. E_2' is proportional to E_T. E_L, to which E_2 is equal, is comparatively reliable as obtained experimentally by standard test, but in the present case, because of material availability, it was necessary to use sub-standard size

specimens. Particularly in yellow birch, buckling was apparent and probably reduced the observed values for Young's modulus. However, it is known (25) that E_T (or E_R) is even more sensitive to specimen size and shape, and is much more variable betwen replicates than E_L. Since the values used were based on only three specimens of sub-standard size, it is possible to suggest that the tests on the matched specimens did not provide a close estimate of the properties of the specimens used in cutting tests. Under such conditions, the species mean, based on many more specimens of standard size, may offer a better estimate of the property than a few measurements of matched specimens. It is to be noted that in the case of both yellow birch and white ash the ratios of E_T/E_L obtained from Table 6 are very different from the values given in the Wood Handbook (12), and in each case the experimental data were better fitted by theoretical curves based on the species-mean values, which are shown dashed in Fig. 31.

Equation (40) suggests that cutting forces increase with the value of c, though its effect is not as great as that of a, since the partial derivative of P with respect to c is given approximately by

$$\frac{\partial P}{\partial c} = \frac{1}{\sqrt{a}} \tag{43}$$

which is smaller than $\frac{\partial P}{\partial a}$ as given in equation (41) since a is much less than unity. In view of equation (43) the

effect of c on the slope of the curves in Figs. 32 and 33 is slight. The expression for c involves E_1', which is a function of E_T/E_L, and hence the latter ratio has some slight inverse effect on P. It also involves the tensile strength, indicating an increase of P with increasing tensile strength. Again, tensile strength is highly variable, and for the matched material was based on a few specimens of sub-standard size, so that it is possible that some error in the theoretical curves was introduced here, affecting principally their levels with respect to the experimental points.

It is evident from the expression for b in equation (38) that variations of the friction angle β, have the same effect as α, the dependent variable in Figs. 31 and 33. The friction angle β may vary over much the same range (20 - 40 deg.) as was used for α, so that theoretical curves plotted with β as abscissa, with α constant, would have a somewhat similar appearance as those in Figs. 31 - 33. Since the effect of β is thus considerable, it was found necessary to use values of β_c experimentally determined for the material being cut. β_c is the cutting friction coefficient given by equation (8) - that is it depends on cutting conditions in addition to the true friction coefficient as discussed earlier. It is known (21) that the cutting friction coefficient normally decreases with cutting angle, but the relationship has not been precisely established, and in any case data on physical friction coefficients for wood are very few. As shown in

Table 7, at 0.030 in. chip thickness the cutting friction coefficients showed little regular change in the range from 20 to 40 deg. cutting angle, and it is apparent that variation in β_c was mainly associated with wood species and moisture content. Since it was desirable to adopt a single value for each species and moisture content, the mean value of β_c associated with maximum P_x on the recording charts, at 40 deg. rake angle and 0.030 in. chip thickness, was used to compute each curve. In so doing, the effect of edge radius is at least partly taken into account, but effects due to varying cutting angle and chip thickness are not. However, these differences were small for the work-sharp cutters used. The problem of the specific effect of edge radius and blunting on cutting forces is side-stepped at this juncture, being regarded as requiring a separate investigation of considerable magnitude. However, some method of measuring friction must be used to take account of the variation with species and moisture content.

In Fig. 32, P is plotted against cutting angle for 0.010 in. nominal chip thickness, and it is evident that the fit of the theoretical curves is not as good for 0.030 in. chip thickness, especially in the case of the dry wood. Discrepancies could be partly explained as for 0.030 in., and by the difficulty, in dry wood, of preparing a surface free of faults that will not affect a cut at this chip thickness. However, when, at a fixed cutting angle of 40 deg., P is plotted against nominal chip thickness up to

TABLE 7

EFFECT OF SPECIES, MOISTURE CONTENT AND CUTTING ANGLE ON CUTTING FRICTION COEFFICIENTS

Nominal chip thickness 0.030 in.

Species	Moisture Content	Cutting Angle, Deg.		
		20	30	40
Sugar pine	4%	31.6	32.1	24.1
	Sat.	28.4	28.0	23.3
Yellow birch	4%	27.4	25.6	28.1
	Sat.	23.2	24.1	20.5
White ash	4%	37.5	39.2	35.2
	Sat.	24.6	23.9	21.4

0.070 in., as in Figs. 34 - 36, it is apparent that the double-beam model as described above does not respond correctly at high chip thicknesses. At a chip thickness of 0.070 in., the theoretical values for P are much smaller than the observed values. Speaking in terms of the model, this would require that one of the two beam systems should, at the higher chip thicknesses, have a higher stiffness. Because of shear deflections the zone above the cutting plane is expected to be actually less stiff than Beam 1 of the model, and hence there remains the possibility that for Beam 2, the deflection Θ might be less at the higher chip thicknesses, than equation (35) requires. It is possible to argue that with increasing chip thickness it is less feasible to consider Beam 2 as having a concentrated load at its end, and that some modification is necessary to account for the actual loading. Considering equation (34), for a concentrated load at a distance from the end, the factor $(e^{-\lambda t}\cos\lambda t)^2$ is less than unity and decreases with distance from the end (or chip thickness t). However, this factor is uncertain, because it depends on the exact point (with respect to the load point) at which Θ is measured, and further, λ involves the ratio B'/B and the beam height h. Therefore it is difficult to account correctly for the effect of varying t. However, to illustrate the effect of introducing a factor of the form $(e^{-\lambda' t}\cos\lambda' t)^2$, an arbitrary value for λ' was introduced, and a adjusted so that there was no change in P at 0.030 in. chip

thickness (this involved using h = 0.0062 instead of 0.005). Then the new expression for a in equation (38) becomes

$$a = \frac{4370\left(\frac{E_2'}{E_2}\right)^{\frac{1}{3}}\left(e^{-3\cdot6t}\cos 3\cdot6t\right)^2}{E_2'} \qquad (44)$$

On this basis the effect of nominal chip thickness on P is as shown by the dashed curves in Figs. 34 - 36. There is an improvement in fit, though only slight for the green material. The fit could be improved further by additional arbitrary adjustments of h and either the constant λ' or the form of the exponential-trigonometrical factor in equation (44), but this was not considered fruitful theoretically.

Although it has proved necessary to place arbitrary values upon some of the factors introduced by the double-beam model, these are constant throughout, and hence do not reduce the generality of the equations over the considered range of the principal factors. This will be discussed further after a criterion for type II failure based on another beam model has been considered.

CHAPTER 13

CRITERION FOR TYPE II FAILURE BASED ON ELASTICALLY SUPPORTED BEAM

As discussed earlier, the failures in zone (4) characteristic of type II are viewed as being due to combined bending and axial stresses. An attempt may be made to assess the magnitude of the bending stresses by creating a third model beam as indicated in Fig. 37. It is suggested that the shear failures which may occur ahead of the cutter edge are shallow (short in the y direction), and with their ending, the stresses developed at the cutter edge are distributed to a wider zone of wood. It is to be noted that the deflections relative to Beam 2 rapidly become negligible. As remarked by Hetényi (23), this occurs at a distance $\frac{\pi}{\lambda}$ from the loaded point. For Beam 2, with depth 0.005 in., the value of $\frac{\pi}{\lambda}$, obtained using equation (28), is approximately 0.030 in. Hence, below this level, deflections relate to a deeper "beam", and the third model beam, Beam 3, is conceived as being such a beam distinct from Beam 2.

At least in the case of type II(a) the x dimension of the laminae which fail in bending is quite apparent, and corresponds to oscillations in the recorded force

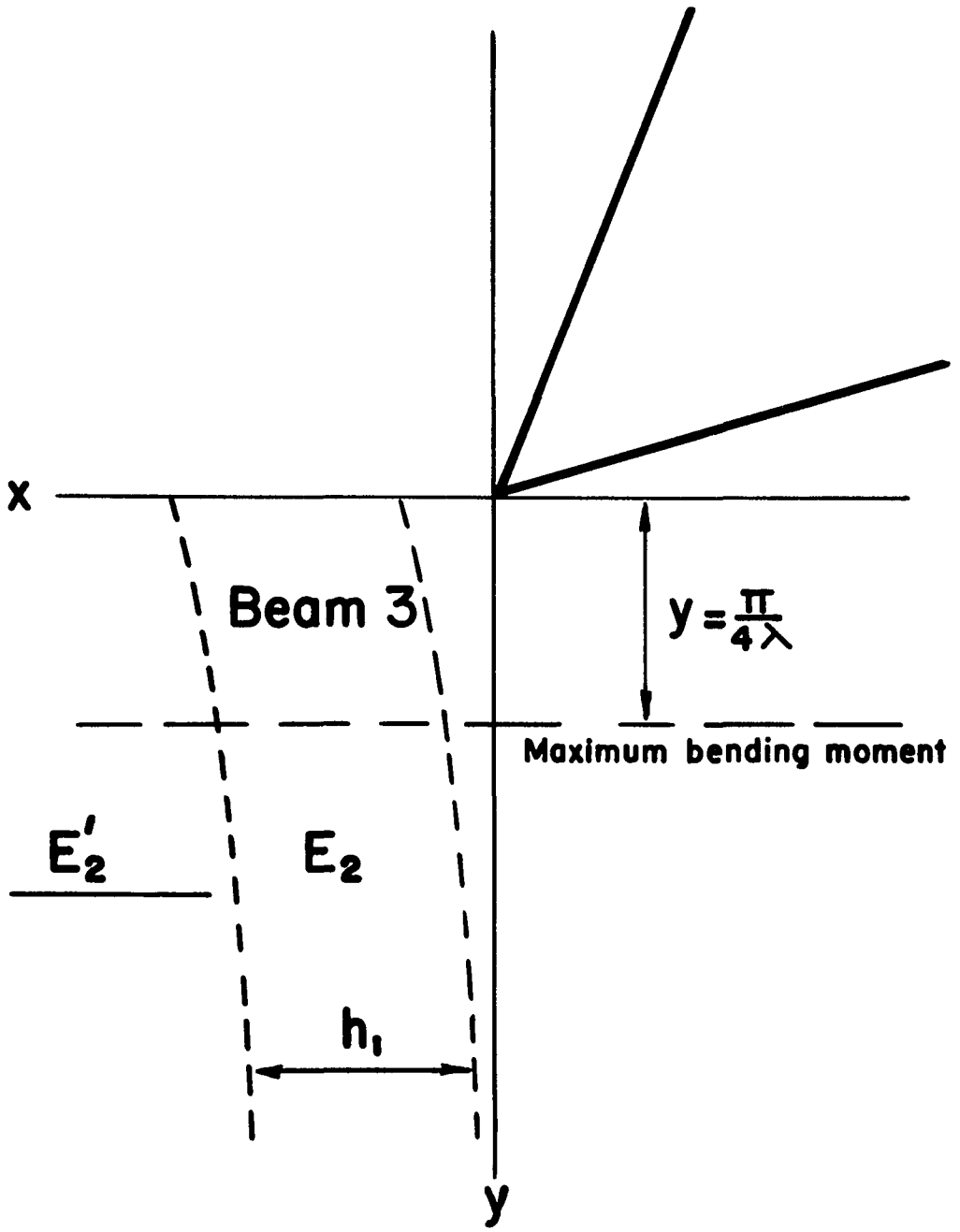


Fig. 37. Criterion for type II failure - Beam 3.

components. Oscillations with wave length of the same order are present in the force recordings in the case of type II(b) failure, and frequently a corresponding oscillation in the level of failure zone (4) below the cutting plane is also apparent. The wave lengths of the force oscillations are recorded in Table 5. They vary from 0.028 in. to 0.047 in., with a mean value of approximately 0.040 in., and this value was adopted for the depth (x dimension) h_1 of Beam 3.

This model beam is again semi-infinite with a concentrated load at its free end, and the bending moment, if axial forces are ignored, is given by (23)

$$M = -\frac{P_x}{\lambda_3} e^{-\lambda_3 y} \sin \lambda_3 y \qquad (45)$$

where λ_3 is the parameter for Beam 3 given by equation (28). The bending moment is at a maximum where

$$\frac{dM}{dy} = P_x e^{-\lambda_3 y} (\sin \lambda_3 y - \cos \lambda_3 y) = 0$$

that is, where

$$\sin \lambda_3 y - \cos \lambda_3 y = 0 \ ,$$

$$\tan \lambda_3 y = 1 \ ,$$

$$y = \frac{\pi}{4\lambda_3}$$

Thus, in view of equation (28) the point of maximum bending moment for Beam 3 is given by

$$y = \frac{\pi}{1.18} \frac{h_1}{\left(\frac{E_2'}{E_2}\right)^{\frac{1}{3}}} \tag{46}$$

using the same values for E' and E as for Beam 2.
Thus the distance of zone (4) below the cutting plane is given as a function of h_1 and the ratio $\left(\frac{E_2'}{E_2}\right)^{\frac{1}{3}}$. The maximum bending moment is

$$M_{max} = -\frac{P_x}{\lambda_3} e^{-\frac{\pi}{4}} \sin\frac{\pi}{4} \tag{47}$$

Elementary beam theory gives

$$\sigma_{y_{max}} = \frac{M}{Z} ,$$

where in this case $Z = \frac{bh_1^2}{6}$

Applying this to (47),

$$\sigma_{y_{max}} = \frac{6}{bh_1^2} P_x e^{-\frac{\pi}{4}} \sin\frac{\pi}{4}$$

and using Biot's expression for λ_3 given in equation (28)

$$\sigma_{y_{max}} = \frac{6 \times 0.322}{1.18} \cdot \frac{P_x}{bh_1\left(\frac{E_2'}{E_2}\right)^{\frac{1}{3}}}$$

$$= 1.64 \frac{P_x}{bh_1 \left(\frac{E_2'}{E_2}\right)^{\frac{1}{3}}} \qquad (48)$$

It is evident from equation (48) that if bending only is considered, the maximum bending stress would increase with force and hence with decreasing cutting angle. Thus cutting angle would have a greater influence on incidence of type II failure than is apparent from observation, and in particular would indicate a type II failure in some of the saturated specimens at cutting angles of 30 deg. or lower. One possible factor is the normal cutting force component, which would superimpose an axial stress on Beam 3, and at the lower cutting angles this stress would be compressive, thus reducing the tension stress at the convex face of Beam 3. The difficulty in taking this stress into account is to decide its distribution. The normal component cannot be considered as distributed uniformly over the end of the beam, as is normally assumed, since it is concentrated mainly toward the tension side.

Experimental stress analysis would be required to provide a firm basis for deciding the distribution of the axial stress at the level of zone (4). However, to observe the effect on the theoretical maximum stress of an assumed distribution, the normal component was considered to be uniformly distributed over the tension half, or 0.020 in. of the beam depth, so that the maximum tension stresses would be as given by the equation

$$\sigma_{max} = 1.64 \frac{P_x}{bh_1\left(\frac{E_2'}{E_2}\right)^{\frac{1}{3}}} - \frac{P\tan(\beta-\alpha)}{\frac{bh_1}{2}} \qquad (49)$$

The effect of doing so is shown in Table 8 which compares the theoretical maximum tension stress, considering bending alone, and considering combined stresses, with the tensile strength of the wood. The failure type is also given.

Discussion

Considering entries in the last three columns of Table 8 for 40 deg. cutting angle, it is evident that, where the theoretical maximum stress approaches or exceeds the tensile strength of the material, type II failure can generally be expected. There are cases where this is not so, but the values are within a few per cent and hence within reasonable limits of error. In the case of yellow birch and white ash at 4 per cent, it is to be noted that the estimated forces, on which the theoretical stresses are based, were considerably in error, as indicated by Fig. 31. Brittle failure was evident in some tensile specimens in ash, and since brittle material may have been irregularly distributed, it is possible that the tensile values given for tensile strength were not representative of the material cut. In the case of green material, it is evident that the theoretical maximum bending stresses tend to exceed the tensile strength at low cutting angles and this criterion would require type II failure where type I failure is observed. It appears from observation that the wood fails in shear in a wide zone ahead of the cutter due

TABLE 8(a)

COMPARISON OF THEORETICAL MAXIMUM STRESSES WITH TENSILE STRENGTH

Nominal chip thickness 0.030 in.

Species	Moisture Content	Cutting Angle deg.	Theoretical Stresses: Maximum Bending Stress p.s.i.	Theoretical Stresses: Combined Bending and Axial Tensile Stress p.s.i.	Tensile Strength p.s.i.	Failure Type
Sugar pine	4%	20	16,910	16,110	13,770*	II(a)
		30	13,220	12,900		II(a)
		40	11,380	12,470		II(a)
	Sat.	20	10,800	10,480	10,240*	-
		30	8,870	9,030		I(a)
		40	6,940	7,680		I(a)
Yellow birch	4%	20	34,650	30,050	27,860*	II(a)
		30	27,500	29,040		II(a)
		40	22,550	22,920		I-II(a)
	Sat.	20	15,310	15,230	17,150*	I(a)
		30	13,070	13,890		I(a)
		40	11,950	13,890		I(a)
White ash	4%	20	22,980	17,650	21,140*	II(b)
		30	19,230	16,590		II(b)
		40	15,940	17,080		II(a) II(b)
	Sat.	20	14,120	11,640	11,863*	I(a)
		30	11,070	11,930		I(a)
		40	8,860	10,620		I(a)

* obtained from tests on matched material

TABLE 8(b)

COMPARISON OF THEORETICAL MAXIMUM STRESSES WITH TENSILE STRENGTH

Nominal chip thickness 0.030 in.

Species	Moisture Content	Cutting Angle deg.	Theoretical Stresses: Maximum Bending Stress p.s.i.	Theoretical Stresses: Combined Bending and Axial Tensile Stress p.s.i.	Tensile Strength p.s.i.	Failure Type
Eastern white pine	5%	30	11,700	11,200	13,000+	I(b) II(a)
		40	9,920	11,220		I(b) II(a)
	Sat.	30	8,900	8,790	9,300+	I(a)
		40	7,050	7,640		I(a)
Yellow-poplar	5%	30	14,740	15,670	14,800+	II(a)
		40	10,830	12,810		II(a)
	Sat.	30	9,270	8,760	10,000+	I(a)
		40	7,790	8,110		I(a)
Sugar maple	5%	30	27,770	24,910	24,140+	II(b)
		40	21,570	22,160		II(b)
	Sat.	30	14,830	14,880	16,910+	I(a)
		40	12,240	13,460		I(a)

+ Species averages obtained from tests on a few specimens by Markwardt and Wilson (26), and others (unpublished).

to large deflections. It is possible that shear failures, occurring near the cutter edge, as discussed earlier in connection with Beam I, extend up and down from the shear plane, and in terms of the model, bending may cause Beam 3 to fail in shear, rather than in tension on the convex side.

Yellow birch shows less tendency to type II failure, and more tendency to deep splitting than white ash, and it is noted from Table 6 that its shear strength, saturated and dry, is less than ash. The shear strength values of both these species are less than sugar maple and persimmon, which are more prone to type II(b) failure.

Because of the uncertainty as to stress distribution ahead of the cutter, it appears impossible to predict occurrence of shear failure in this zone, and it appears that the criterion based on the beam model is not applicable to saturated wood at cutting angles of 20 deg. and lower.

For the cutting conditions covered in the experimental work, it appears that the best criterion for type II failure is whether the wood is saturated or at 4-5 per cent moisture content. At some moisture contents between these extremes there would be a critical value where a transition between failure types I and II occurs. Previous discussion shows that this point would depend principally on E_T and the ratio E_T/E_L. Unfortunately, no information on the effect of moisture content on these quantities was available to test this point. However, cuts

were made at moisture contents of 8, 12 and 14 per cent in white pine, yellow-poplar and sugar maple. The transition points for white pine and yellow-poplar appeared to be above 12 per cent, and that for sugar maple to be about 12 per cent, since above this the failure was of type I, resulting in a very good surface as shown in Fig. 38. There appear to be two factors contributing to this. The ratio E_T/E_L is in any case lower, and in this species the friction coefficient is also reduced rapidly with increasing moisture content, since Table 7 shows the value to be much higher at 5 per cent than when saturated. On the other hand, Table 7 shows that the friction coefficients for white pine and yellow-poplar are increased or reduced very little as moisture content increases, and consequently their critical moisture contents would be higher.

The role of friction is obscure. It was noted that the relationship between P_y and P_x changed with a transition from one failure type to another, where this occurred in the same specimen. During type I failure, maximum P_x is associated with P_y greatest in the downward (negative) direction, whereas during type II failure, maximum P_x is associated with maximum (positive) P_y. Therefore the friction value associated with maximum P_x is much less in type I than in type II failure. A closer investigation of the factors deciding failure type should take account of changes in frictional phenomena with moisture content, working especially with moisture contents above the critical values.

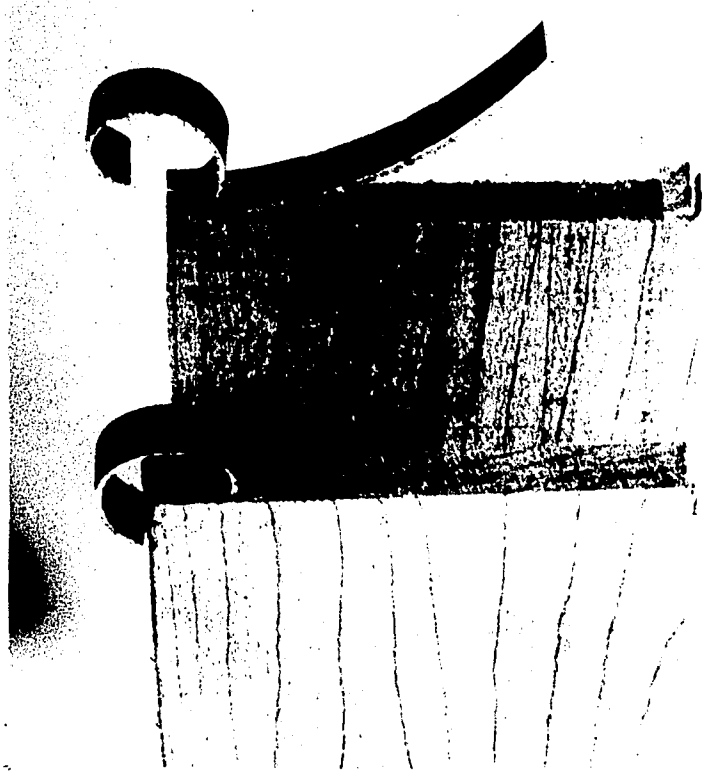


Fig. 38. The effect of moisture content on failure type in sugar maple.
Top: 5 per cent moisture content.
Bottom: 14 per cent moisture content.
Cutting angle 30 deg., nominal chip thickness 0.030 in.

CHAPTER 14

APPLICATION OF THE BEAM MODELS TO CUTTING AT 90^{o}-0^{o} AND 0^{o}-90^{o}

There is no theoretical reason why the double-beam model should not be applied to any situation in which the cutter edge and cutting velocity vector are orthogonal to the axes of symmetry of the wood, using the mechanical properties appropriate to the particular cutting direction. Physically, this model may be more appropriate in the other directions than in 90^{o}-90^{o} cutting. However, it is to be expected that the modes of failure in the other cutting situations will be different, and this has been established by Franz (1), McMillan (18) and Leney (3). Thus, although the double-beam model might give the cutting force associated with a failure in tension across the cutting plane at the cutter edge, where such a failure is appropriate, in situations other than at 90^{o}-90^{o} this force will not usually represent the maximum. Again it is necessary to investigate the relationship between the cutting force and the stresses at each zone of potential failure, and this was not considered to be part of the present study. Nevertheless, brief consideration was given to the 90^{o}-0^{o} and the 0^{o}-90^{o} cutting situations with a view to making suggestions as to

the application of the theory of the elastically supported beam.

Application of the Beam Model to Cutting at 90^{o}-0^{o}

Franz (1) developed an analysis for this situation by considering the zone above the cutting plane as a free elastic body of length equal to the nominal chip thickness (t) and subject to shear and tensile restraint at the cutting plane, both decaying from the cutting edge to zero at distance t. A third reaction is introduced in the form of a bending moment due to stresses at the distance t. To substitute fully for this system with a beam model, Beam 1 must be considered as subject to both lateral and axial loading by the cutter, and to normal and shear reactions at the cutting plane. Because of the stiffness in the x direction, Beam 2 appears to be not necessary, and the resultant of the tensile stresses across the cutting plane can be considered to be perpendicular to it. This model for the 90^{o}-0^{o} situation is illustrated in Fig. 39. In this case the model beam is readily identified with reality since the zone above the cutting plane is strongest in the x direction and its behaviour can be expected to be more typical of a beam.

If a possible interaction between the axial component and lateral deflection is ignored, a resultant force P acting on this model has two components, one producing lateral deflection and bending of the beam model, the other producing axial compression, and shear in the cutting plane.

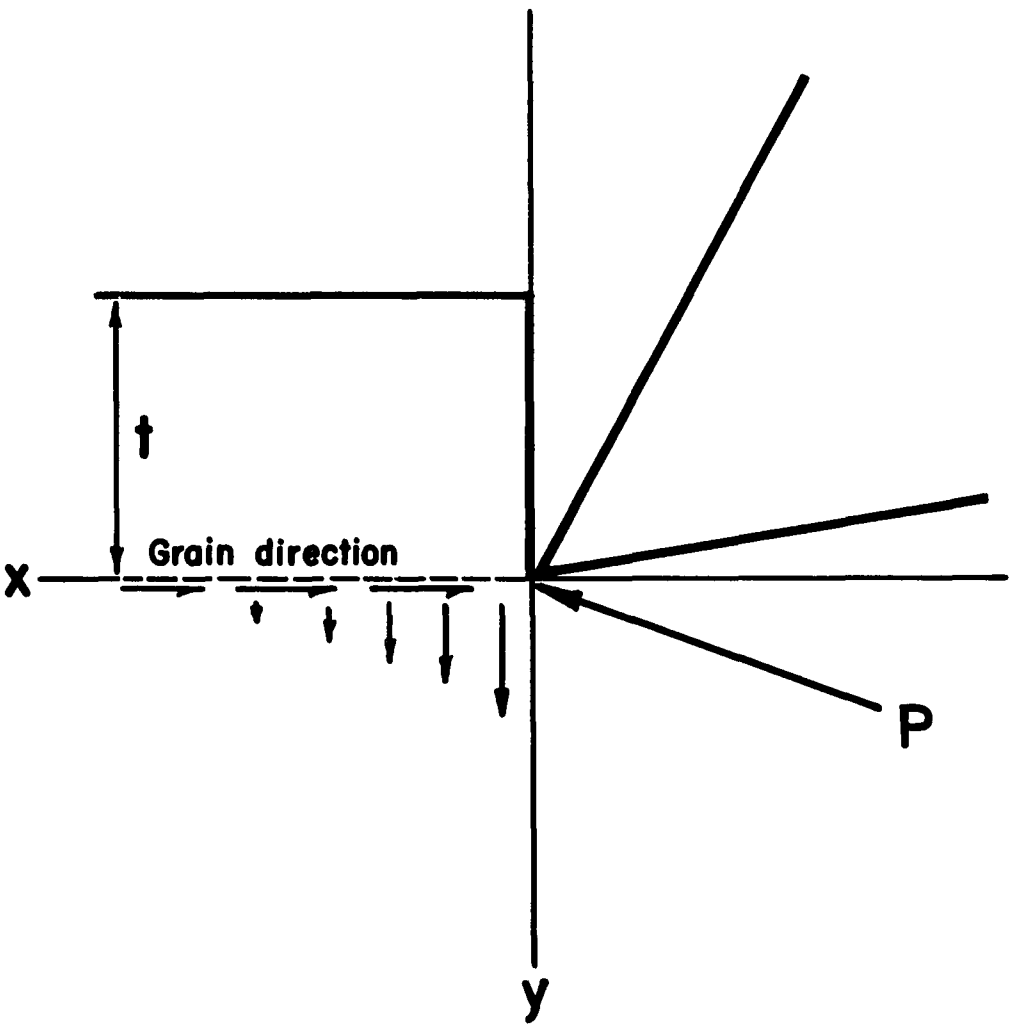


Fig. 39. Model for 90°-0° cutting situation.

The equation for bending is similar to equation (24). The axial and shear stresses are interdependent in a way such that all the axial force is transmitted to the workpiece by shear along the cutting plane. This relationship may be derived by considering Fig. 40 which shows a bar of width b and depth t, subject to an axial force P_x distributed uniformly over its end. The only reaction is due to the foundation exerting a shear force on the bar at its lower face.

The compression force in an element ΔX of the bar is given by

$$P' = - bt E \frac{\partial u}{\partial x} \tag{50}$$

where $\frac{\partial u}{\partial x}$ is the strain in the element, and E is the Young's modulus in compression. The reduction in compression stress across the length of the element is solely due to shear on its bottom face, resulting from the displacement (u) of the element from its original position. Thus

$$\frac{\Delta P'}{b \Delta x} = - C u$$

or,

$$\frac{dP'}{dx} = - Cbu \tag{51}$$

where C is a constant relating the displacement u and the shear stress.

Eliminating P' from (50) and (51) gives

$$\frac{d^2u}{dx^2} - \frac{C}{tE} u = 0,$$

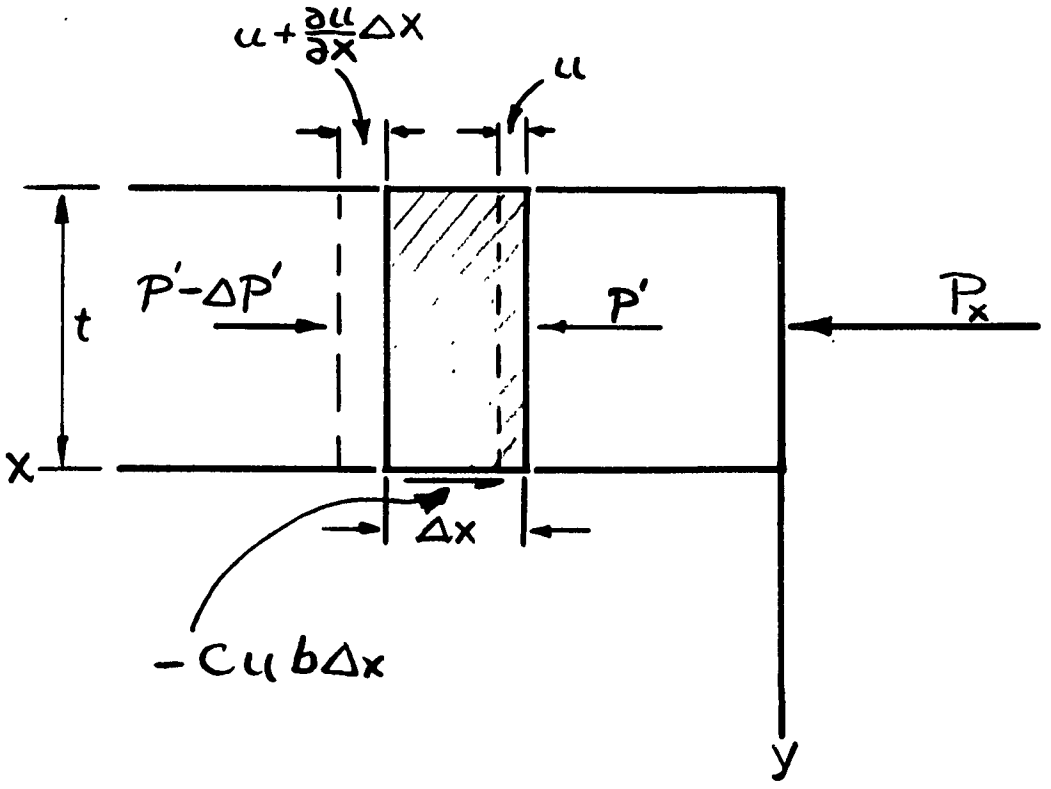


Fig. 40. Relationship between axial force and shear at cutting plane in model for 90°-0° cutting situation.

or

$$\left.\begin{aligned} &\frac{d^2u}{dx^2} - \eta^2 u = 0 \\ &\text{where} \\ &\eta^2 = \frac{C}{tE} \end{aligned}\right\} \quad (52)$$

The general solution of (52) is

$$u = Ae^{\eta x} + Be^{-\eta x} \quad (53)$$

Since the displacement u diminishes to zero as x becomes infinite, the constant A is required to be zero.

By differentiating (53) the strain is given by

$$\frac{du}{dx} = -\eta e^{-\eta x}$$

and at x = 0, where $P' = P_x$ this is prescribed by equation (50). Thus,

$$\frac{du}{dx}_{(x=0)} = -\eta B = \frac{P_x}{btE}$$

so that

$$B = \frac{-P_x}{\eta btE}$$

Hence,

$$u = \frac{P_x}{\eta btE} e^{-\eta x} \quad (54)$$

relating displacements in the x direction to the axial force.

For $x = 0$,

$$u_o = \frac{P_x}{\eta b t E} , \qquad (55)$$

relating the displacement at the end of the beam to P_x. The resultant cutting force P is given by

$$P = \frac{E b t \eta u_o}{\cos(\beta - \alpha)} \qquad (56)$$

This equation and equation (33) provide two expressions for P. In principle they could be used to assess whether a failure in bending, compression or shear may occur first, but the difficulty is to provide a value for η which embodies C, the constant relating displacement u and the shearing stress.

Further, the problem becomes one of elastic stability under some conditions, involving new considerations. Investigation of these two points was considered too great a diversion from the main theme for the application of the above theory to be pursued further.

Application of the Beam Model to Cutting at 0^o-90^o

If the transverse axes of symmetry are orthogonal to the x and y axes of Figs. 29 and 30, the double-beam model appears to represent the 0^o-90^o cutting situation, and here Beam 2 should be retained to account for angular deflections near the cutter edge. Again in this situation the physical identity of the beams is not clear, but a starting point is to consider Beam 1 to have depth equal to the nominal chip thickness t, and Beam 2 to have a depth equal

to the spacing of the "veneer checks" which commonly occur in this cutting situation.

On this basis a theoretical value for P was calculated using equation (38), for comparison with the experimental results from cutting saturated birch in the tangential direction at 45 deg. cutting angle and 0.050 in. nominal chip thickness. Since the anisotropy is only of the order of 2 to 1, the B'/B ratios were not corrected for anisotropy. The friction coefficients and mechanical properties were taken from Franz (1). The computed value of 4.5 lb. for P compared with the minimum value of the parallel force component taken from the recording chart. This was to be expected since in this case there was little deflection of wood before the edge, of the type described by Leney (3). The failure was of the type A ascribed by McMillan (18) to failure as a beam. The failure of Beam I at its point of maximum bending moment was considered, and computations using equation (48) gave a force of 20 lb., which compared with a maximum force from the recording chart of 21 lb. Failure by continuous shear (Type B (18)) might be treated by using equation (3) derived from metal cutting, and equation (35) relating to Beam 2 of the double-beam model. This brief consideration suggests that a beam model may prove useful in considering the modes of failure in this cutting situation.

PART V

CHAPTER 15

GENERAL DISCUSSION

Although lack of knowledge concerning stress distribution and material properties make some of the assumptions involved in the beam models difficult to justify, it is nevertheless concluded that the resulting equations include the important variables affecting cutting, in a way that has some resemblance to reality over certain ranges of cutting conditions. The analytical results for 90^{o}-90^{o} are considered to be of practical use in predicting cutting forces. For instance, an estimate of the maximum force required for a saw tooth in a ripping cut might be made by adding terms to P as estimated from equation (38). One important term would involve friction at the sides of the unsevered chip due to lateral spreading, obtainable from Poisson's ratio. The remaining important term would involve friction of the severed sub-chips.

The results for cutting at 90^{o}-90^{o} confirm Antoine's contention (19) that cutting in this direction is inefficient, involving high deformation and damage. However, there are indications that these deficiencies may be reduced by control of moisture content and friction, or by introducing

a lateral component in the velocity of the cutter.

Models based on the elastically supported beam appear to have application in the other cutting situations orthogonal to the axes of symmetry, especially since deflections are not so great before failure occurs. The cutter is not attempting to dictate failure in the strongest direction of the material, and failures are more simply related to the cutting conditions. Thus the model developed for a particular cutting situation (90^{o}-90^{o}) appears to have limited but important generality, in that it may have application to the other principal cutting directions.

Probably one of the principal defects of these models is that they do not take shear stresses fully into account. The modulus of rigidity is involved in the use of Green's theory (22) to adjust the foundation modulus, but it was not possible to assess the influence of shear stresses on failure. As a result, the occurrence of shear failures in zone (5) to form laminae could not be dealt with. Further, the tendency for shear failure to occur, instead of type II failure in zone (4), at cutting angles below about 20 deg. in saturated wood, could not be predicted. The assumption that failure at the cutter edge is due to tension parallel to the fibres appears to have some connection with reality, but because of arbitrary factors introduced, it is possible that this is due to correlation of tensile strength parallel to the grain with some other property. One possibility is that a shear failure of a plastic type may

occur in the highly densified and compressed area near the cutter edge, and that this is related to tensile strength. However, nothing is known concerning the failure of wood in this way, or of the distribution and stressing of the densified zone.

Although the present analysis recognized an edge of finite radius, and its success testifies to the importance of edge rounding, edge radius is not directly taken into account. It is implicated in the use of experimentally determined cutting coefficients of friction, but no direct relation between edge condition and stresses is provided. This appears to require a special experimental study, with positive control of edge shape.

The analyses presented here, like previous analyses such as those of Voskresenski (6) and Franz (1) have been based on deductions from observations of failures in the region of the cutter edge. Their soundness depends to an important extent on the accuracy of assumptions made concerning the stresses causing failure. To test their validity more fully, an experimental investigation of the relation between the stress distribution and the important cutting conditions, especially in the zones where failure may occur, appears to be necessary. It appears possible, by use of techniques such as application of a grid, photoelastic layer, or brittle coating, to measure the strains in the zones of interest. These strains could be related empirically to the advance of the cutter, the cutting forces,

and the various factors operating. Then the stresses at points of interest may be obtained by applying the stress-strain equations for an orthotropic material (28). Using the failure criterion developed by Norris (17) to derive the force values associated with failure at the various points, the sequence of failure could be related empirically to the factors involved.

Considering the properties indicated by the analysis to be important, equation (38) shows that these are the elastic constants, especially the Young's moduli perpendicular and parallel to the grain (E_T and E_L), tensile strength and coefficient of friction. The string model also placed emphasis on the ratio E_T/E_L. It becomes apparent why density alone is not a good criterion of machinability since these factors are variously related to density. The analysis appears to place correct emphasis on the effect of moisture content, through its effects on E_L and E_T. In its effects on failure type, moisture content is indicated to be as important as species, because of its influence on the ratio E_T/E_L. However, as discussed earlier it is probable that shear properties are also involved here, especially at the lower cutting angles.

Unfortunately almost all of the properties involved in equation (38) are difficult to measure, or are not obtained in standard tests, which have the object of providing data for structural engineering. For instance, data on the influence of moisture content on the ratio of

Young's moduli, and on modulus of rigidity are entirely lacking. Therefore, the task of consolidating the indications of the present work will be considerable, and if they are to be applied in practice, much testing, or correlation with existing standard tests will be necessary. There is also an indication that the standard tests for shear may be unsatisfactory for the present purposes, since the lubrication experiments suggest the possibility that normal stress may, through frictional effects, increase the maximum shear stress sustained at the shear plane.

The frictional properties of wood have had very little investigation, and the work of Atack and Tabor (29) is the only known application to wood of modern concepts of frictional phenomena. Their work suggests that variables such as moisture content may affect the frictional phenomena at the edge and at the face differently. Further such study of frictional phenomena occurring in contact between wood and wood, and wood and metals, as related to wood species, moisture content and normal pressure would contribute greatly to fundamental machining research.

It is felt that the models developed for a particular cutting direction have been valuable in providing a basis for a critical examination of the cutting process, suggesting causes and effects, properties that may be expected to affect the process, and directions for further investigation.

SUMMARY

This research was based on the premise that the diverse wood machining processes have vital problems in common, and that the most basic of these concerns the action of a wedge-shaped cutter on a wooden work-piece, in the simplest possible cutting situation. The object was to investigate how far an analytical study of this simple situation might supply the principal information ultimately required for all machining processes, concerning the forces acting on the tool and the work, the nature of the chip, and the surface formed.

Since evidence concerning the effects of cutting speed on forces and surface formed was contradictory, cutting experiments were carried out using a lathe, at cutting speeds ranging from 0.5 in. to 28,000 ft. per min. The results showed a small linear effect of cutting speed on cutting forces, attributable to chip acceleration, and it was concluded that this factor need not be considered further in developing an analysis.

Because of the extreme anisotropy of wood, it was found necessary to investigate a situation at a particular grain angle, that in which both the cutter edge and velocity vector were perpendicular to the grain. Preliminary observations included cutting force determination and

microscopic study of cutting action, and provided the basis for a classification of modes of chip formation to be accounted for analytically. An important feature revealed was an "indentation phase" involving deformation before incision, associated with the maximum amplitude of the recorded cutting forces. This appeared even with sharp cutters, and was attributed to the existence of a cutter edge radius of the same order as cell wall thickness. On the assumption that incision requires that fibres at a point on the curved edge profile be stressed to their ultimate strength in tension, models were developed to represent the cutting process. The principal models were based on the reactions of an elastically supported beam.

Despite certain limitations of these models, the results for forces and failure types derived from them showed some accord with reality, and are considered to be of practical value in predicting cutting forces and surface quality.

Similar models appear to be applicable to the other important cutting directions in which the cutter edge and cutting speed are orthogonal to the axes of symmetry of the wood, and hence the analysis appears to have limited but important generality.

Other results, with practical implications, suggest that lateral vibration and lubrication may, under certain conditions, modify the indentation phase and greatly improve surface quality. The beam models appeared to involve the more important variables acting, except perhaps shear

properties. They emphasise the importance of the ratio between the Young's moduli respectively perpendicular and parallel to the grain, and since this is very sensitive to moisture content, take into account the dominant influence of this factor on the chip formation process and resulting surface quality. Frictional properties are also indicated as being of general importance. It is concluded that fuller validation of these indications will require an empirical approach based on experimental stress analysis, aimed at determining the stresses in certain zones of interest in the vicinity of the cutting edge, defined in the present study. The models served to define certain areas of ignorance concerning the properties of wood, and several problems basic to further understanding of the fundamental action of a cutting edge. These are :-

(1) The effect of strain rate on mechanical properties, in the range between standard testing rates and those occurring in cutting at 0.5 in. per min.

(2) The effect of moisture content on the elastic constants.

(3) The influence of normal stress on shear strength in the longitudinal plane of wood.

(4) The influence of the cutter edge itself on cell wall deformations and the resulting stress and force relations.

(5) The frictional properties of wood as related to wood species, moisture content and normal pressure.

BIBLIOGRAPHY

1. Franz, N. C. 1957. "An Analysis of the Wood Cutting Process" Univ. of Michigan, Ann Arbor, Mich.

2. Reineke, L. H. 1950. Sawteeth in Action. Proc. For. Prod. Res. Soc. 4 : 36-51.

3. Leney, L. 1960. A Photographic Study of Veneer Formation. For. Prod. J. 10(3):133.

4. Merchant, M. E. 1945. Mechanics of the Metal Cutting Process I. Orthogonal Cutting and a Type II Chip. J. Appl. Phys. 16 : 267-75.

5. Lubkin, J. L. 1957. "A Status Report on Research in the Circular Sawing of Wood. Volume I." Cent. Res. Lab. Amer. Mach. & Foundry Co. Stamford, Conn.

6. Voskresenski, S. A. 1955. "Rezanie Derevesiny" (Wood Cutting). Govt. Forestry Printing Office, Moscow.

7. Liska, J. A. 1950. Effect of Rapid Loading on the Compression and Flexural Strength of Wood. U.S. Dept. Agric. For. Prod. Lab. Report No. 1767.

8. Koch, P. 1955-56. An Analysis of the Lumber Planing Process. For. Prod. J. 5 : 255, 6 : 393.

9. Kollmann, F. 1955. "Technologie des Holzes und der Holzwerkstoffe." Springer - Verlag, Berlin.

10. Bershadskii, A. L. 1951. (High Speed Sawing with Reduced Power Consumption) Lesnaia Promyshlennost 2 : 25-28. C.S.I.R.O. Australia. Trans. 1637.

11. Freudenthal, A. M. 1950. "The Inelastic Behaviour of Engineering Materials and Structures" Wiley & Sons, New York.

12. U.S. Dept. Agric. 1955. "Wood Handbook" Agric. Handbook No. 72.

13. Reichel, W. 1936. Das Temperaturefeld beim Zerspanen. Maschinenbau der Beitrieb. 15 : 495; 16:187.

14. Kivimaa, E. 1950. "The Cutting Force in Woodworking" State Institute for Technical Research, Helsinki, Finland, Publ. No. 18.

15. Thunell, B. 1958. Schnittkraftbestimmung bei der Holzbearbeitung. Holz als Roh- und Werkstoff 16 : 138-145.

16. Chardin, A. 1957. L'Etude du Sciage par Photographie Ultra-Rapide. Bois et Forets des Tropiques no. 51 : 40.

17. Norris, C. B. 1955. Strength of Orthotropic Materials Subjected to Combined Stresses. F.P.L. Madison Report No. 1816.

18. McMillan, C. W. 1958. The Relation of Mechanical Properties of Wood and Nose-Bar Pressure in the Production of Veneer. For. Prod. J. 8 (1) : 23.

19. Antoine, M. R. 1959. La Scie Statique - apporterait-elle une solution aux illogismes du sciage du bois? Rev. de Bois No. 4, April, p.47.

20. Shaw, M. T. 1954. Metal Cutting Principles. 3rd Edit. M.I.T. Camb., Mass.

21. Albrecht, P. 1960. New Developments in the Theory of the Metal-Cutting Process : The Ploughing Process in Metal Cutting. A.S.T.M.E. 28th Annual Meeting Collected Papers 60(1). Paper No. 251.

22. Green, A. E. 1939. Stress Systems in Aeolotropic Plates. II. Proc. Roy. Soc. A 173 : 173.

23. Hetényi, M. 1946. "Beams on Elastic Foundation" Univ. of Mich. Press, Ann Arbor, Mich.

24. Biot, M. A. 1937. Bending of an Infinite Beam on an Elastic Foundation. Trans. A.S.M.E. 59 : A 1-7.

25. Doyle, D. V., Drow, J. T., and McBurney, R. S. 1945. Elastic Properties of Wood : The Young's Moduli, Moduli of Rigidity and Poisson's Ratios of Balsa and Quipo. U.S.F.P.L. Report No. 1528.

26. Markwardt, L. J. and Wilson, T. R. C. 1935. Strength and Related Properties of Woods Grown in the United States. U.S.D.A. Tech. Bull. 479.

27. Haythornthwaite, R. M. 1959. "Theory of Plasticity and Practical Engineering Problems" Brown University : Manuscript.

28. Sokolnikoff, I. S. 1956. "Mathematical Theory of Elasticity" McGraw-Hill Book Co. N.Y.

29. Atack, D. and Tabor, D. 1958. The Friction of Wood. Proc. Roy. Soc. 246 : 539.